



**Simulation & Analysis of the Helicopter Transmission
System**

محاكاة و تحليل نظام نقل الحركة الخاص بالطائرة العمودية

by

ABDALLAH LASFER

**Dissertation submitted in fulfilment
of the requirements for the degree of
MSc SYSTEMS ENGINEERING
at
The British University in Dubai**

January 2019

DECLARATION

I warrant that the content of this research is the direct result of my own work and that any use made in it of published or unpublished copyright material falls within the limits permitted by international copyright conventions. I understand that a copy of my research will be deposited in the University Library for permanent retention. I hereby agree that the material mentioned above for which I am author and copyright holder may be copied and distributed by The British University in Dubai for the purposes of research, private study or education and that The British University in Dubai may recover from purchasers the costs incurred in such copying and distribution, where appropriate. I understand that The British University in Dubai may make a digital copy available in the institutional repository. I understand that I may apply to the University to retain the right to withhold or to restrict access to my thesis for a period which shall not normally exceed four calendar years from the congregation at which the degree is conferred, the length of the period to be specified in the application, together with the precise reasons for making that application.

Signature of the student

COPYRIGHT AND INFORMATION TO USERS

The author whose copyright is declared on the title page of the work has granted to the British University in Dubai the right to lend his/her research work to users of its library and to make partial or single copies for educational and research use. The author has also granted permission to the University to keep or make a digital copy for similar use and for the purpose of preservation of the work digitally. Multiple copying of this work for scholarly purposes may be granted by either the author, the Registrar or the Dean only. Copying for financial gain shall only be allowed with the author's express permission. Any use of this work in whole or in part shall respect the moral rights of the author to be acknowledged and to reflect in good faith and without detriment the meaning of the content, and the original authorship.

Abstract

This report analyzes the main shafts of the helicopter transmission box. The corresponding behavior of the shafts, gears, and blades are monitored and studied. Three different methods were used to analyze the set of systems describing the behavior of the shafts. The first method is the lumped model analysis, which considers each element of the shaft to be discrete. The second method is the finite element method, which separates the shaft itself into smaller elements. The last method is the hybrid model, where the gears are taken as discrete elements, while the shaft characteristics are continuous functions of the shafts' length. The speed at each end of each shaft is recorded and studied, as well as, the shafts threshold to the shear stress applied. The model results are compared for accuracy, precision and difficulty. Results conclude of simplicity of the lumped model but also impracticality. While the finite elements model is difficult to produce as it requires tedious solving of high order polynomials. The hybrid model is the most accurate in terms of shaft properties however; it faces difficulty in determining the critical speeds for mechanical failure.

ملخص

يحلل هذا التقرير الأعمدة الرئيسية لصندوق إرسال الهليكوبتر. يتم مراقبة ودراسة السلوك المقابل للأعمدة والتروس والشفرات. تم استخدام ثلاث طرق مختلفة لتحليل مجموعة من النظم التي تصف سلوك الأعمدة. الطريقة الأولى هي تحليل النموذج المقطوع ، والذي يعتبر كل عنصر من عناصر عمود المنبع منفصلاً. الطريقة الثانية هي طريقة العناصر المحدودة ، التي تفصل العمود نفسه إلى عناصر أصغر. والطريقة الأخيرة هي النموذج الهجين ، حيث يتم أخذ التروس كعناصر منفصلة ، في حين تكون خصائص العمود صفات تعتمد على طول العمود. يتم تسجيل ودراسة السرعة عند كل نهاية لكل عمود ، وكذلك عتبة العمود إلى إجهاد القص المطبقة. تتم مقارنة نتائج النموذج من حيث الدقة والصعوبة. تلخص النتائج من ناحية النموذج المقطوع أنها بسيطة ولكن غير عملية. في حين يصعب حل معادلات نموذج العناصر المحدودة لأنها تتطلب حلاً شاقاً. النموذج الهجين هو الأكثر دقة من حيث خصائص ربح ومع ذلك ؛ تواجه صعوبة في تحديد السرعة الحرجة للفشل الميكانيكي.

Acknowledgment

I would like to thank my supervisor, Dr Alaa Ameer for his continuous guidance and for providing assistance and advice when needed.

I also would like to show gratitude towards Professor Robert Whalley (deceased) for his teachings and help throughout the whole program.

I am grateful towards my family, friends and colleagues for providing the physical and mental encouragement to pursue this degree.

Table of Contents

List of Illustrations	
List of Abbreviations.....	
Chapter I: Introduction	1
1.1 Control Systems Engineering Background	1
1.2 Mathematical Modelling	4
1.2.1 Lumped Parameter Method.....	4
1.2.2 Finite Element Method.....	5
1.2.3 Hybrid (Distributed-Lumped) Method.....	5
1.3 Problem Statement	6
1.4 Aims and Objectives	7
1.5 Organization of the Dissertation	7
Chapter II: Literature Review	9
2.1 History of the Helicopter Aircraft	9
2.2 Helicopter Flight Principle	9
2.3 Helicopter Transmission Line Components	10
2.3.1 Gas Turbine & Turbo shaft	11
2.3.2 Clutch	14
2.3.3 Gears	16
2.4 Lumped Parameter Method.....	17
2.5 Finite Element Method.....	18
2.6 Impedance Analogy.....	19
2.7 Hybrid (Distributed-Lumped) Method.....	20
Chapter III: Mathematical Modeling.....	22
3.1 Helicopter Transmission System Model	22
3.2 Lumped Parameter Model.....	23
3.3 Finite Elements Model	35
3.4 Hybrid (Distributed-Lumped) Model.....	52
3.5 Defining of Parameter Values & Equations for each Modeling Method	66

3.5.1 Lumped Parameter Model Equations	66
3.5.2 Finite Element Model Equations	74
3.5.3 Hybrid (Distributed-Lumped) Model Equations	79
Chapter IV: Simulation, Results & Discussion of Results	82
4.1 Lumped Parameter Model Simulation	82
4.2 Lumped Parameter Model Results	85
4.3 Lumped Parameter Model Analysis	93
4.4 Finite Element Model Simulation	99
4.5 Finite Element Model Results	102
4.6 Finite Element Model Analysis	112
4.7 Hybrid (Distributed-Lumped) Model Simulation	117
4.8 Hybrid (Distributed-Lumped) Model Results	121
4.9 Hybrid (Distributed-Lumped) Model Analysis	127
Chapter V: Conclusions & Recommendations	131
References	133
Appendix I	136
Appendix II	150
8.1 Definition of Concepts	150
8.1.1 Torque & Torsion	150
8.1.2 Shear Stress	151
8.1.3 Angular Displacement, Velocity, Acceleration	151
8.1.4 Inertia & Moment of inertia	152
8.1.5 Power	153
8.1.6 Density	153
8.2 Differential Equations	153

List of Illustrations

Figure 1: Overview of the Components of the Helicopter Transmission System (FAA Safety Team, Accessed 6 Jan 2019)	11
Figure 2: Compressor Flow Characteristics (Fundamentals of Gas Turbine Engines, Accessed 14 Oct 2018)	13
Figure 3: Turbine Flow Characteristics (Fundamentals of Gas Turbine Engines, Accessed 14 Oct 2018)	13
Figure 4: Side View of the Components of a Turbo Shaft (Turbo Shaft Operation, Accessed on Jan 3 2019)	14
Figure 5: The Belt Drive Clutch (Padfield, 2013).....	15
Figure 6: Illustration of a Gear Train (Integrated Publishing, Accessed on Dec 21 2018)	17
Figure 7: Schematic Model of the Helicopter Transmission System	23
Figure 8: Main Rotor Shaft (MRS)	24
Figure 9: Main Rotor Shaft (MRS): Labeled	25
Figure 10: Block Diagram of Lumped Model on Main Rotor Shaft.....	31
Figure 11: Block Diagram of Main Shaft.....	34
Figure 12: Finite Element Model on Main Rotor Shaft	35
Figure 13: Block Diagram of the Finite Element Model on Main Rotor Shaft.....	44
Figure 14: The Block Diagram of the Finite Element Model on Main Shaft.....	51
Figure 15: Hybrid Model Main Rotor Shaft Labeled.....	52
Figure 16: Transmission Line Representation (Whalley, Ebrahimi, Jamil, 2005).....	53
Figure 17: Block Diagram of the Hybrid Model on Main Rotor Shaft	62
Figure 18: Block Diagram of the Hybrid Model on the Main Shaft	65
Figure 19: Representation of SIMULINK Model of Main Rotor Shaft	82
Figure 20: Representation of SIMULINK Model Main Shaft	84
Figure 21: Load End (Angular Speed 1) of Lumped Model	85
Figure 22: Drive End (Angular Speed 2) of Lumped Model	86
Figure 23: Load End (Angular Speed 1) Bode Plot for Lumped Model	86
Figure 24: Load End (Angular Speed 2) Bode Plot for Lumped Model	87
Figure 25: Shear Stress of Main Rotor Shaft for Lumped Model	88
Figure 26: Tail Rotor Speed for Lumped Model.....	89
Figure 27: Drive End (Angular Speed 4) of Main Shaft for Lumped Model.....	89
Figure 28: Blade Angular Speed of Main Shaft for Lumped Model.....	90
Figure 29: Drive End (Angular Speed 4) of Main Shaft Bode plot for Lumped Model	91
Figure 30: Blade Angular Speed of Main Shaft Bode Plot for Lumped Model.....	92
Figure 31: Shear Stress of Main Shaft for Lumped Model	93
Figure 32: Representation of SIMULINK Model of Finite Elements on Main Rotor Shaft.....	100
Figure 33: Representation of SIMULINK Model of Main Shaft for the Finite Elements	101
Figure 34: Load End (Angular Speed 1) of Finite Model	102

Figure 35: Drive End (Angular Speed 2) of Finite Element Model	103
Figure 36: Load End (Angular Speed 1) Bode Plot for Finite Element Model.....	104
Figure 37: Load End (Angular Speed 2) Bode Plot for Finite Element Model.....	105
Figure 38: Shear Stress of Main Rotor Shaft for Finite Element Model.....	106
Figure 39: Tail Rotor Speed for Finite Element Model	107
Figure 40: Drive End (Angular Speed 4) of Main Shaft for Finite Element Model.....	108
Figure 41: Blade Angular Speed of Main Shaft for Finite Element Model	109
Figure 42: Drive End (Angular Speed 4) of Main Shaft Bode plot for Finite Element Model.....	110
Figure 43: Blade Angular Speed of Main Shaft Bode Plot for Finite Element Model.....	111
Figure 44: Shear Stress of Main Shaft for Finite Element Model	112
Figure 45: Representation of SIMULINK Model on Main Rotor Shaft for Hybrid Model.....	118
Figure 46: Representation of SIMULINK Model on Main Shaft for Hybrid Model.....	120
Figure 47: Load End (Angular Speed 1) of Hybrid Model	121
Figure 48: Drive End (Angular Speed 2) of Hybrid Model	122
Figure 49: Shear Stress Main Rotor Shaft Hybrid Model	123
Figure 50: Tail Rotor Speed Hybrid Model	124
Figure 51: Drive End (Angular Speed 4) of Main Shaft for Hybrid Model.....	125
Figure 52: Blade Angular Speed of Main Shaft for Hybrid Model.....	126
Figure 53: Shear Stress Main Shaft Hybrid Model	127
Figure 54: Shear stress distribution across Solid and Hollow Shafts.....	151
Figure 55: Equations of moment and polar moment of inertia for different shapes of rigid bodies ...	153

List of Abbreviations

Annotation	Meaning	Unit
F	Force on the shaft	N
m	Mass of the element	Kg
a	Acceleration of the element	$\frac{m}{s^2}$
c	Damping Coefficient on the shaft	
k	Stiffness of the shaft	$N * \frac{m}{radians}$
x	Linear displacement from the point of origin	m
v	Linear speed of the element	$\frac{m}{s}$
T	Torque on the shaft	Nm
θ	Angular Displacement of the element	$radians$
J	Polar Moment of Inertia	m^4 or Kgm^2
D	Diameter of the element	m
ρ	Density of the material	$\frac{Kg}{m^3}$
H	Height/Thickness of the element	m

G	Modulus of Elasticity	Pa
L	Length/Depth of the element	m
P	Power produced by the turbo shaft	$HP \text{ or } KW$
SS	Shear Stress along the shaft	Pa
V	Voltage across the capacitor	V
i	Current induced in the inductor	A
L (<i>inductance</i>)	Inductance of inductor	H
C (<i>capacitance</i>)	Capacitance of capacitor	F
ζ	Impedance of the shaft	$KgNm^3$
I (<i>mass moment</i>)	Mass moment of inertia	Kgm^2
L (<i>shaft inductance</i>)	A term equivalent to inertia per meter	Kgm
C (<i>shaft compliance</i>)	Inverse of stiffness per meter	$in N^{-1}m^{-2}$
τ	Time constant (Finite delay)	s
w	Angular velocity of the shaft	$\frac{radians}{s}$

Chapter I: Introduction

1.1 Control Systems Engineering Background

The discipline of control system engineering is the study that uses the control theory to manipulate different and a wide range of systems based and derived from their mathematical roots. Sensors are used to measure the output of the modelled and analysed system. The signals from the output measurement are used as a method of corrective feedback to correct the input signal and reach the desired outcome of the system. Control systems engineering is a very large field with many sub specialties originating from different disciplines of engineering, such as mechanical, electrical, chemical, and computer engineering. The very first work in automatic control was the speed control of a rotor powered by a steam engine in the eighteenth century (Ogata, 1997). In the early 1900s engineers such as Harry Nyquist started developing different ways in terms of finding stability of closed loop systems. During the mid-1900s, the frequency response and root locus methods were fully developed as a basis and core of classical control theory.

The analysis of any controlled system is divided in two categories.

- Modelling and Simulation
- Control Theory

The study of modelling in control systems engineering involves going back to the roots of practical physics, and deriving the mathematical equations that describe the

analysed dynamic system. Current modelling techniques involves the use of frequency response to turn ordinary and partial differential equations into polynomials that are easier to solve. The model of the dynamic controlled system covers the governing equations as well as some assumptions and constraints. This is an integral part of the determining the solution of the equations. As mathematics dictate, the solutions of differential equations are generated from a general format. This general format is made smaller and more specific to one specific case by the use of initial boundary conditions (A.D.Polyanin, 2003). These boundary conditions are specific to the problem at hand and determined by the engineer.

With the help of new software and the mechanical to electrical analogies, it is possible to simulate the dynamic system. Simulation is done after modelling; it helps in understanding the behaviour of the designated system without the requirement of building the prototype (up to an extent). With simulation, it is possible to duplicate and imitate the initial signals sent to the system in order to observe the behavioural response of the output.

Different modelling techniques exist, with different accuracies and difficulties; it is the job of the engineer to analyse and optimise the best solution according to the desired and required performance. For the case of drive line systems, the models are linear, dynamic, discrete and continuous depending on the method used. Further details will be explained in the following chapter.

The application of the control theory is related to the feedback control system. The governing equations of the dynamic system can be represented in a block

model, this is also known as the open loop response. In order to close the loop, a controller must be added; however, the design of the controller depends on the system dynamics. In case of a single input command, and a single output from the actuator, a more classical approach is used. A feedback is added that takes the measured output signal and feeds it to the controller (Ogata, 1997). The controller compares the output with the input signal it receives and corrects the input. This is done continuously while the system is running; decreasing the margin of error every time the signal passes through the loop until a steady state is achieved. The main function of the controller is to be able to keep this steady state output in case of any disturbances on the system. An example of a single input-output controller is the PID, or the Proportional Integral Differential controller, which regulates the response output of the system by increasing the amplitude (of the signal), reducing the steady state error, regulating the overshoot and the settling time (Sontag, 1998). In case of multiple input-output systems, a more modern approach is used. The mathematical modelling for these type of systems usually need a state space representation, and is solved in a matrix. Designing a controller for these types of systems usually involves a lot more complex methods with the help of software to produce more accurate results, as the math can get very tedious. This becomes much more complicated in higher order systems (3 or more input to outputs).

This is the case for all stable open-loop systems, in case of unstable systems a test of controllability must be done first to determine if closing the loop can

control the Eigenvalues (roots of the equations) of the system (and to what extent).

This dissertation will not cover the control theory, but only the modelling and simulation of the main transmission of a helicopter vehicle.

1.2 Mathematical Modelling

The modeling of helicopter transmission is used to derive the basic mathematical equations that describe the rotor shaft dynamic system.

Three different modeling techniques are used to study the behavior of the helicopter transmission:

- 1- The Lumped Parameter Method
- 2- The Finite Element Method
- 3- The Hybrid (Distributed-Lumped) Method

The three models are used to describe the dynamic system in terms of differential and partial differential equations within certain assumptions in order to analyze the dynamic shear stresses and angular speeds of the shafts.

1.2.1 Lumped Parameter Method

The lumped parameter method is a method that describes the distributed system in a topology. This topology is made of discrete elements that explain how the system behaves under certain conditions and constraints. However, the lumped model usually consists of an element having one important physical property (Doebelin, E.O, 1998.). That physical property of concern will be a function of

one variable. What this signifies is that it reduces the set of equations that describe the system into a number of ordinary differential equations with finite number of parameters. This method is mainly but not entirely used in electrical, thermal and mechanical systems.

1.2.2 Finite Element Method

The finite element method is a type of numerical methods to solve problems in physics and engineering by approximating solutions of complex differential equations. Differential equations are solved usually by having initial boundary conditions to be set, so that the general solution is extracted. Some partial differential equations are unsolvable unless a boundary condition is set, to extract a specific solution for a specific problem. The finite element method divides a problem into smaller parts named after the method. These equations are transformed into algebraic polynomials, and then combined to form the system of equations that model the problem (K.J.Bathe, 1976). The finite element method is used in many disciplines of engineering and physics usually involving dynamics of elements such as heat transfer, fluid flow dynamics, structural analysis, and rotor systems.

1.2.3 Hybrid (Distributed-Lumped) Method

The model is derived based on the electrical transmission line using two linear differential equations. These equations are called the telegrapher equations; they were developed by Oliver Heaviside sometime in the late 19th century. The equations are described by voltage and current those vary with time and the

length of the transmission line. These equations can be applied to all types of transmission lines regardless of frequency. The transmission line model consists of a resistor and an inductor in series, followed by another resistor and a capacitor connected to it in parallel (Karakash, John,1950). The effect of the inductance in the model is similar to that of the inertia in rigid bodies. The effect of the capacitance is the same as of that of the spring, as it behaves as a restoring force. The resistors exist as an energy dissipater, but in the lossless transmission line model, they are equal to zero. All elements in the model are variables of length. This is the base model used to derive the equations used in the hybrid model analysis. This is because the hybrid model describes the shaft length as a function of its inductance and compliance, similarly to the transmission line model. However, lumped elements also exists in the model, such as the inertia of the shafts/gears, length, diameter, and damping.

1.3 Problem Statement

The reason the helicopter transmission is studied, analysed and simulated is to understand the difficulties in design in order to control and reduce the problems that could occur due to torsional stresses in the shafts. The main purpose of this dissertation is to apply the lumped, finite element, and transmission line modelling techniques to the helicopter transmission system, and to compare the accuracy and precision, difficulty, complexity, and the response of each model in order to fully understand the behaviour of the system. The analysis will include

the speed of the shafts, as well as the shear stress. Bode diagrams will be used to identify resonance speeds.

1.4 Aims and Objectives

At the end of the dissertation, the reader will be able to comprehend the following:

- Mathematical modelling of the helicopter transmission model using lumped, finite element and hybrid model techniques.
- Simulation of the helicopter transmission model on SIMULINK software.
- Study and analyse the behaviour of the system from the response and bode plots in terms of angular speed and dynamic torsional stress.
- Comparing all modelling techniques in terms of response, complexity, accuracy and feasibility to conclude the optimised way of analysis.

1.5 Organization of the Dissertation

The dissertation will consist of five different chapters:

Chapter one contains the introduction and background. This introduces the reader mathematical modelling. Moreover, it presents the fundamental basics behind the three methods that will be used.

Chapter two contains the literature review. This is the history of the helicopter, how it was made, the flight principle, and the components that make the aircraft. The three modelling techniques developed to simulate and analyse the helicopter

transmission is discussed as used by mathematicians, engineers, researchers and scholars; showing what has been done (work) and their opinion (conclusions).

Chapter three covers the actual mathematical modelling and derivation. This section covers the explanation of how the model is derived, as well as the solution for the equations. The parameter definitions, values and calculations are all completed in this chapter.

Chapter four shows the simulation, results, and the discussion of the three models. This section describes the results in terms of the responses of the system. The angular speed and shear stresses of each shaft is analysed. In addition, the settling time, overshoot, magnitude, phase, and resonance speeds are recorded and studied. Results are explained based on values reached.

Chapter five explains the conclusions reached. This is the author's scientific opinion based on the results obtained from the simulation. Each model's results are compared based on their qualities in terms of complexity, accuracy and difficulty. A final conclusion is reached, and recommendations can be given if needed.

Chapter II: Literature Review

2.1 History of the Helicopter Aircraft

The word helicopter comes from the greek words “helix” and “pteron” meaning “spiral” and “wing”. The very first inventor (that was recorded in history) is said to be the famous Leonardo da Vinci (Prime Industries, 2015). He was fascinated with the idea of a flying machine with a helical screw which he designed in 1488. However, due to lack of means he was never able to build it. This inspiration took on into Sikorsky, the first man to build the base design of many modern helicopters. The main struggle in creating the helicopter was the maneuvering of the main rotor blades, which was solved by the mechanics of the swash plate. The swash plate is able to move the rotor blades at different angles to allow sideway movements; the main difference between a helicopter and an airplane. Another problem was the design of the tail rotor blade, this was used to counter act the torque from the main rotor blades. It was only until 1942 where Sikorsky was able to design the very first successful helicopter.

2.2 Helicopter Flight Principle

The helicopter flight principle is based on the lift force produced from the main rotor. When the fuel burns, the turbo shaft rotates the shaft, and power is transmitted to the main rotor through the helicopter transmission. When the rotor blades rotate, due to the shape of the blade, it creates a pressure difference which causes a force upwards (Lift Force).

When the lift is more than the weight of the helicopter, it starts to move upwards (Seddon and Newman, 2011). Navigation on the helicopter (movement to the right/left or upwards/downwards) is done through changing the angle of attack. This is the angle between the edge of the blade and the streamline of air hitting the blade. The change in angle of attack decomposes the force vector into different axes depending of direction of desire. This change is done using a swashbuckler located at the hub connected below the rotor. When moving the controls of the helicopter, the swashbuckle slips and twists accordingly to change the angle of attack of the blades in order to manoeuvre around. Rotation of the main rotor blades causes a problem that can be explained using Newton's third law of motion. For every action there is an equal and opposite reaction. Because the main rotor blade rotates in one direction it will cause the body of the helicopter to rotate as well. This is solved by installing the tail blade rotor. The tail blade rotor's main function is to counter act the force of rotation caused by the main blade rotor (Padfield, 2013). The tail blade rotor produces a force in a plane perpendicular to the main blade rotor, and is also powered from the main transmission. The tail blade rotor is a lot smaller, and power/speed transmitted is reduced a lot compared to the main blade rotor.

2.3 Helicopter Transmission Line Components

The helicopter main transmission is a basic form of drive line system containing a series of interconnected shafts and gears for torque and power transfer. The model starts with a turbo shaft engine (an optimised jet engine for high power

and low weight vehicles) rotating at 6000 rpm. This is the source of power that moves the whole system, and follows the rules of the thermodynamics of a gas turbine engine that converts energy into torque. The transmission shaft from the turbo shaft is connected via a series of gear meshes to transmit torque and speed to rest of the system (Padfield, 2013). The main transmission splits in functionality to provide torque for both the main rotor and the tail rotor. At both ends of the transmission lines, the shafts are connected to the hubs and rotary blades.

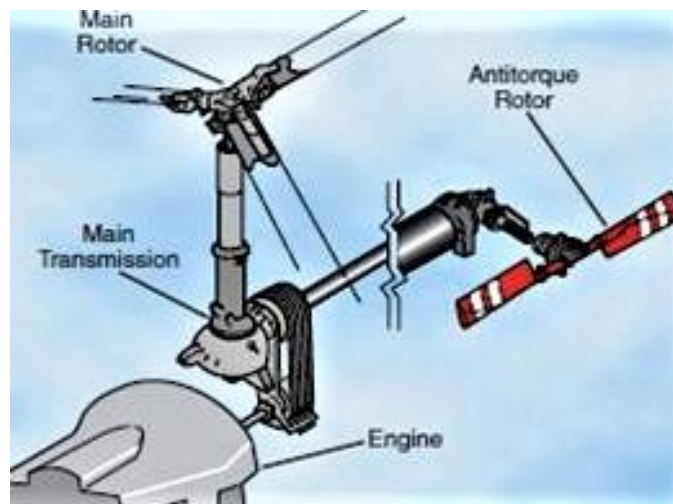


Figure 1: Overview of the Components of the Helicopter Transmission System (FAA Safety Team, Accessed 6 Jan 2019)

2.3.1 Gas Turbine & Turbo shaft

The gas turbine is a form of an internal combustion engine that converts fuel and air into torque to be used in the transmission. The turbine comprises of 3 main components: the compressor, the combustion chamber, and the turbine. These 3 components are connected (usually) in one shaft called the rotor. The compressor

is made of many stages of rotary blades and stationary vanes. These blades and vanes are in a bent shape named the air foil. The air foils have this specific shape for a reason, when air travels through the compressor at fast speed, the foils due to their profile, convert the kinetic energy into pressure energy; increasing the pressure and temperature of the air (El Nagggar, 2015). This process is isentropic (ideally), meaning there is no heat transfer outside of the system, and reversible, meaning no losses of energy occurs during the compression. When air exits the compressor, it enters the combustion chamber, where it mixes with fuel. Inside the combustion chamber are burners in order to heat the air and fuel mixture to very high levels of temperature (around 1000 degrees Celsius, depending on gas turbine operation and type). Combustion is an Isobaric process, meaning it occurs at constant pressure (ideally). Finally, the hot fuel air mixture enters the turbine section. The turbine section is also made of blades and vanes that serve the function that is the opposite of the compressor. Here the high temperature and pressure of fuel air mixture is converted to into kinetic energy (in case of a jet engine) or mechanical energy in the form of torque to rotate the shaft (gas turbine).The gas turbine follows the rules of a Brayton cycle (Cengel & Boles, 2007). For helicopter vehicles, the gas turbine engine has been optimised to produce a lot of power to weight ratio, and is now being used instead of the conventional reciprocating engine. This type of engine is now called the turbo shaft.

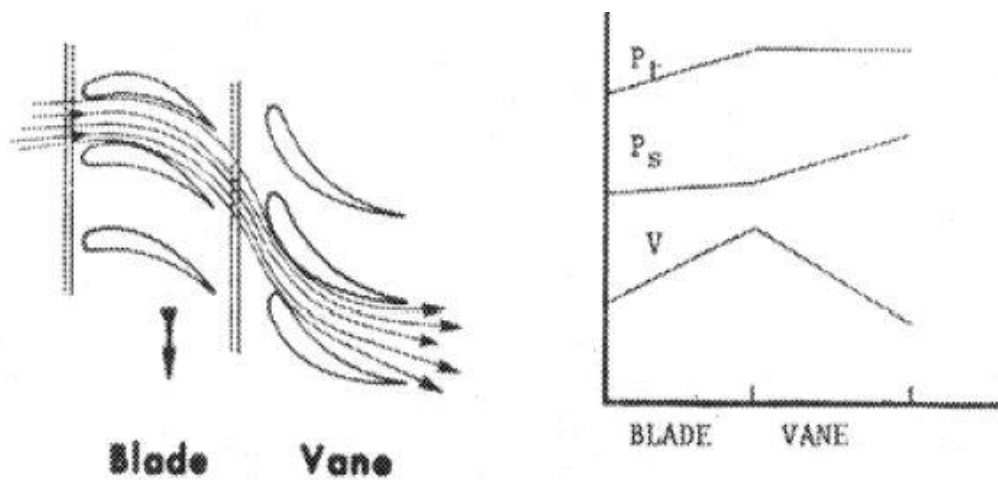


Figure 2: Compressor Flow Characteristics (Fundamentals of Gas Turbine Engines, Accessed 14 Oct 2018)

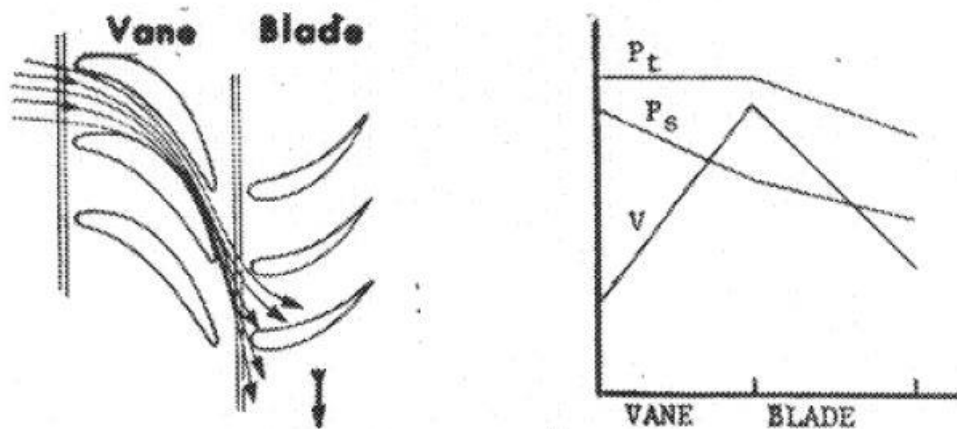


Figure 3: Turbine Flow Characteristics (Fundamentals of Gas Turbine Engines, Accessed 14 Oct 2018)

The turbo shaft is the optimised form of the gas turbine designed specifically for helicopter vehicles. It is a compact form of gas turbine that is small in size, lightly weighted and still able to produce high amount of power to drive the helicopter vehicle (Aero, 2015). The turbo shaft is made up of two sections.

The first section is the gas turbine itself, with a multi stage compressor and a two (usually) stage turbine section. The second section is a different shaft that is connected very close to the turbine section (but is not touching) and starts with another 2 stage turbine. This section is often called the free power turbine because the turbine blades that rotate, and consequently the shaft, are run freely by the exhaust gases of the first section turbine (Gunston, 2006). Both sections make up the turbo shaft engine. The free power turbine shaft is connected directly to the main transmission.

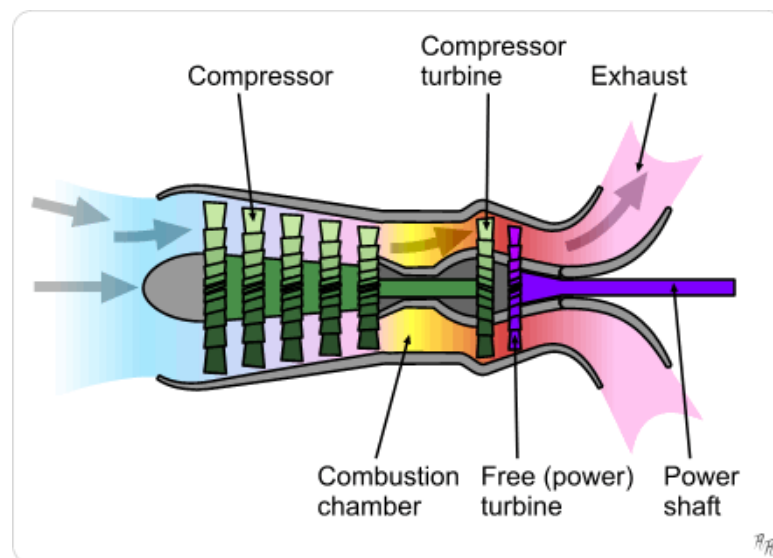


Figure 4: Side View of the Components of a Turbo Shaft (Turbo Shaft Operation, Accessed on Jan 3 2019)

2.3.2 Clutch

The clutch is mechanical device which links or disconnects two shafts in the form of engagement and disengagement. Clutches are used in all types of power transmission vehicles and mechanical drive line systems that require two shafts to be of the same speed at different times.

Normally, one of the shafts is considered to be the driving shaft and is connected to a motor or an engine. The other shaft is the driven shaft and is connected to the output of the system (Padfield, 2013). In helicopter design, there are different types of clutches developed depending on practicality and feasibility.

The belt drive clutch consists of two pulleys, one connected to the engine drive shaft while the other connected the main rotor transmission. The pulleys themselves are inter-connected with a set of belts as in gear train. When the engine starts, the throttle is activated to engage the clutch. As the engine starts to accelerate and gain speed, the tension in the belts starts to activate pulling the pulley and thus activating the rotation of the main transmission (Padfield, 2013). The main issue with this type of clutch is the throttle timing, as fast or not properly controlled throttles may cause over speed of the rotor shaft.

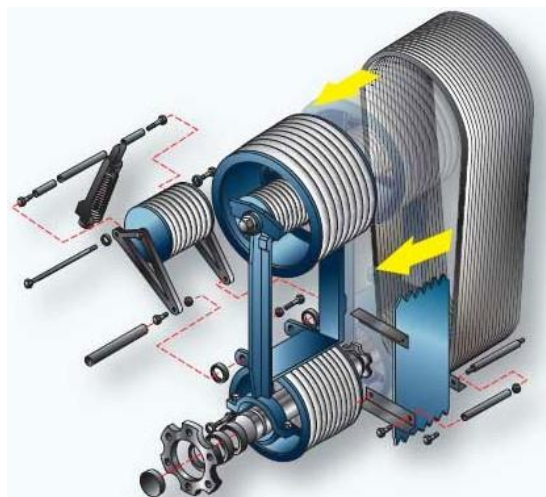


Figure 5: The Belt Drive Clutch (Padfield, 2013)

The centrifugal clutch consists of an inner plate and an outer drum. The inner plate is connected to the drive shaft, while the outer drum is connected to the main rotor transmission. The inner plate consists of pads similar to break pads that are held inside by springs. As the rotor speeds up, the centrifugal force of the pads push the springs outward until the outer drum is touched. This is when the clutch becomes fully engaged and the rotor drive shaft and driven shaft are synchronised (Padfield,2013).

2.3.3 Gears

The gear is a simple rotating machine part that has teeth carefully cut from the outer layer of the circular disk shape. The gears are usually hollow in the middle for the shaft to be inserted. Two or more gears can be meshed together to transmit power and rotational speed between the shafts connected. This combination is called a gear train. A gear train can be a mesh of more than two gears. This is usually the case inside the gear box of any vehicle. What is special about meshed gears is that they can change (increase or decrease) the power, rotational speed, and even the direction (depending on the type of gear) from one shaft to another (Nibsett, 2011). This property is a function of the number of teeth the gears have; and is called the gear ratio.

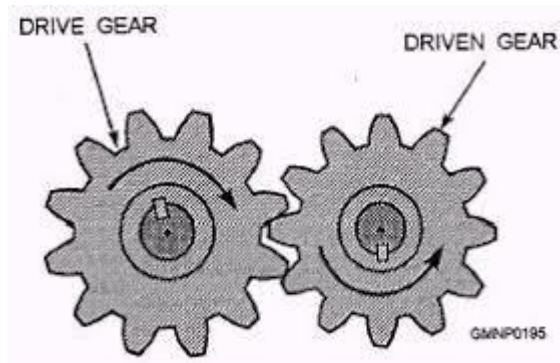


Figure 6: Illustration of a Gear Train (Integrated Publishing, Accessed on Dec 21 2018)

2.4 Lumped Parameter Method

The lumped parameter method is a method derived from analysis of electrical systems; in electrical systems consisting of resistors, capacitors and inductors. The lumped parameter method assumes no change in the magnetic field or charge in the circuit. This results in the Kirchhoff's laws of electrical circuit analysis. Another assumption states that the propagation time is less than the period of the signal inside the circuit (Doebelin, E.O, 1998.). When the propagation time increases to of a significant value, it must be considered in the analysis and a distributed system model must be used. In mechanical systems such as the current model (the helicopter transmission), the method is similar, except it involves rigid bodies of mechanical parts. The rigid bodies have significant characteristics such as inertia, mass, dimensions, force and acceleration. These rigid bodies are linked by joints, clutches, gears. Considering all of these elements as rigid bodies; this means that we do not study each element as a set of small different parts but one as a whole.

We do not consider the temperature, stresses, behavior of each section of the shaft, but the shaft as a whole. This is what defines a lumped parameter model. In terms of mathematical modeling, non-linearities in the system are not considered.

2.5 Finite Element Method

The finite element method is a method that sub divides the analyzed system into small sub sections; thus the name finite elements. Each sub section of the division will have its own equation model. These equations are then constructed together to solve the entire problem (K.J.Bathe, 1976). In the helicopter transmission, the shaft is modeled as a combination of smaller shafts with gears at the end of each sub section. Equations are modeled for each sub shaft between each two gears. This creates a series of equations based on the number of sub shafts (or more correctly; finite elements) taken. The equations themselves are similar to the lumped parameter model and are dependent on each other. Solving these model equations is difficult and complex due to the increasing number of the order of the polynomials (after conversion from differential equations). Software (such as MATLAB) is best used to avoid calculation errors. The more finite elements taken, the more the system is sub divided, the higher the order, the higher the difficulty. In the paper “The Torsional Response of Rotor Systems” the authors applied the finite element method in drive line systems with 2 rotors by taking 5 to 10 finite elements (Whalley, Ebrahmi, Jamil, 2005). Results displayed the complexity of the method which gives prone to inaccuracies.

2.6 Impedance Analogy

The impedance analogy is one of the main analogies to describe mechanical systems as electrical systems; converting the system as whole to easily reach the mathematical representation model. This analogy is used in the hybrid model technique, which is derived originally from the transmission line model. Each element in the mechanical system has a similar and corresponding element in the electrical system (Dorf, Bishop, 2010).

The mechanical loss of energy due to a resistive force such as friction is what is known as electrical resistance. The mechanical effect of a damper (or a shock absorber) is to reduce or dissipate kinetic energy. The corresponding effect of a resistor is to reduce current flow, or dissipate electrical power.

The shaft itself and the gears have a mass. According to Newton's first law of dynamics: when an object (of a certain mass) moves, it continues to move in a straight line. Thus the object resists the change in velocity, this is called inertia. The analogous term for the electrical system is inductance. The inductor is a coil wrapped around an insulator core. When electricity passes through the coil, it creates a magnetic field around the coil with a direction specified according to Faraday's law. When current changes in the coil, this induces an electro motive force in the coil and this opposes the change in the current. This is resistive property is analogous to inertia.

The stiffness of a rigid body is the resistance to deformation. Since the shaft is rotating due to torque, the stiffness in this model is mostly used as the resistance to angular deformation. The weight for the shaft cause a bending stress on the shaft, and thus the stiffness regards also resistance to linear deformation. This is however ignored in the model for simplicity and the relation with the topic (not related). The capacitance is analogous to the inverse of stiffness, which is called, the compliance (Whalley, Ebrahimi, Jamil, 2005). The capacitor is a component that stores electrical energy. It is made of two conducting metal plates with a solid insulator in between. The insulator is referred to as a dielectric solid because of its ability to polarize the charge passing through; this way the capacitor stores the voltage when charge passes through.

2.7 Hybrid (Distributed-Lumped) Method

The hybrid method is a method that utilizes both the lumped and distributed parameters into one representation. This is possible by taking the elements of interest as a distributed sum, while other elements remain as lumped. In the helicopter transmission, the shaft stiffness and compliance becomes a function of the shaft's properties such as length. Using the transmission line theory, as well as the impedance analogy, it is possible to compare a mechanical system to an electrical transmission line. In a long transmission line, the line behaves as a combination of inductor and capacitor repeated infinitely across the line length. The inductance and capacitance of this line become partial differential equations that are dependent on both time and length.

These can be accessed from the equations of current and voltage for the inductor and capacitor. Similarly, in the helicopter transmission, the compliance and stiffness of the shaft vary across the length (of the shaft) and time. These partial differential equations can be accessed from the equations of torque and speed. The rest of the elements of the shaft, such as the mass/inertia of the gears are considered as lumped parameters. In the paper “The Computational of Torsional, Dynamic Stresses” the authors applied this method to 2, 3 and derived the equations for multiple rotor systems (Whalley, Ameer, 2009). The results showed complexity in understanding the determination of critical speeds.

Chapter III: Mathematical Modeling

3.1 Helicopter Transmission System Model

The section of the helicopter that will be looked at is the Transmission. The Transmission extends from the output of the gas turbine engine into the gear box. From the gearbox it splits into two paths, one is to the tail rotor and the other is to the main rotor. The first path (to the tail rotor) is governed by two shafts. The first shaft, the Main Rotor Shaft, has two gears of inertias J_1 and J_2 and a length of L (These variables exact names have not been used for simplicity purposes). The second shaft, the Tail Rotor Shaft, is assumed to be very small in length with one gear on one side and the tail blades at the other. Since the shaft is modeled to be very small the speed of the gear is equal to the speed of the blades; the mechanics of the shaft can be ignored. The second path emerges from the gear 1 into an intermediate shaft. This shaft is also very small, and for simplicity purposes the mechanics of the shaft are ignored. At the end of the intermediate shaft, is a small gear, which is connected via a gear train (of two) to the main shaft. The main shaft consists of one gear on one side and the hub and blades on the other. Each of these components exerts inertia of J_4 , J_{1B1} , and J_{H1} respectively. The following can be easily represented using the diagram below:

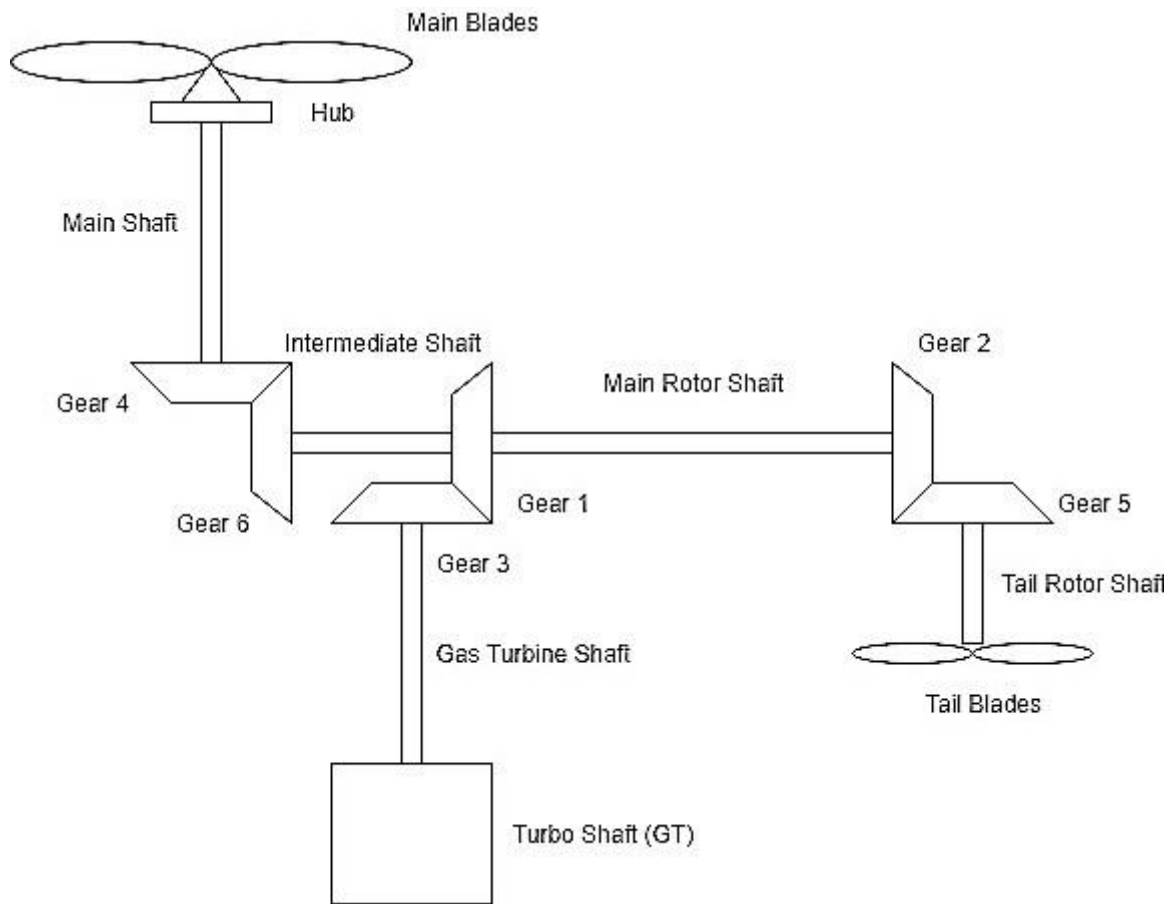


Figure 7: Schematic Model of the Helicopter Transmission System

This model can be analyzed in 3 different ways. These 3 ways can be categorized into 2 different sections. The first section is the lumped model analysis and the second section is the distributed model analysis. The distributed model utilizes two different methods, the finite element method and the hybrid method.

3.2 Lumped Parameter Model

The lump model analysis utilizes each element in the system as discrete figures, which is what engineers usually do when modeling mechanical elements in a mechanical system.

To simplify the modeling, the system will be cut to different sections in order to calculate their properties.

Starting with the Main Rotor Shaft, which is the basis of the whole model (thus the name).

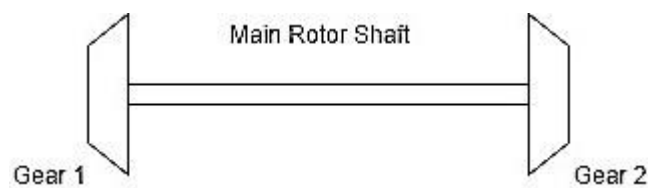


Figure 8: Main Rotor Shaft (MRS)

The model of this system comes from Newton's second law of motion, which states: The sum of the forces acting on an object is equal to the object mass multiplied by its acceleration.

$$F = ma \tag{3-1}$$

Considering this is a system with resistive forces: damping C and stiffness K :

$$F - cv - kx = ma \tag{3-2}$$

Rearranging:

$$F = ma + cv + kx \tag{3-3}$$

Considering acceleration is the derivative of velocity, and velocity itself is the derivative of displacement, then:

$$F = mx'' + cx' + kx \quad (3-4)$$

This is a simple form of the second order differential equation.

However, the concern in our model is not linear displacement, but angular position, thus turning the equation into:

$$T = J\theta'' + c\theta' + k\theta \quad (3-5)$$

Where T is the Torque acting on the shaft, and J is the mass moment of Inertia of modeled object.

Since the Main Rotor Shaft, has two gears acting on the shaft, in other words, two forms of inertia (separate), the equation has to be applied on two different point of axes, at Gear 1 and Gear 2.

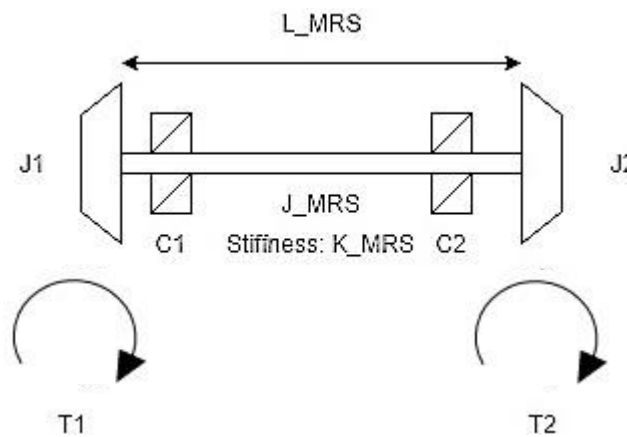


Figure 9: Main Rotor Shaft (MRS): Labeled

J_1 and J_2 represent the Polar moment of inertia (mass) of gear 1 and gear 2. C_1 and C_2 represent the damping, or the resistance to speed, at each side of the shaft. K

(MRS) is the stiffness, or the resistance to torsion of the shaft. L is the length of the shaft.

J (MRS) is the Polar moment of inertia (mass) of the shaft itself. T_1 and T_2 are the torques at each end of the shaft due to external forces

The direction of the torque is assumed and can be correctly represented in the equation using signs “+” and “-“.

By taking the point at one end of the shaft it is possible to represent each equation in terms of acting torque (one at a time).

The differential equations that represent the dynamic system are:

$$T_1 = J_1\theta_1'' + c_1\theta_1' + k(\theta_1 - \theta_2) \quad (3-6)$$

$$T_2 = J_2\theta_2'' + c_2\theta_2' + k(\theta_2 - \theta_1) \quad (3-7)$$

These are 2 second order differential equations that depend on each other. To solve this, just like any other differential equation, a method is used in order to transform them to polynomials. The method is called Laplace Transform.

Taking the Laplace Transform of both equations:

$$T_1(s) = J_1(S^2)\theta_1(s) + c_1S\theta_1(s) + k(\theta_1(s) - \theta_2(s)) \quad (3-8)$$

$$T_2(s) = J_2(S^2)\theta_2(s) + c_2S\theta_2(s) + k(\theta_2(s) - \theta_1(s)) \quad (3-9)$$

These equations are easily solved by many methods, for easier representation independent of the number of equations or variables, these equations will be represented in matrix form.

$$[T_1(s), T_2(s)] = [JS^2 + CS + K][W_1(s), W_2(s)] \quad (3-10)$$

$W(s)$ represents the angular speed and is equal to $S * \theta(s)$.

The angular speed is more of a concern than the angle of rotation, and since the angular speed is the derivative of angular position, when one is known the other will follow.

$[JS^2 + CS + K] = [A]$ matrix, which is just a representation for easier naming purposes. A detailed look into the A matrix is:

$$[A] = [J_1S^2 + C_1S + K \quad K, K \quad J_2S^2 + C_2S + K] \quad (3-11)$$

This implies that in order to find the speeds at the end of each shaft, this equation must be solved:

$$[W_1(s), W_2(s)] = [A]^{-1} [T_1(s), T_2(s)] \quad (3-12)$$

The inverse of the A matrix is easily found as described in “Modern Control Systems” from the matrix property equation (Dorf and Bishop, 2010):

$$\text{Inverse of A matrix} = \frac{Adj(A)}{Det(A)} \quad (3-13)$$

If the A matrix is represented with the elements a,b,c,d in a 2x2 matrix, then:

$$A = [a \quad b, c \quad d] \quad (3-14)$$

$$Adj(A) = [d - b, -c \quad a] \quad (3-15)$$

$$Det(A) = \Delta(s) = |ad - bc| \quad (3-16)$$

Solving these equations:

$$Adj(A) = [J_2 S^2 + C_2 S + K - K, -K J_1 S^2 + C_1 S + K] \quad (3-17)$$

$$Det(A) = S * [(J_1 * J_2) S^3 ((J_2 * C_1) + (J_1 * C_2)) S^2 ((J_2 * K) + (J_1 * K) + (C_1 * C_2)) S (K * (C_1 + C_2))] \quad (3-18)$$

S from the determinant is removed to change $\theta(s)$ to $W(s)$

The solved equation becomes:

$$\begin{aligned} [W_1(s), W_2(s)] & \quad (3-19) \\ & = \left(\frac{1}{\Delta(s)}\right) * [J_2 S^2 + C_2 S + K - K, -K J_1 S^2 + C_1 S \\ & \quad + K] [T_1(s), T_2(s)] \end{aligned}$$

If the assumption is the torque provided to the shaft is coming from the gas turbine only, then:

$$T_2(t) = T_2(s) = 0. \quad (3-20)$$

The final equation becomes:

$$\begin{aligned} [W_1(s), W_2(s)] & \quad (3-21) \\ & = \left(\frac{1}{\Delta(s)}\right) * [J_2 S^2 + C_2 S + K - K, -K J_1 S^2 + C_1 S \\ & \quad + K] [T_1(s), 0] \end{aligned}$$

Where the angular speed 1 is:

$$W_1(s) = (1/\Delta(s)) * [J_2 S^2 + C_2 S + K] * T_1(s) \quad (3-22)$$

And the angular speed 2 is:

$$W_2(s) = \left(\frac{1}{\Delta(s)}\right) * [-K] * T_1(s) \quad (3-23)$$

Normally these Laplace transformed equations are reverted from frequency response back to the time domain; however, it is still possible to study the behavior without the inversion using MATLAB and SIMULINK to simulate the response of the system.

Ultimately, the angular speeds are dependent on the design of the shaft and gears, which is to be expected. The values themselves will be discussed in the discussion of results section; moreover, the calculated numbers will be shown in the appendix section (done on MATLAB). However, the equations will be shown here for the purpose of clarity.

This is done for every gear in the whole model (not just the MRS), taking gear 1 for example:

Outer Diameter = D_2 , measured in m (converted)

Inner Diameter = D_1 , measured in m

$$J_1 = \pi * \rho * H * \left(\frac{1}{32}\right) * ((D_2^4) - (D_1^4)); \quad (3-24)$$

(Polar mass moment of inertia (Kgm²))

Where ρ , is the density of the material the gear is made of (Steel, in $\frac{Kg}{m^3}$), and H is the height of the gear cross section or the Depth (in m).

The same way, J_2 and J_{MRS} are calculated.

C , the damping, is assumed from practice (in $\frac{N}{m}$)

K , the stiffness of the shaft is calculated:

$$K = G * \frac{J}{L} \quad (3-25)$$

However, due to the fact that stiffness is independent mass, J here is Polar moment of inertia not the Polar mass moment of inertia, the equation must be adjusted for consistency.

The equation becomes:

$$K = \frac{G * J}{\rho * (L^2)} \quad (3-26)$$

Where G is the modulus of rigidity, which is dependent on the shaft material (Steel, in N/m^2).

J is Polar mass moment of inertia of the shaft.

ρ is the density of the material.

L is the length of the shaft.

Finally, T_1 is dependent on the transmitted torque from the gas turbine.

The power produced by the gas turbine is:

$$P_T = 350 \text{ HP} \quad (3-27)$$

Converting the power to KW with a conversion factor:

$$P_T = 350 * Kf \quad (3-28)$$

The turbine speed is needed to determine the torque:

$$W_T = 6000 \text{ rpm} \quad (3-29)$$

Again, the angular speed of the turbine is converted to Hz with a conversion factor:

$$W_T = 6000 * Kh \tag{3-30}$$

The Torque produced on the gas turbine shaft is:

$$T_T = P_T/W_T = \left(\frac{350}{6000}\right) * \left(\frac{Kf}{Kh}\right) \tag{3-31}$$

The Gear Ratio between Gear 3 and Gear 1 determines the torque transmitted to the Main Rotor Shaft, T_1 .

The Gear Ratio between Gear 3 and 1 is:

$$GR_1 = \frac{N_3}{N_1} \tag{3-32}$$

Where N_3 and N_1 are the number of teeth of gear 3 and gear 1 respectively.

Finally, the torque on Main Rotor Shaft is:

$$T_1 = \left(\frac{350}{6000}\right) * \left(\frac{Kf}{Kh}\right) * \left(\frac{N_3}{N_1}\right) \tag{3-33}$$

The Block Diagram can be drawn be as the following:

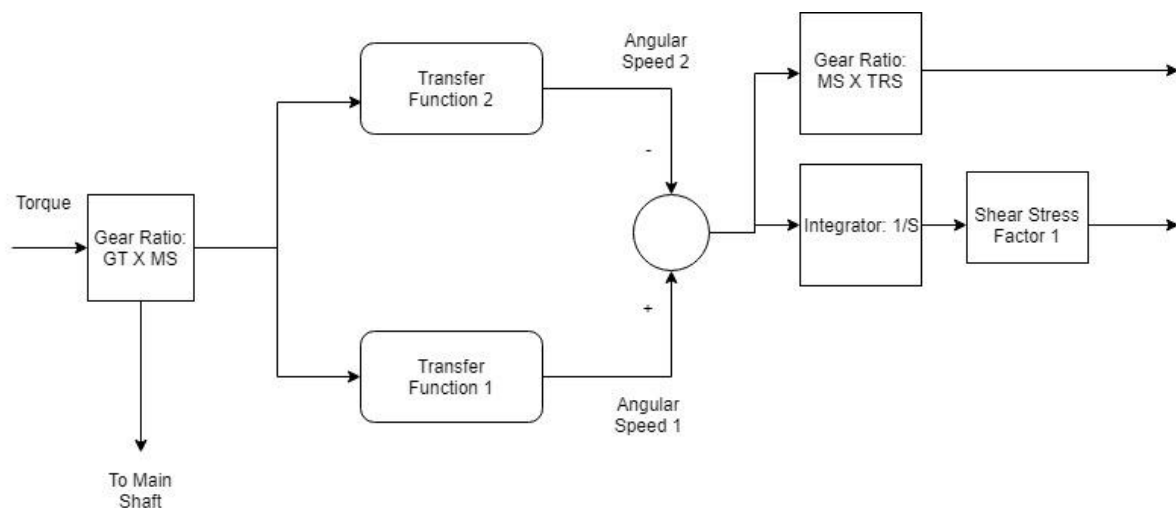


Figure 10: Block Diagram of Lumped Model on Main Rotor Shaft

Equations of Transfer functions used in SIMULINK and MATLAB can be found in the

Appendix I.

On the Main Shaft, the analysis is very similar to the Main Rotor Shaft with the exception of the inertia. Instead of two gears at two ends, it is one gear at one end and blades + Hub on the other end.

The equation of the Main Shaft becomes:

$$[W_4(s), W_{B1}(s)] \quad (3-34)$$

$$= \left(\frac{1}{\Delta(s)} \right) * [J_{B1}S^2 + C_{B1}S + K_2 - K_2, -K_2 J_4 S^2 + C_4 S + K_2] [T_4(s), 0]$$

$$J_4 = \pi * \rho * H * \left(\frac{1}{32} \right) * ((D_2^4) - (D_1^4)) \quad (3-35)$$

Where ρ , is the density of the material the gear is made of (Steel, in $\frac{Kg}{m^3}$), and H is the height of the gear cross section or the Depth (in m).

The same way, J_{MS} is calculated.

$$J_{B1} = J_B + J_H \quad (3-36)$$

J_{B1} is the combined Polar mass moment of inertia (Kgm^2) of the blades and the hub.

To assume the inertia of the blades, the blades are assumed to be long and thin rods.

J_B is the Polar mass moment of inertia (Kgm^2) of the blades and is equal to:

$$J_B = N_B * \pi * \rho * L * \left(\frac{1}{32} \right) * (D_1^4) \quad (3-37)$$

N_B is the number of blades

D is the density of the blades (Aluminum Alloy, in $\frac{Kg}{m^3}$)

L is the length of the blades (in m)

D_1 is the diameter of the blades (assumed as rods, in m)

The hub is then calculated to be:

$$J_H = \pi * \rho * L * \left(\frac{1}{32}\right) * (D^4) \quad (3-38)$$

In which the variables represent the same characteristics but for the hub.

C , the damping, is assumed from practice (in N/m)

K_2 , the stiffness of the shaft is calculated from:

$$K_2 = \frac{G * J}{\rho * (L^2)} \quad (3-39)$$

T_4 , is the torque at the Main Shaft and is equal to:

$$T_4 = \left(\frac{350}{6000}\right) * \left(\frac{Kf}{Kh}\right) * \left(\frac{N_3}{N_1}\right) * \left(\frac{N_6}{N_4}\right) \quad (3-40)$$

The Block Diagram is as the following:

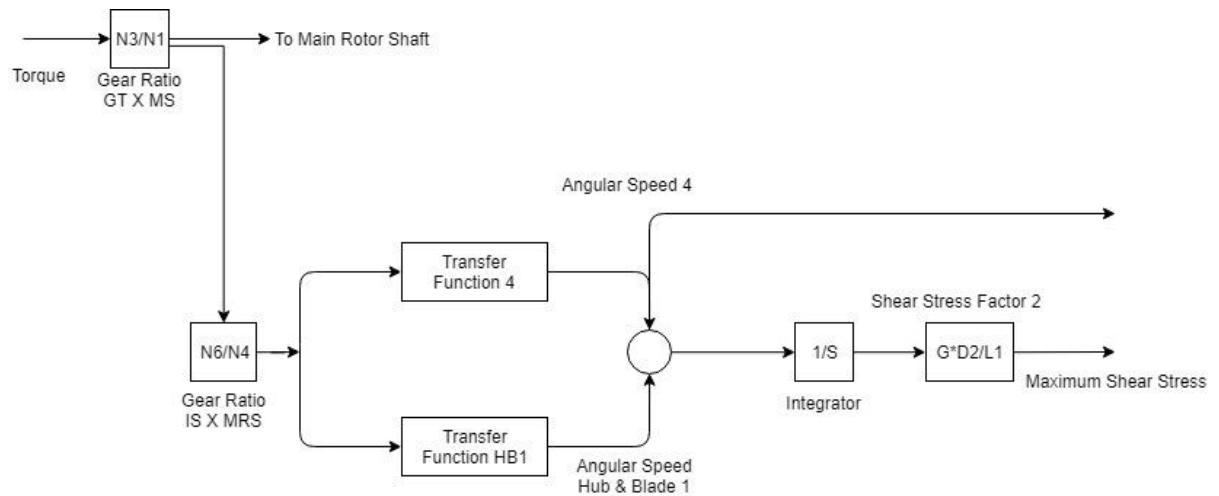


Figure 11: Block Diagram of Main Shaft

Equations of Transfer functions used in SIMULINK and MATLAB can be found in the

Appendix I.

3.3 Finite Elements Model

The next method for comparison is the Finite Element Method. The shaft is assumed to be continuous small shafts packed together into one. The smaller shafts are called finite elements. The number of finite elements is dependent on the designer; keep in mind that the higher the number of elements, the more complicated the system becomes. For the current design, the number of finite elements used is 5.

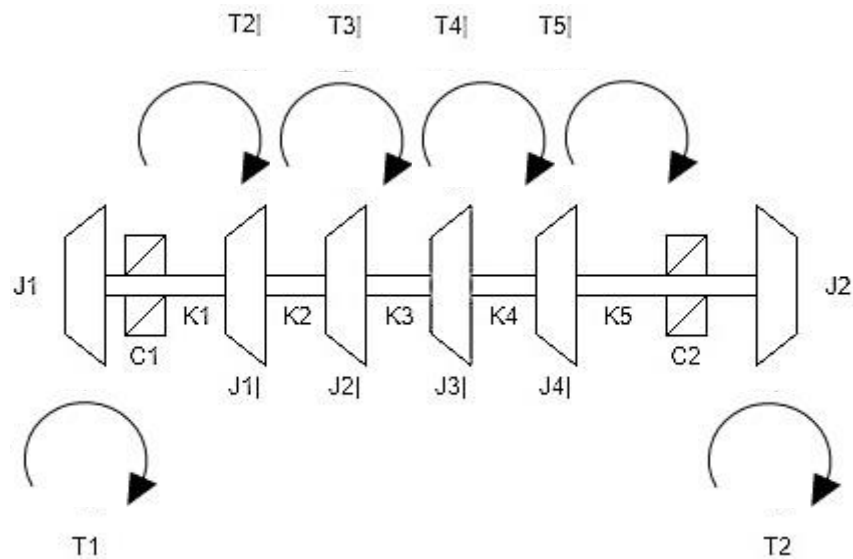


Figure 12: Finite Element Model on Main Rotor Shaft

By assuming the applied torque is applied on different sections of the shaft, the equations that represent the system can be given by:

$$T_1 = J_1\theta_1'' + c_1\theta_1' + k_1(\theta_1 - \theta_1|) \quad (3-41)$$

$$T_2| = J_1|\theta_1|'' + k_1(\theta_1| - \theta_1) + k_2(\theta_1| - \theta_2|) \quad (3-41)$$

$$T_3| = J_2|\theta_2|'' + k_2(\theta_2| - \theta_1|) + k_3(\theta_2| - \theta_3|) \quad (3-42)$$

$$T_4| = J_3|\theta_3|'' + k_3(\theta_3| - \theta_2|) + k_4(\theta_3| - \theta_4|) \quad (3-34)$$

$$T_5| = J_4|\theta_4|'' + k_4(\theta_4| - \theta_3|) + k_5(\theta_4| - \theta_2) \quad (3-44)$$

$$T_6| = J_2\theta_2'' + c_2\theta_2' + k_5(\theta_2 - \theta_4|) \quad (3-45)$$

Since the torque is coming from the gas turbine only:

$$T_2| = T_3| = T_4| = T_5| = T_6| = 0 \quad (3-46)$$

The finite elements are assumed to be equal:

The polar moment of inertia of the elements is:

$$J_1 = J_2 = J_3 = J_4 = J \quad (3-47)$$

Where the inertia of the 5 elements is equal to:

$$J = \frac{J_{MRS}}{5} \quad (3-48)$$

The stiffness of the shaft between each element is represented in the model, making the combined stiffness to be:

$$K = k_1 + k_2 + k_3 + k_4 + k_5 \quad (3-9)$$

The stiffness between each element is also assumed to be equal:

$$k_1 = k_2 = k_3 = k_4 = k_5 = k \quad (3-10)$$

The total stiffness of the shaft increases, and is equal to:

$$K = 5 * k \quad (3-11)$$

On the other hand the length between each element is:

$$L_i = \frac{L}{5} \quad (3-12)$$

Taking the Laplace transform of the equations:

$$T_1(s) = J_1(S^2)\theta_1(s) + c_1(S)\theta_1(s) + k_1(\theta_1(s) - \theta_1|_1(s)) \quad (3-13)$$

$$0 = J_1|(S^2)\theta_1|_1(s) + k_1(\theta_1|_1(s) - \theta_1(s)) + k_2(\theta_1|_1(s) - \theta_2|_1(s)) \quad (3-14)$$

$$0 = J_2|(S^2)\theta_2|_1(s) + k_2(\theta_2|_1(s) - \theta_1|_1(s)) + k_3(\theta_2|_1(s) - \theta_3|_1(s)) \quad (3-15)$$

$$0 = J_3|(S^2)\theta_3|_1(s) + k_3(\theta_3|_1(s) - \theta_2|_1(s)) + k_4(\theta_3|_1(s) - \theta_4|_1(s)) \quad (3-16)$$

$$0 = J_4|(S^2)\theta_4|_1(s) + k_4(\theta_4|_1(s) - \theta_3|_1(s)) + k_5(\theta_4|_1(s) - \theta_2(s)) \quad (3-17)$$

$$0 = J_2(S^2)\theta_2(s) + c_2(S)\theta_2(s) + k_5(\theta_2(s) - \theta_4|_1(s)) \quad (3-18)$$

These 6 equations represent the mechanics of the Main Rotor Shaft Taking the matrix from of the equations, (Whalley, Ebrahimi and Jamil, 2005):

$$\begin{aligned} [T_1(s), 0, 0, 0, 0, 0] & \quad (3-19) \\ & = [J(S^2) + C(S) + K] \\ & * [\theta_1(s), \theta_1|_1(s), \theta_2|_1(s), \theta_3|_1(s), \theta_4|_1(s), \theta_2(s)] \end{aligned}$$

Since $S * \theta(s) = W(S)$, the $[J(S^2) + C(S) + K]$ is just multiplied by S , in which $Delta(S)$ will be of 1 lower power.

This does not change the equation:

$$[T_1(s), 0, 0, 0, 0, 0] \quad (3-20)$$

$$= [J(S^2) + C(S) + K] \\ * [W_1(s), W_1|(s), W_2|(s), W_3|(s), W_4|(s), W_2(s)]$$

The angular speeds of the finite elements is not to be concerned about, as the main objective is to compare speeds of the ends of the shaft W_1 and W_2 to other models.

Matrix A is again made to be:

$$[A] = [J(S^2) + C(S) + K] \quad (3-21)$$

Where the Polar moment of inertia matrix is equal to:

$$[J] = [J_1 \ 0 \ 0 \ 0 \ 0 \ 0, 0 \ J \ 0 \ 0 \ 0 \ 0, 0 \ 0 \ J \ 0 \ 0 \ 0, 0 \ 0 \ 0 \ J \ 0 \ 0 \ 0, 0 \ 0 \ 0 \ 0 \ J \ 0 \ 0 \ 0 \ 0, 0 \ 0 \ 0 \ 0 \ 0 \ J_2] \quad (3-22)$$

The damping matrix is:

$$[C] \quad (3-23) \\ = [C_1 \ 0 \ 0 \ 0 \ 0 \ 0, 0 \ 0 \ 0 \ 0 \ 0 \ 0, 0 \ 0 \ 0 \ 0 \ 0 \ 0, 0 \ 0 \ 0 \ 0 \ 0 \ 0, 0 \ 0 \ 0 \ 0 \ 0 \ 0, 0 \ 0 \ 0 \ 0 \ 0 \ C_2]$$

The stiffness is matrix is:

$$[K] = [k \ -k \ 0 \ 0 \ 0 \ 0, -k \ 2k \ -k \ 0 \ 0 \ 0, 0 \ -k \ 2k \ -k \ 0 \ 0, 0 \ 0 \ -k \ 2k \ - \\ k \ 0, 0 \ 0 \ 0 \ -k \ 2k \ -k, 0 \ 0 \ 0 \ 0 \ -k \ k] \quad (3-24)$$

The equation of the model now becomes:

$$[W_1(s), W_1|(s), W_2|(s), W_3|(s), W_4|(s), W_2(s)] = [A]^{-1} * [T_1(s), 0, 0, 0, 0, 0] \quad (3-25)$$

Where the inverse matrix of A is equal to:

$$[A]^{-1} = \frac{Adj}{Det} \quad (3-26)$$

It is not easy finding the inverse of a 6x6 matrix on paper without computational mistakes; therefore, the use of computational software such as MATLAB is used:

The inverse matrix is way too large to show on paper (or even MATLAB); however, the format of the 6x6 matrix can be shown:

$$\begin{aligned}
 [A]^{-1} & \quad (3-27) \\
 & = 1/(\Delta(s)) \\
 & * [a_{11} \ a_{12} \ a_{13} \ a_{14} \ a_{15} \ a_{16}, a_{21} \ a_{22} \ a_{23} \ a_{24} \ a_{25} \ a_{26}, a_{31} \ a_{32} \ a_{33} \ a_{34} \ a_{35} \ a_{36}, \\
 & \quad a_{41} \ a_{42} \ a_{43} \ a_{44} \ a_{45} \ a_{46}, a_{51} \ a_{52} \ a_{53} \ a_{54} \ a_{55} \ a_{56}, a_{61} \ a_{62} \ a_{63} \ a_{64} \ a_{65} \ a_{66}]
 \end{aligned}$$

Where $\Delta(s) = \det(A)$

Since all elements in vector $T(s)$ is 0 except $T_1(s)$, then the angular speeds of concern are equal to:

$$W_1(s) = \frac{a_{11}}{\Delta(s)} * T_1(s) \quad (3-28)$$

$$W_2(s) = \frac{a_{61}}{\Delta(s)} * T_1(s) \quad (3-29)$$

$$\begin{aligned}
a_{11} = & J_{MRS}^4 * K * S^8 + J_2 * J_{MRS}^4 * S^{10} + C_2 * J_{MRS}^4 * S^9 + 35 * J_{MRS}^3 * K^2 \\
& * S^6 + 40 * J_2 * J_{MRS}^3 * K * S^8 + 40 * C_2 * J_{MRS}^3 * K * S^7 \\
& + 375 * J_{MRS}^2 * K^3 * S^4 + 525 * J_2 * J_{MRS}^2 * K^2 * S^6 + 525 \\
& * C_2 * J_{MRS}^2 * K^2 * S^5 + 1250 * J_{MRS} * K^4 * S^2 + 2500 * J_2 \\
& * J_{MRS} * K^3 * S^4 + 2500 * C_2 * J_{MRS} * K^3 * S^3 + 625 * K^5 \\
& + 3125 * J_2 * K^4 * S^2 + 3125 * C_2 * K^4 * S
\end{aligned} \tag{3-30}$$

As expected the values of the terms are long and in terms of high powers (power 10), these values can be rearranged in MATLAB in the form of matrix Y, where each term of matrix Y represent the co-efficient of S. Matrix Y is represented by:

$$a_{11} = [Y] = [Y_{10} Y_9 Y_8 Y_7 Y_6 Y_5 Y_4 Y_3 Y_2 Y_1 Y_0] \tag{3-31}$$

Where the values of Y equal to:

$$Y_0 = (K^5) \tag{3-32}$$

$$Y_1 = (5 * (K^4) * C_2) \tag{3-33}$$

$$Y_2 = (5 * (K^4) * J_2) + (10 * (K^4) * J) \tag{3-34}$$

$$Y_3 = (20 * (K^3) * J * C_2) \tag{3-35}$$

$$Y_4 = (15 * (K^3) * (J^2)) + (20 * (K^3) * J * J_2) \tag{3-36}$$

$$Y_5 = (21 * (K^2) * (J^2) * C_2) \tag{3-37}$$

$$Y_6 = (7 * (J^3) * (K^2)) + (21 * (K^2) * (J^2) * J_2) \tag{3-38}$$

$$Y_7 = (8 * K * (J^3) * C_2) \tag{3-39}$$

$$Y_8 = (8 * K * (J^3) * J_2) + (K * (J^4)) \tag{3-40}$$

$$Y_9 = ((J^4) * C_2) \tag{3-41}$$

$$Y_{10} = (J^4) * J_2 \tag{3-42}$$

$$a_{61} = K^5 \tag{3-43}$$

In terms of matrix Y:

$$a_{61} = [Y_0] \tag{3-44}$$

$$\begin{aligned}
\Delta(s) = & (625 * J_1 * K^5 * S^2 + 625 * J_2 * K^5 * S^2 + 500 * J_{MRS} * K^5 * S^2 & (3-45) \\
& + 250 * J_{MRS}^2 * K^4 * S^4 + 30 * J_{MRS}^3 * K^3 * S^6 + J_{MRS}^4 * K^2 \\
& * S^8 + 625 * C_1 * K^5 * S + 625 * C_2 * K^5 * S + C_1 * C_2 \\
& * J_{MRS}^4 * S^{10} + 3125 * C_1 * C_2 * K^4 * S^2 + C_1 * J_2 * J_{MRS}^4 \\
& * S^{11} + C_2 * J_1 * J_{MRS}^4 * S^{11} + 3125 * C_1 * J_2 * K^4 * S^3 \\
& + 3125 * C_2 * J_1 * K^4 * S^3 + 1250 * C_1 * J_{MRS} * K^4 * S^3 \\
& + 1250 * C_2 * J_{MRS} * K^4 * S^3 + C_1 * J_{MRS}^4 * K * S^9 + C_2 \\
& * J_{MRS}^4 * K * S^9 + J_1 * J_2 * J_{MRS}^4 * S^{12} + 3125 * J_1 * J_2 * K^4 \\
& * S^4 + 1250 * J_1 * J_{MRS} * K^4 * S^4 + 1250 * J_2 * J_{MRS} * K^4 \\
& * S^4 + J_1 * J_{MRS}^4 * K * S^{10} + J_2 * J_{MRS}^4 * K * S^{10} + 375 * C_1 \\
& * J_{MRS}^2 * K^3 * S^5 + 375 * C_2 * J_{MRS}^2 * K^3 * S^5 + 35 * C_1 * J_{MRS}^3 \\
& * K^2 * S^7 + 35 * C_2 * J_{MRS}^3 * K^2 * S^7 + 375 * J_1 * J_{MRS}^2 * K^3 \\
& * S^6 + 375 * J_2 * J_{MRS}^2 * K^3 * S^6 + 35 * J_1 * J_{MRS}^3 * K^2 * S^8 \\
& + 35 * J_2 * J_{MRS}^3 * K^2 * S^8 + 2500 * C_1 * C_2 * J_{MRS} * K^3 * S^4 \\
& + 40 * C_1 * C_2 * J_{MRS}^3 * K * S^8 + 2500 * C_1 * J_2 * J_{MRS} * K^3 \\
& * S^5 + 2500 * C_2 * J_1 * J_{MRS} * K^3 * S^5 + 40 * C_1 * J_2 * J_{MRS}^3 \\
& * K * S^9 + 40 * C_2 * J_1 * J_{MRS}^3 * K * S^9 + 2500 * J_1 * J_2 * J_{MRS} \\
& * K^3 * S^6 + 40 * J_1 * J_2 * J_{MRS}^3 * K * S^{10} + 525 * C_1 * C_2 \\
& * J_{MRS}^2 * K^2 * S^6 + 525 * C_1 * J_2 * J_{MRS}^2 * K^2 * S^7 + 525 * C_2 \\
& * J_1 * J_{MRS}^2 * K^2 * S^7 + 525 * J_1 * J_2 * J_{MRS}^2 * K^2 * S^8)
\end{aligned}$$

$\Delta(s)$ can also be written in matrix form in MATLAB. Matrix [X] is used to describe it and is equal to:

$$\Delta(s) = [X] = [X_{11} X_{10} X_9 X_8 X_7 X_6 X_5 X_4 X_3 X_2 X_1 X_0] \quad (3-46)$$

Where the values of X are equal to:

$$X_0 = ((K^5) * C_1) + ((K^5) * C_2) \quad (3-47)$$

$$X_1 = ((K^5) * J_2) + (4 * (K^5) * J) + ((K^5) * J_1) + (5 * (K^4) * C_1 * C_2) \quad (3-48)$$

$$X_2 = (5 * (K^4) * C_1 * J_2) + (10 * (K^4) * J * C_2) + (5 * (K^4) * J_1 * C_2) \quad (3-49)$$

$$+ (10 * (K^4) * C_1 * J)$$

$$X_3 = (5 * (K^4) * J_1 * J_2) + (20 * (K^3) * C_1 * J * C_2) + (10 * (K^4) * J_1 * J) \quad (3-50)$$

$$+ (10 * (J^2) * (K^4)) + (10 * (K^4) * J * J_2)$$

$$X_4 = (15 * (K^3) * C_1 * (J^2)) + (15 * (K^3) * (J^2) * C_2) + (20 * (K^3) * C_1 \quad (3-51)$$

$$* J * J_2) + (20 * (K^3) * J_1 * J * C_2)$$

$$X_5 = (15 * (K^3) * (J^2) * J_2) + (20 * (K^3) * J_1 * J * J_2) + (6 * (J^3) * (K^3)) \quad (3-52)$$

$$+ (15 * (K^3) * J_1 * (J^2)) + (21 * (K^2) * C_1 * (J^2) * C_2)$$

$$X_6 = (21 * (K^2) * J_1 * (J^2) * C_2) + (7 * C_1 * (J^3) * (K^2)) + (21 * (K^2) \quad (3-53)$$

$$* C_1 * (J^2) * J_2) + (7 * (K^2) * (J^3) * C_2);$$

$$X_7 = (7 * J_1 * (J^3) * (K^2)) + (21 * (K^2) * J_1 * (J^2) * J_2) + ((K^2) * (J^4)) \quad (3-54)$$

$$+ (8 * K * C_1 * (J^3) * C_2) + (7 * (K^2) * (J^3) * J_2)$$

$$X_8 = (K * C_1 * (J^4)) + (8 * K * C_1 * (J^3) * J_2) + (8 * K * J_1 * (J^3) * C_2) \quad (3-55)$$

$$+ (K * (J^4) * C_2)$$

$$X_9 = (K * (J^4) * J_2) + (8 * K * J_1 * (J^3) * J_2) + (K * J_1 * (J^4)) + (C_1 \quad (3-56)$$

$$* (J^4) * C_2)$$

$$X_{10} = (C_1 * (J^4) * J_2) + (J_1 * (J^4) * C_2) \quad (3-57)$$

$$X_{11} = (J_1 * (J^4) * J_2) \quad (3-58)$$

This answer is already divided by S since $W(s) = s * \theta(s)$

The Block Diagram is represented by:

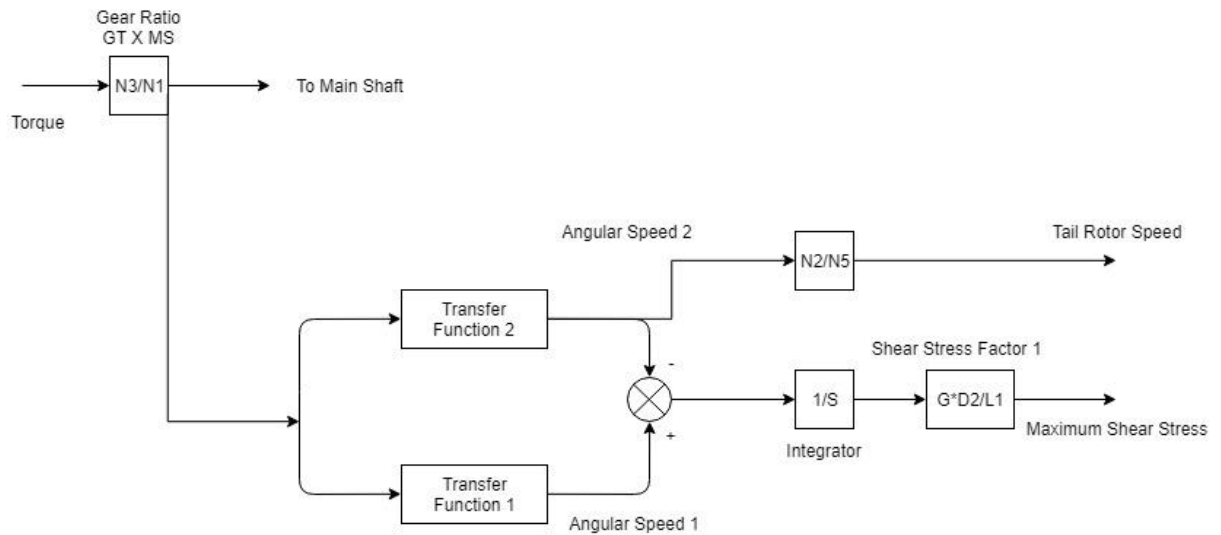


Figure 13: Block Diagram of the Finite Element Model on Main Rotor Shaft

Equations of Transfer functions used in SIMULINK and MATLAB can be found in the

Appendix I.

The same procedure is repeated for the Main Shaft, the equation is represented by:

$$\begin{aligned}
 [T_1(s), 0, 0, 0, 0, 0] & \quad (3-59) \\
 & = [J(S^2) + C(S) + K] \\
 & * [\theta_4(s), \theta_1(s), \theta_2(s), \theta_3(s), \theta_4(s), \theta_{B1}(s)]
 \end{aligned}$$

The difference in the equation variables will be:

T_1 will be multiplied by another gear ratio, GR_3 to adjust the torque converted to the Main Shaft from gear 6 and gear 4.

Matrix A is again made to be:

$$[A] = [J(S^2) + C(S) + K] \quad (3-60)$$

Where the Polar moment of inertia matrix is equal to:

$$[J] = [J_4 \ 0 \ 0 \ 0 \ 0 \ 0, 0 \ J \ 0 \ 0 \ 0 \ 0, 0 \ 0 \ J \ 0 \ 0 \ 0, 0 \ 0 \ 0 \ J \ 0 \ 0, 0 \ 0 \ 0 \ 0 \ J \ 0, 0 \ 0 \ 0 \ 0 \ 0 \ J_{B1}] \quad (3-61)$$

The damping matrix is:

$$\begin{aligned}
 [C] & \quad (3-62) \\
 & = [C_4 \ 0 \ 0 \ 0 \ 0 \ 0, 0 \ 0 \ 0 \ 0 \ 0 \ 0, 0 \ 0 \ 0 \ 0 \ 0 \ 0, 0 \ 0 \ 0 \ 0 \ 0 \ 0, 0 \ 0 \ 0 \ 0 \ 0 \ 0, 0 \ 0 \ 0 \ 0 \ 0 \ C_{B1}]
 \end{aligned}$$

The stiffness matrix is:

$$\begin{aligned}
 [K] & = [k \ -k \ 0 \ 0 \ 0 \ 0, -k \ 2k \ -k \ 0 \ 0 \ 0, 0 \ -k \ 2k \ -k \ 0 \ 0, 0 \ 0 \ -k \ 2k \\
 & \quad -k \ 0, 0 \ 0 \ 0 \ -k \ 2k \ -k, 0 \ 0 \ 0 \ 0 \ -k \ k] \quad (3-63)
 \end{aligned}$$

The values inside the matrixes are:

$$J = J_{MS}/5 \quad (3-64)$$

$K = 5 * k$ (stiffness value used will be of the Main Shaft)

The equation of the model now becomes:

$$\begin{aligned} [W_4(s), W_1(s), W_2(s), W_3(s), W_4(s), W_{B1}(s)] \\ = [A]^{-1} * [T_1(s), 0, 0, 0, 0, 0] \end{aligned} \quad (3-65)$$

Again, the inverse matrix of A is equal to:

$$[A]^{-1} = \frac{Adj}{Det} \quad (3-66)$$

The 6x6 matrix is represented in MATLAB, in order to get the inverse, and the elements of the inverse are:

$$\begin{aligned} [A]^{-1} \\ = \frac{1}{\Delta(s)} \end{aligned} \quad (3-67)$$

$$\begin{aligned} * [a_{11} \ a_{12} \ a_{13} \ a_{14} \ a_{15} \ a_{16}, a_{21} \ a_{22} \ a_{23} \ a_{24} \ a_{25} \ a_{26}, a_{31} \ a_{32} \ a_{33} \ a_{34} \ a_{35} \ a_{36}, \\ a_{41} \ a_{42} \ a_{43} \ a_{44} \ a_{45} \ a_{46}, a_{51} \ a_{52} \ a_{53} \ a_{54} \ a_{55} \ a_{56}, a_{61} \ a_{62} \ a_{63} \ a_{64} \ a_{65} \ a_{66}] \end{aligned}$$

Where $\Delta(s) = det(A)$

Again, all elements in vector $T(s)$ is 0 except $T_1(s)$, then the angular speeds of concern are equal to:

$$W_1(s) = \frac{a_{11}}{\Delta(s)} * T_1(s) \quad (3-68)$$

$$W_2(s) = \frac{a_{61}}{\Delta(s)} * T_1(s) \quad (3-69)$$

$$\begin{aligned}
A_{11} = & J_{MS}^4 * K * S^8 + J_{B1} * J_{MS}^4 * S^{10} + C_{B1} * J_{MS}^4 * S^9 + 35 * J_{MS}^3 * K^2 \\
& * S^6 + 40 * J_{B1} * J_{MS}^3 * K * S^8 + 40 * C_{B1} * J_{MS}^3 * K * S^7 \\
& + 375 * J_{MS}^2 * K^3 * S^4 + 525 * J_{B1} * J_{MS}^2 * K^2 * S^6 + 525 \\
& * C_{B1} * J_{MS}^2 * K^2 * S^5 + 1250 * J_{MS} * K^4 * S^2 + 2500 * J_{B1} \\
& * J_{MS} * K^3 * S^4 + 2500 * C_{B1} * J_{MS} * K^3 * S^3 + 625 * K^5 \\
& + 3125 * J_{B1} * K^4 * S^2 + 3125 * C_{B1} * K^4 * S
\end{aligned} \tag{3-70}$$

$$A_{61} = K^5 \tag{3-71}$$

The values can be represented in a more proper fashion and rearranged as of descending powers of S, in MATLAB this is done by writing it in form of a matrix [W]

$$A_{11} = [W] = [W_{10} \ W_9 \ W_8 \ W_7 \ W_6 \ W_5 \ W_4 \ W_3 \ W_2 \ W_1 \ W_0] \tag{3-72}$$

Where the values of W are:

$$W_0 = (K^5) \tag{3-73}$$

$$W_1 = (5 * (K^4) * C_{B1}) \tag{3-74}$$

$$W_2 = (5 * (K^4) * J_{B1}) + (10 * (K^4) * J) \tag{3-75}$$

$$W_3 = (20 * (K^3) * J * C_{B1}) \tag{3-76}$$

$$W_4 = (15 * (K^3) * (J^2)) + (20 * (K^3) * J * J_{B1}) \tag{3-77}$$

$$W_5 = (21 * (K^2) * (J^2) * C_{B1}) \tag{3-78}$$

$$W_6 = (7 * (J^3) * (K^2)) + (21 * (K^2) * (J^2) * J_{B1}) \tag{3-79}$$

$$W_7 = (8 * K * (J^3) * C_{B1}) \tag{3-80}$$

$$W_8 = (8 * K * (J^3) * J_{B1}) + (K * (J^4)) \tag{3-81}$$

$$W_9 = (J^4) * C_{B1} \tag{3-82}$$

$$W_{10} = (J^4) * J_{B1} \tag{3-83}$$

$$A_{61} = [W_0] \tag{3-84}$$

$\Delta(s)$ is also found to be:

$$\begin{aligned}
\Delta(s) = & 625 * J_4 * K^5 * S^2 + 500 * J_{MS} * K^5 * S^2 + 625 * J_{B1} * K^5 * S^2 & (3-85) \\
& + 250 * J_{MS}^2 * K^4 * S^4 + 30 * J_{MS}^3 * K^3 * S^6 + J_{MS}^4 * K^2 * S^8 \\
& + 625 * C_4 * K^5 * S + 625 * C_{B1} * K^5 * S + C_4 * C_{B1} * J_{MS}^4 \\
& * S^{10} + 3125 * C_4 * C_{B1} * K^4 * S^2 + C_4 * J_{MS}^4 * J_{B1} * S^{11} \\
& + C_{B1} * J_4 * J_{MS}^4 * S^{11} + 1250 * C_4 * J_{MS} * K^4 * S^3 + C_4 * J_{MS}^4 \\
& * K * S^9 + 3125 * C_4 * J_{B1} * K^4 * S^3 + 3125 * C_{B1} * J_4 * K^4 \\
& * S^3 + 1250 * C_{B1} * J_{MS} * K^4 * S^3 + C_{B1} * J_{MS}^4 * K * S^9 + J_4 \\
& * J_{MS}^4 * J_{B1} * S^{12} + 1250 * J_4 * J_{MS} * K^4 * S^4 + J_4 * J_{MS}^4 * K \\
& * S^{10} + 3125 * J_4 * J_{B1} * K^4 * S^4 + 1250 * J_{MS} * J_{B1} * K^4 \\
& * S^4 + J_{MS}^4 * J_{B1} * K * S^{10} + 375 * C_4 * J_{MS}^2 * K^3 * S^5 + 35 \\
& * C_4 * J_{MS}^3 * K^2 * S^7 + 375 * C_{B1} * J_{MS}^2 * K^3 * S^5 + 35 * C_{B1} \\
& * J_{MS}^3 * K^2 * S^7 + 375 * J_4 * J_{MS}^2 * K^3 * S^6 + 35 * J_4 * J_{MS}^3 \\
& * K^2 * S^8 + 375 * J_{MS}^2 * J_{B1} * K^3 * S^6 + 35 * J_{MS}^3 * J_{B1} * K^2 \\
& * S^8 + 2500 * C_4 * C_{B1} * J_{MS} * K^3 * S^4 + 40 * C_4 * C_{B1} * J_{MS}^3 \\
& * K * S^8 + 2500 * C_4 * J_{MS} * J_{B1} * K^3 * S^5 + 2500 * C_{B1} * J_4 \\
& * J_{MS} * K^3 * S^5 + 40 * C_4 * J_{MS}^3 * J_{B1} * K * S^9 + 40 * C_{B1} * J_4 \\
& * J_{MS}^3 * K * S^9 + 2500 * J_4 * J_{MS} * J_{B1} * K^3 * S^6 + 40 * J_4 \\
& * J_{MS}^3 * J_{B1} * K * S^{10} + 525 * C_4 * C_{B1} * J_{MS}^2 * K^2 * S^6 + 525 \\
& * C_4 * J_{MS}^2 * J_{B1} * K^2 * S^7 + 525 * C_{B1} * J_4 * J_{MS}^2 * K^2 * S^7 \\
& + 525 * J_4 * J_{MS}^2 * J_{B1} * K^2 * S^8
\end{aligned}$$

$\Delta(s)$ is also represented by a matrix in MATLAB, the matrix of [V]:

$$\Delta(s) = [V] = [V_{11} \ V_{10} \ V_9 \ V_8 \ V_7 \ V_6 \ V_5 \ V_4 \ V_3 \ V_2 \ V_1 \ V_0] \quad (3-86)$$

Where the values of matrix V are:

$$V_0 = ((K^5) * C_4) + ((K^5) * C_{B1}) \quad (3-87)$$

$$V_1 = ((K^5) * J_{B1}) + (4 * (K^5) * J) + ((K^5) * J_4) + (5 * (K^4) * C_4 * C_{B1}) \quad (3-88)$$

$$V_2 = (5 * (K^4) * C_4 * J_{B1}) + (10 * (K^4) * J * C_{B1}) + (5 * (K^4) * J_4 * C_{B1}) \quad (3-89)$$

$$+ (10 * (K^4) * C_4 * J)$$

$$V_3 = (5 * (K^4) * J_4 * J_{B1}) + (20 * (K^3) * C_4 * J * C_{B1}) + (10 * (K^4) * J_4 \quad (3-90)$$

$$* J) + (10 * (J^2) * (K^4)) + (10 * (K^4) * J * J_{B1})$$

$$V_4 = (15 * (K^3) * C_4 * (J^2)) + (15 * (K^3) * (J^2) * C_{B1}) + (20 * (K^3) * C_4 \quad (3-91)$$

$$* J * J_{B1}) + (20 * (K^3) * J_4 * J * C_{B1})$$

$$V_5 = (15 * (K^3) * (J^2) * J_{B1}) + (20 * (K^3) * J_4 * J * J_{B1}) + (6 * (J^3) \quad (3-92)$$

$$* (K^3)) + (15 * (K^3) * J_4 * (J^2)) + (21 * (K^2) * C_4 * (J^2)$$

$$* C_{B1})$$

$$V_6 = (21 * (K^2) * J_4 * (J^2) * C_{B1}) + (7 * C_4 * (J^3) * (K^2)) + (21 * (K^2) \quad (3-93)$$

$$* C_4 * (J^2) * J_{B1}) + (7 * (K^2) * (J^3) * C_{B1})$$

$$V_7 = (7 * J_4 * (J^3) * (K^2)) + (21 * (K^2) * J_4 * (J^2) * J_{B1}) + ((K^2) * (J^4)) \quad (3-94)$$

$$+ (8 * K * C_4 * (J^3) * C_{B1}) + (7 * (K^2) * (J^3) * J_{B1})$$

$$V_8 = (K * C_4 * (J^4)) + (8 * K * C_4 * (J^3) * J_{B1}) + (8 * K * J_4 * (J^3) * C_{B1}) \quad (3-95)$$

$$+ (K * (J^4) * C_{B1})$$

$$V_9 = (K * (J^4) * J_{B1}) + (8 * K * J_4 * (J^3) * J_{B1}) + (K * J_4 * (J^4)) + (C_4 \quad (3-96)$$

$$* (J^4) * C_{B1})$$

$$V_{10} = (C_4 * (J^4) * J_{B1}) + (J_4 * (J^4) * C_{B1}) \quad (3-97)$$

$$V_{11} = (J_4 * (J^4) * J_{B1}) \quad (3-98)$$

This answer is already divided by S since $W(s) = s * \theta(s)$

The Block Diagram representation is:

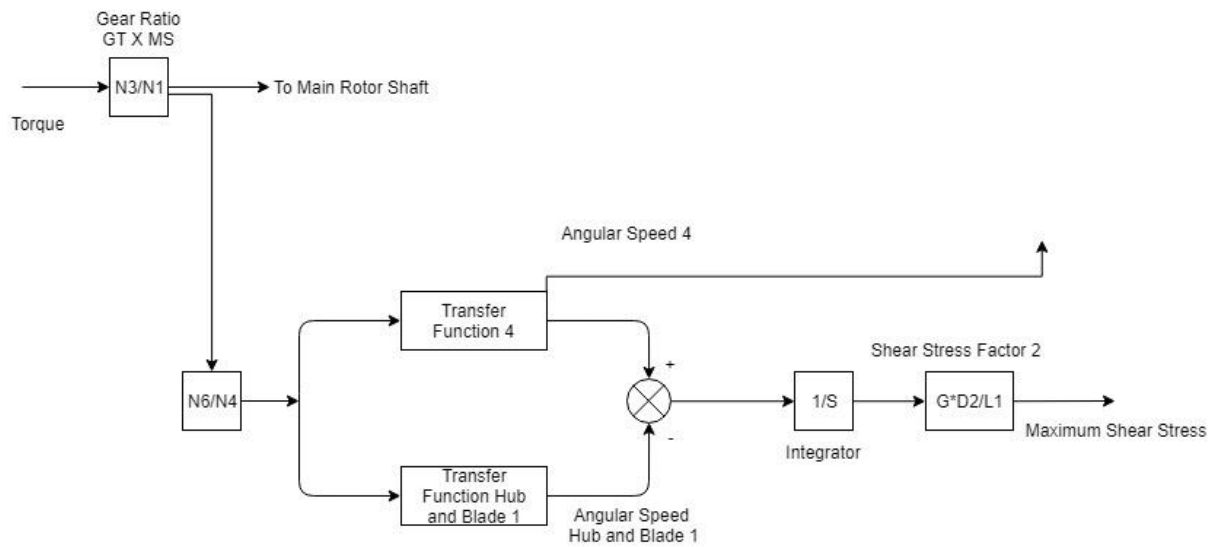


Figure 14: The Block Diagram of the Finite Element Model on Main Shaft

Equations of Transfer functions used in SIMULINK and MATLAB can be found in the

Appendix I.

3.4 Hybrid (Distributed-Lumped) Model

This method considers the shaft as distributed model while the gears and bearings to be lumped; thus the name: Hybrid analysis model. The shaft properties, namely the polar moment of inertia and stiffness, will be a function of the shaft's dimensions, mainly the length.

The Main Rotor Shaft is modeled as:

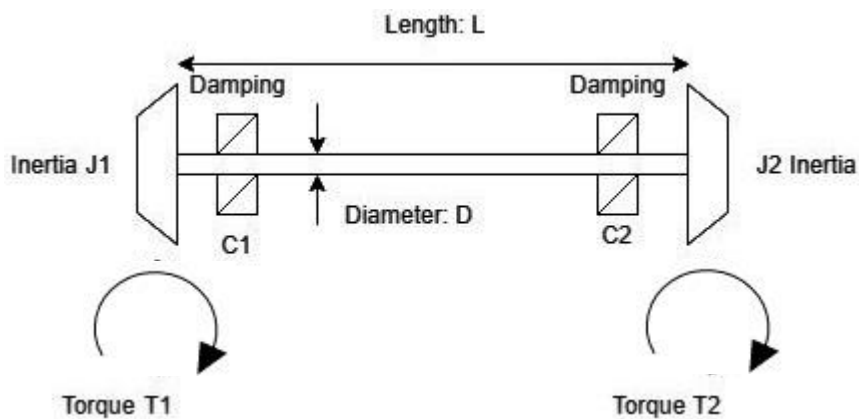


Figure 15: Hybrid Model Main Rotor Shaft Labeled

Normally, when the shaft is considered as a lumped model, it is modeled with the idea of solving ordinary differential equations. However, as used in long transmission lines, the dynamics of the long transmission lines is represented by a series of inductors and capacitors along the length of the line. These representations are realized using partial differential equations:

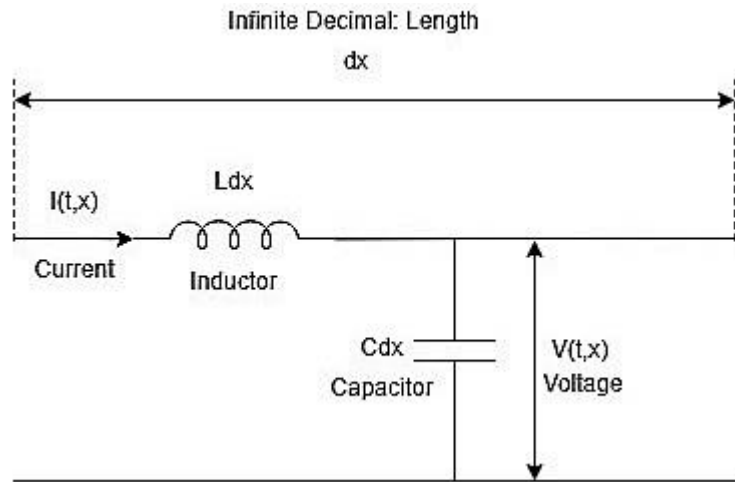


Figure 16: Transmission Line Representation (Whalley, Ebrahimi, Jamil, 2005)

The equations of inductor and capacitor can be represented by ordinary differential equations:

$$V = -L * \frac{di}{dt} \quad (3-140)$$

$$I = -C * \frac{dv}{dt} \quad (3-141)$$

These ordinary differential equations become partial differential equations when the length of the line dx varies:

$$\frac{dV(t,x)}{dx} = - \frac{Ldi(t,x)}{dt} \quad (3-142)$$

$$\frac{dI(t,x)}{dx} = - \frac{Cdv(t,x)}{dt} \quad (3-143)$$

This is in a long transmission line, or in other words, a circuit. In a mechanical shaft, the driving force (Voltage) is the torque, and the charge movement (Current) is the angular speed.

The partial differential equations become:

$$\frac{dT(t, x)}{dx} = -\frac{Ldw(t, x)}{dt} \quad (3-144)$$

$$\frac{dw(t, x)}{dx} = -\frac{CdT(t, x)}{dt} \quad (3-145)$$

Taking the Laplace Transform of these equations:

$$\frac{dT}{dx} = -LwS \quad (3-146)$$

$$\frac{dw}{dx} = -CTS \quad (3-147)$$

[Laplace transform changes only the time domain to frequency domain]

Differentiating both equations with respect to x:

$$\frac{D^2T}{dx^2} = -L * \frac{dw}{dx} * S \quad (3-148)$$

$$\frac{D^2w}{dx^2} = -C * \frac{dT}{dx} * S \quad (3-2)$$

But dw/dx and dT/dx are already known values, substituting them in the equations holds:

$$\frac{D^2T}{dx^2} = LCT * S^2 \quad (3-150)$$

$$\frac{D^2w}{dx^2} = CLw * S^2 \quad (3-151)$$

Suggested solution to the equations above is:

$$P(s) = S * \sqrt{LC} \quad (3-3)$$

This would be called: the propagation function

Applying the propagation function to the partial differential equations; the general solution becomes:

$$T = P_1 * \text{Cosh}[P(s)x] + P_2 * \text{Sinh}[P(s)x] \quad (3-4)$$

$$W = P_3 * \text{Sinh}[P(s)x] + P_4 * \text{Cosh}[P(s)x] \quad (3-53)$$

To find the constants, $P_1 P_2 P_3 P_4$, initial conditions have to be satisfied.

Using the properties of hyperbolic functions:

$$\text{Sinh}(0) = 0 \quad (3-154)$$

$$\text{Cosh}(0) = 1 \quad (3-155)$$

Initial condition $x = 0$

$$T(s = s, x = 0) = P_1 \quad (3-156)$$

$$W(s = s, x = 0) = P_4 \quad (3-157)$$

Differentiating the general solutions:

$$\frac{dT}{dx} = P_1 * P(s) * \text{Sinh}[P(s)x] + P_2 * P(s) * \text{Cosh}[P(s)x] \quad (3-158)$$

$$\frac{dW}{dx} = P_3 * P(s) * \text{Cosh}[P(s)x] + P_4 * P(s) * \text{Sinh}[P(s)x] \quad (3-159)$$

But also:

$$\frac{dT}{dx} = -LwS \quad (3-160)$$

$$\frac{dW}{dx} = -CTS \quad (3-161)$$

Equating both equations:

$$-LwS = P_1 * P(s) * Sinh[P(s)x] + P_2 * P(s) * Cosh[P(s)x] \quad (3-162)$$

$$-CTS = P_3 * P(s) * Cosh[P(s)x] + P_4 * P(s) * Sinh[P(s)x] \quad (3-4-163)$$

Initial condition at $x=0$:

$$-LwS = P_2 * P(s) \quad (3-164)$$

$$-CTS = P_3 * P(s) \quad (3-165)$$

$$P_2 = -L * w * \frac{S}{P(s)} \quad (3-165)$$

$$P_3 = -C * T * \frac{S}{P(s)} \quad (3-166)$$

Where w is $w(s = s, x = 0)$ and T is $T(s = s, x = 0)$

Since $P(s) = S * \sqrt{LC}$

$$P_2 = -L * w(s = s, x = 0) * \frac{S}{S} * \sqrt{LC} \quad (3-167)$$

$$P_2 = -\sqrt{\frac{L}{C}} * w(s = s, x = 0) \quad (3-168)$$

$$P_3 = -C * T(s = ls, x = 0) * \frac{S}{S} * \sqrt{LC} \quad (3-169)$$

$$P_3 = -\sqrt{\frac{C}{L}} * T(s = s, x = 0) \quad (3-170)$$

The term $\sqrt{\frac{L}{C}}$ is defined as the impedance:

$$\zeta = \sqrt{\frac{L}{C}} \quad (3-171)$$

$$\frac{1}{\zeta} = \sqrt{\frac{C}{L}} \quad (3-172)$$

This defines P_2 and P_3 to be:

$$P_2 = -\sqrt{\frac{L}{C}} * w(s = s, x = 0) \quad (3-173)$$

$$P_2 = -\zeta * w(s = s, x = 0) \quad (3-174)$$

$$P_3 = -\sqrt{\frac{C}{L}} * T(s = s, x = 0) \quad (3-175)$$

$$P_3 = -\left(\frac{1}{\zeta}\right) * T(s = s, x = 0) \quad (3-176)$$

The general solution for the partial differential equations becomes:

$$T = T(s = s, x = 0) * \text{Cosh}[P(s)x] - \zeta * w(s = s, x = 0) * \text{Sinh}[P(s)x] \quad (3-177)$$

$$W = -\left(\frac{1}{\zeta}\right) * T(s = s, x = 0) * \text{Sinh}[P(s)x] + W(s = s, x = 0) * \text{Cosh}[P(s)x] \quad (3-178)$$

To write the equation in matrix form:

$$[T] = [A] * [W] \quad (3-179)$$

From W :

$$W = -\left(\frac{1}{\zeta}\right) * T(s = s, x = 0) * Sinh[P(s)x] + W(s = s, x \quad (3-180)$$

$$= 0) * Cosh[P(s)x]$$

$$T(s = s, x = 0) = -\zeta * \left(\frac{1}{Sinh[P(s)x]}\right) * W + \zeta * Coth[P(s)x] * W(s \quad (3-181)$$

$$= s, x = 0)$$

$$Cosech[P(s)x] = 1/Sinh[P(s)x] \quad (3-182)$$

$$T(s = s, x = 0) = -\zeta * Cosech[P(s)x] * W + \zeta * Coth[P(s)x] * W(s \quad (3-183)$$

$$= s, x = 0)$$

Substituting the acquired equation into T :

$$T = [-\zeta * Cosech[P(s)x] * W + \zeta * Coth[P(s)x] * W(s = s, x \quad (3-184)$$

$$= 0)] * Cosh[P(s)x] - \zeta * w(s = s, x = 0) * Sinh[P(s)x]$$

Where:

$$Cosech * Cosh = Coth \quad (3-185)$$

$$Coth * Cosh = \frac{Cosh^2}{Sinh} \quad (3-186)$$

$$\left(\frac{Cosh^2}{Sinh}\right) - Sinh = \frac{Cosh^2 - Sinh^2}{Sinh} = \frac{1}{Sinh} = Cosech \quad (3-187)$$

This implies that:

$$T = -\zeta * Colth[P(s)x] * W + \zeta * W(s = s, x = 0) * Cosech[P(s)x] \quad (3-188)$$

Taking both equations of T and $T(s = s, x = 0)$, putting them in matrix form:

$$[T, T(s = s, x = 0)] \quad (3-189)$$

$$= [-\zeta * Coth[P(s)x] \zeta * Cosech[P(s)x], -\zeta * Cosech[P(s)x] \zeta * Coth[P(s)x]] * [W, W(s = s, x = 0)]$$

Defining the parameters: T and W

$$T = T(s = s, x = L) = T_2 \quad (3-190)$$

$$T(s = s, x = 0) = T_1 \quad (3-191)$$

$$W = W(s = s, x = L) = W_2 \quad (3-192)$$

$$W(s = s, x = 0) = W_1 \quad (3-193)$$

In order to simulate the trigonometric functions, they have to be written in exponential format, this because exponential functions can be simulated as a finite time delay:

$$Coth[P(s)x] = \frac{[e^{2P(s)*L} + 1]}{[e^{2P(s)*L} - 1]} = G(s) \quad (3-194)$$

$$Cosech[P(s)x] = \frac{[2e^{2P(s)*L}]}{[e^{2P(s)*L} - 1]} = H(s) \quad (3-195)$$

Both can be related from the equation:

$$H(s) = \sqrt{G(s)^2 - 1} \quad (3-196)$$

The defining equation becomes:

$$[T_1(s), T_2(s)] = [-\zeta * G(s) \zeta * \sqrt{G(s)^2 - 1}, -\zeta * \sqrt{(G(s)^2 - 1)} \zeta * G(s)] \quad (3-197)$$

$$* [W_1(s), W_2(s)]$$

Since the Gears 1 and 2 are still considered as discrete, the equation becomes:

$$[T_1(s) - J_1 * S * W_1(s) - C_1 * W_1(s), T_2(s) + J_2 * S * W_2(s) + C_2 * \quad (3-198)$$

$$W_2(s)] = [-\zeta * G(s) \zeta * \sqrt{G(s)^2 - 1}, -\zeta * \sqrt{G(s)^2 - 1} \zeta * G(s)] *$$

$$[W_1(s), W_2(s)]$$

T_2 is assumed to be in the opposite direction of T_1 .

This can be separated as:

$$[T_1(s), T_2(s)] - [J_1 * S + C_1 \ 0, 0 \ J_2 * S + C_2] * [W_1(s), W_2(s)] \quad (3-199)$$

And then recombined to:

$$[T_1(s), T_2(s)] = [-\zeta * G(s) + [J_1 * S + C_1] \zeta * \sqrt{G(s)^2 - 1}, -\zeta \quad (3-200)$$

$$* \sqrt{G(s)^2 - 1} \zeta * G(s) + [J_2 * S + C_2]] * [W_1(s), W_2(s)]$$

Defining some terms:

$$T_2(s) = 0 \text{ [Torque only coming from the gas turbine]}$$

$$\gamma_1(s) = J_1 * S + C_1 \text{ [For simplicity]} \quad (3-201)$$

$$\gamma_2(s) = J_2 * S + C_2 \quad (3-202)$$

The Torque equation for the model becomes:

$$[T_1(s), 0] = [-\zeta * G(s) + \gamma_1(s) \zeta * \sqrt{G(s)^2 - 1}, -\zeta * \sqrt{G(s)^2 - 1} \zeta \quad (3-203)$$

$$* G(s) + \gamma_2(s)] * [W_1(s), W_2(s)]$$

The parameters of inductance and capacitance:

$$L = \rho * J_{MRS} \quad (3-204)$$

$$C = \frac{1}{G * J_{MRS}} \quad (3-205)$$

The matrix A becomes:

$$[A] = [-\zeta * G(s) + \gamma_1(s) \zeta * \sqrt{G(s)^2 - 1}, -\zeta * \sqrt{G(s)^2 - 1} \zeta * G(s) + \gamma_2(s)] \quad (3-206)$$

Inverting the torque equation to obtain the angular speeds:

$$[W_1(s), W_2(s)] = [A]^{-1} * [T_1(s), 0] \quad (3-205)$$

The inverse of matrix A is:

$$[A]^{-1} = \frac{Adj(A)}{Det(A)} \quad (3-208)$$

If matrix A is considered as:

$$A = [a \ b, \ c \ d] \quad (3-209)$$

$$Adj(A) = [d - b, -c \ a] \quad (3-210)$$

$$Det(A) = \Delta(s) = |ad - bc| \quad (3-211)$$

Then:

$$Adj(A) = [\zeta * G(s) + \gamma_2(s) - \zeta * \sqrt{G(s)^2 - 1}, \zeta * \sqrt{G(s)^2 - 1} - \zeta * G(s) + \gamma_1(s)] \quad (3-212)$$

$$Det(A) = \zeta * (\gamma_1(s) + \gamma_2(s)) * G(s) + \gamma_1(s) * \gamma_2(s) + \zeta^2 \quad (3-213)$$

The Hybrid Model Equation becomes:

$$[W_1(s), W_2(s)] = \zeta * [\zeta * G(s) + \gamma_2(s) - \zeta * \sqrt{G(s)^2 - 1}, \zeta * \sqrt{G(s)^2 - 1} - \zeta * G(s) + \gamma_1(s)] * [T_1(s), 0] \quad (3-214)$$

Where:

$$W_1(s) = \frac{[\zeta * G(s) + \gamma_2(s)]}{[\zeta * (\gamma_1(s) + \gamma_2(s)) * G(s) + \gamma_1(s) * \gamma_2(s) + \zeta^2]} * T_1(s) \quad (3-215)$$

$$W_2(s) = \frac{[\zeta * \sqrt{G(s)^2 - 1}]}{[\zeta * (\gamma_1(s) + \gamma_2(s)) * G(s) + \gamma_1(s) * \gamma_2(s) + \zeta^2]} * T_1(s) \quad (3-216)$$

The Block Diagram for this model is:

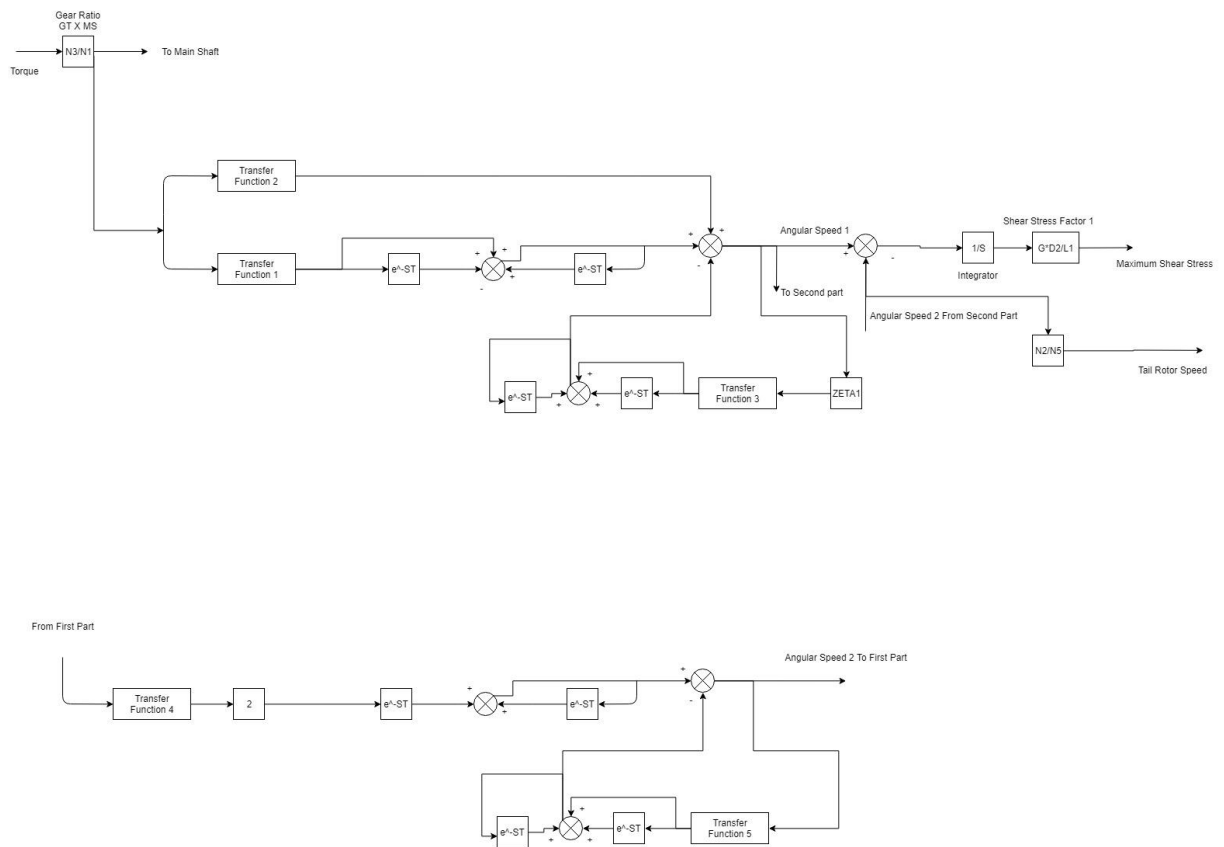


Figure 17: Block Diagram of the Hybrid Model on Main Rotor Shaft

Equations of Transfer functions used in SIMULINK and MATLAB can be found in the

Appendix I.

For the Main Shaft, the same equations will be used, and some parameters will be changed:

$$L = \rho * JMS \quad (3-217)$$

$$C = \frac{1}{G * JMS} \quad (3-218)$$

The propagation function:

$$P_2(s) = S * \sqrt{LC} \quad (3-219)$$

$$G_2(s) = \frac{[e^{2P_2(s)*L} + 1]}{[e^{2P_2(s)*L} - 1]} \quad (3-220)$$

$$H_2(s) = \sqrt{G_2(s)^2 - 1} \quad (3-221)$$

$$\zeta_2 = \sqrt{\frac{L}{C}} \quad (3-222)$$

$$\gamma_3(s) = J_4 * S + C_4 \quad (3-223)$$

$$\gamma_4(s) = J_{B1} * S + C_{B1} \quad (3-224)$$

The Torque equation for the hybrid model is:

$$[T_3(s), 0] = [-\zeta_2 * G_2(s) + \gamma_3(s) \zeta_2 * \sqrt{G_2(s)^2 - 1}, -\zeta_2 * \sqrt{G_2(s)^2 - 1} \zeta_2] \\ * G_2(s) + \gamma_4(s) * [W_4(s), W_{B1}(s)] \quad (3-225)$$

The A matrix becomes:

$$[A] = [-\zeta_2 * G_2(s) + \gamma_3(s) \zeta_2 * \sqrt{G_2(s)^2 - 1}, -\zeta_2 * \sqrt{G_2(s)^2 - 1} \zeta_2] \\ * G_2(s) + \gamma_4(s) \quad (3-226)$$

To find the inverse of A:

$$Adj(A) = [\zeta_2 * G_2(s) + \gamma_4(s) - \zeta_2 * \sqrt{G_2(s)^2 - 1}, \zeta_2 * \sqrt{G_2(s)^2 - 1} - \zeta_2 * G_2(s) + \gamma_3(s)] \quad (3-227)$$

$$Det(A) = \zeta_2 * (\gamma_3(s) + \gamma_4(s)) * G_2(s) + \gamma_3(s) * \gamma_4(s) + \zeta_2^2 \quad (3-228)$$

The Hybrid Model Equation becomes:

$$[W_4(s), W_{B1}(s)] \quad (3-229)$$

$$= \frac{1}{[\zeta_2 * (\gamma_3(s) + \gamma_4(s)) * G_2(s) + \gamma_3(s) * \gamma_4(s) + \zeta_2^2]} * [\zeta_2 * G_2(s) + \gamma_4(s) - \zeta_2 * \sqrt{G_2(s)^2 - 1}, \zeta_2 * \sqrt{G_2(s)^2 - 1} - \zeta_2 * G_2(s) + \gamma_3(s)] * [T_3(s), 0]$$

Where:

$$W_4(s) = \frac{[\zeta_2 * G_2(s) + \gamma_4(s)]}{[\zeta_2 * (\gamma_3(s) + \gamma_4(s)) * G_2(s) + \gamma_3(s) * \gamma_4(s) + \zeta_2^2]} * T_3(s) \quad (3-230)$$

$$W_{B1}(s) = \frac{[\zeta_2 * \sqrt{G_2(s)^2 - 1}]}{[\zeta_2 * (\gamma_3(s) + \gamma_4(s)) * G_2(s) + \gamma_3(s) * \gamma_4(s) + \zeta_2^2]} * T_3(s) \quad (3-231)$$

The Block Diagram for this shaft is:

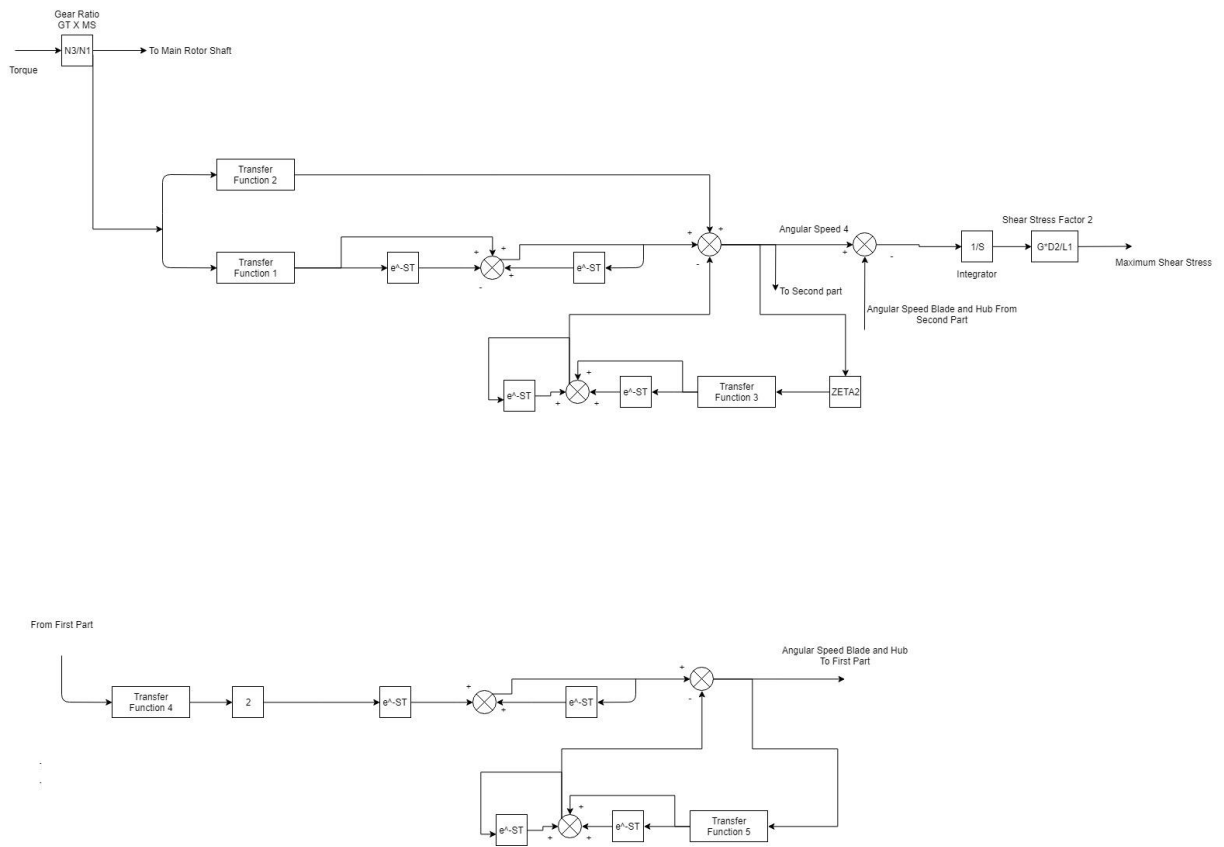


Figure 18: Block Diagram of the Hybrid Model on the Main Shaft

Equations of Transfer functions used in SIMULINK and MATLAB can be found in the

Appendix I.

3.5 Defining of Parameter Values & Equations for each Modeling Method

In this section, the results of the simulated responses including: the angular speeds, the shear stress, the resonance speeds will be displayed. The behavior of the transfer functions in terms of magnitude and decibels will also be shown (aka: the bode plots). This section merely states the behavior, a thorough analysis and discussion is shown in the Chapter 5.

But before any of the results, the design of each element for each type of model is calculated:

The values for the design of gears, blades, hub, and shafts were taken from actual values from different designs such as the R22 Robinson and CH53 Sikorsky; depending on what was available. Values such as damping and density of the blade alloy are estimated. This is because blade material for example is an alloy of different metals depending on the manufacturer (trademark). However, this is not meant to be a design and simulation of a specific helicopter model, but rather a general simulation to the behavior of a helicopter transmission shafts.

3.5.1 Lumped Parameter Model Equations

Defining the density and depth of all gears:

$$H = 0.02 \quad (3-232)$$

$$\rho = 7000 \quad (3-133)$$

The density of the blades is estimated (Aluminum Alloy)

$$\rho_B = 3000 \quad (3-234)$$

Main Rotor Shaft:

Shaft:

Inner and Outer Diameter:

$$D_{1MS} = 10.0655 \quad (3-5235)$$

$$D_{2MS} = 0.07 \quad (3-236)$$

The shaft is hollow in order to hold much more shear stress.

The Length:

$$L_{1MS} = 3.96 \quad (3-237)$$

The Polar Moment of Inertia (Mass):

$$I_{1MS} = \pi * \rho * L_{1MS} * \left(\frac{1}{32}\right) * ((D_{2MS}^4) - (D_{1MS}^4)) \quad (3-238)$$

Gear 1:

Estimated Number of Teeth:

$$NTD_1 = 50 \quad (3-239)$$

Inner and Outer Diameter:

$$D_{1D1} = 0.08 \quad (3-240)$$

$$D_{2D1} = 0.10 \quad (3-241)$$

The Polar Moment of Inertia (Mass):

$$I_1 = \pi * \rho * H * \left(\frac{1}{32}\right) * ((D_{2D1}^4) - (D_{1D1}^4)) \quad (3-242)$$

Gear 2:

Estimated Number of Teeth:

$$NTD_2 = 25 \quad (3-243)$$

Inner and Outer Diameter:

$$D_{1D2} = 0.08 \quad (3-244)$$

$$D_{2D2} = 0.115 \quad (3-245)$$

The Polar Moment of Inertia (Mass):

$$I_2 = \pi * \rho * H * \left(\frac{1}{32}\right) * ((D_{2D2}^4) - (D_{1D2}^4)) \quad (3-246)$$

Main Shaft:

Shaft:

Inner and Outer Diameter:

$$D_{1MRS} = 0.042 \quad (3-247)$$

$$D_{2MRS} = 0.05 \quad (3-248)$$

The shaft is hollow in order to hold much more shear stress.

The Length:

$$L_{1MRS} = 1.34 \quad (3-249)$$

The Polar Moment of Inertia (Mass):

$$I_{1MRS} = \pi * \rho * L_{1MRS} * \left(\frac{1}{32}\right) * ((D_{2MRS}^4) - (D_{1MRS}^4)) \quad (3-250)$$

Gear 4:

Estimated Number of Teeth:

$$NTD_4 = 60 \quad (3-251)$$

Inner and Outer Diameter:

$$D_{1D4} = 0.1 \quad (3-252)$$

$$D_{2D4} = 0.11 \quad (3-253)$$

The Polar Moment of Inertia (Mass):

$$I_4 = \pi * \rho * H * \left(\frac{1}{32}\right) * ((D_{2D4}^4) - (D_{1D4}^4)) \quad (3-254)$$

Blade and Hub 1:

Blade:

Estimated Number of Blades

$$NB_1 = 5 \quad (3-255)$$

Diameter of the blades (estimated to be very thin):

$$D_{1B1} = 0.02 \quad (3-256)$$

The length of each blade:

$$L_{B1} = 4.03 \quad (3-257)$$

The Polar Moment of Inertia (Mass):

$$I_{B1} = NB_1 * \pi * \rho_B * L_{B1} * \left(\frac{1}{32}\right) * (D_{1B1}^4) \quad (3-258)$$

Hub:

Hub Diameter:

$$D_{H1} = 0.1 \quad (3-259)$$

Hub Depth:

$$L_{H1} = 0.35 \quad (3-260)$$

The Polar Moment of Inertia (Mass):

$$I_{H1} = \pi * \rho_B * L_{H1} * \left(\frac{1}{32}\right) * (D_{H1}^4) \quad (3-261)$$

Other Parameters of the Shafts

Main Rotor Shaft:

The Inertia:

$$J_1 = I_1 \quad (3-262)$$

$$J_2 = I_2 \quad (3-263)$$

$$J_{1MS} = I_{1MS}; \quad (3-264)$$

The Damping:

$$C_1 = 2.5 \quad (3-265)$$

$$C_2 = 20 \quad (3-266)$$

The Modulus of Rigidity:

$$G = 80 * 10^9 \quad (3-267)$$

The Stiffness:

$$K = \frac{G * J_{1MS}}{\rho * (L_{1MS}^2)}; \quad (3-268)$$

The Shear Stress Factor [Angle Difference is the signal]:

$$SSF_1 = G * \frac{D_{2MS}}{L_{1MS}}; \quad (3-269)$$

Main Shaft:

The Inertia:

$$J_4 = I_4 \quad (3-270)$$

$$J_{1B1} = I_{B1} \quad (3-271)$$

$$J_{H1} = I_{H1} \quad (3-272)$$

$$J_{1MRS} = I_{1MRS} \quad (3-273)$$

$$J_{B1} = J_{1B1} + J_{H1} \quad (3-274)$$

The Damping:

$$C_4 = 10 \quad (3-275)$$

$$C_{B1} = 20 \quad (3-276)$$

The Modulus of Rigidity:

$$G = 80 * 10^9 \quad (3-277)$$

The Stiffness:

$$K_{MRS} = \frac{G * J_{1MRS}}{\rho * (L_{1MRS}^2)}; \quad (3-278)$$

The Shear Stress Factor:

$$SSF_2 = G * \frac{D_{2MRS}}{L_{1MRS}}; \quad (3-279)$$

Gear Ratios:

Intermediate Shaft:

Gear 6:

Number of Teeth Estimated:

$$NTD_6 = 15 \quad (3-280)$$

Gas Turbine Shaft:

Gear 3:

Number of Teeth Estimated:

$$NTD_3 = 40 \quad (3-281)$$

Tail Rotor Shaft:

Gear 5:

Number of Teeth Estimated:

$$NTD_5 = 45 \quad (3-282)$$

The Ratios:

Gas Turbine X Main Shaft:

$$GR_{GT \times MS} = \frac{NTD_3}{NTD_1} \quad (3-283)$$

Main Shaft x Tail Rotor Shaft:

$$GR_{MS \times TRS} = \frac{NTD_2}{NTD_5} \quad (3-284)$$

Intermediate Shaft x Main Rotor Shaft:

$$GR_{IS \times MRS} = \frac{NTD_6}{NTD_4} \quad (3-285)$$

Torque:

The Torque of the gas turbine is modeled as a 6000rpm turbo shaft:

Conversion to Hz, the Angular speed is:

$$W_T = 6000 * 2 * \frac{\pi}{60} \quad (3-286)$$

The Turbo shaft engine is modeled to have 350 Horse Power:

Conversion to kW, the Power is:

$$P_T = 350 * 745.7 \quad (3-287)$$

The Torque Equation is:

$$T_T = \frac{P_T}{W_T} \quad (3-288)$$

Resonance:

Resonance of the shaft is given by the derived equations:

At End 1:

$$w = \sqrt{\frac{K * (C_1 + C_2)}{(J_1 * C_2) + (J_2 * C_1)}} \quad (3-289)$$

At End 2:

$$w_2 = \sqrt{\frac{K_{MRS} * (C_4 + C_{B1})}{(J_4 * C_{B1}) + (J_{B1} * C_4)}}; \quad (3-290)$$

Calculated Values:

$$J_1 = 8.1147e - 04 \quad (3-291)$$

$$J_2 = 0.0018 \quad (3-292)$$

$$K = 1.1114e + 04 \quad (3-293)$$

$$J_4 = 6.3788e - 04 \quad (3-294)$$

$$J_{B1} = 0.0113 \quad (3-295)$$

$$K_{MRS} = 1.8394e + 04 \quad (3-296)$$

$$J_{1MS} = 0.0153 \quad (3-297)$$

$$J_{1MRS} = 0.0029 \quad (3-298)$$

$$GR_{GTXMS} = 0.8000 \quad (3-299)$$

$$GR_{MSXTRS} = 0.5556 \quad (3-300)$$

$$GR_{ISXMRS} = 0.2500 \quad (3-301)$$

$$T_T = 415.3864 \quad (3-302)$$

$$SSF_1 = 1.4141e + 09 \quad (3-303)$$

$$SSF_2 = 2.9851e + 09 \quad (3-304)$$

$$W = 828.8999 \quad (3-305)$$

$$W_2 = 1.6132e + 03 \quad (3-306)$$

3.5.2 Finite Element Model Equations

Main Rotor Shaft:

Setting the variables of the system:

$$\text{syms } S \ T_1 \ T_2 \ C_1 \ C_2 \ J_1 \ J_2 \ J \ K \quad (3-307)$$

Properties of finite elements:

$$K = 5 * K \quad (3-308)$$

$$J = \frac{J_{1MS}}{5} \quad (3-309)$$

The A Matrix is composed of:

$$KF = [K \ -K \ 0 \ 0 \ 0 \ 0; \ -K \ K + K \ -K \ 0 \ 0 \ 0; \ 0 \ -K \ K + K \ -K \ 0 \ 0; \ 0 \ 0 \ -K \ K + K \ -K \ 0; \ 0 \ 0 \ 0 \ -K \ K + K \ -K; \ 0 \ 0 \ 0 \ 0 \ -K \ K] \quad (3-310)$$

$$C \quad (3-311)$$

$$= [C_1 \ 0 \ 0 \ 0 \ 0 \ 0; \ 0 \ 0 \ 0 \ 0 \ 0 \ 0; \ 0 \ 0 \ 0 \ 0 \ 0 \ 0; \ 0 \ 0 \ 0 \ 0 \ 0 \ 0; \ 0 \ 0 \ 0 \ 0 \ 0 \ 0; \ 0 \ 0 \ 0 \ 0 \ 0 \ C_2]$$

$$JF \quad (3-312)$$

$$= [J_1 \ 0 \ 0 \ 0 \ 0 \ 0; \ 0 \ J \ 0 \ 0 \ 0 \ 0; \ 0 \ 0 \ J \ 0 \ 0 \ 0; \ 0 \ 0 \ 0 \ J \ 0 \ 0; \ 0 \ 0 \ 0 \ 0 \ J \ 0; \ 0 \ 0 \ 0 \ 0 \ 0 \ J]$$

$$A_1 = JF * S^2 \quad (3-313)$$

$$A_2 = C * S \quad (3-314)$$

$$A_3 = KF \quad (3-315)$$

$$A = A_1 + A_2 + A_3 \quad (3-316)$$

The Inverse of A Matrix:

$$Y = \text{inv}(A) \quad (3-317)$$

The Torque Vector:

$$T = [T_1; 0; 0; 0; 0; 0]; \quad (3-318)$$

The Angular Speed Vector:

$$WF = Y * T \quad (3-319)$$

After obtaining the equations in variable form, the variables are re arranged in terms of S, in a matrix form:

Matrix X:

$$X_1 = ((K^5) * J_2) + (4 * (K^5) * J) + ((K^5) * J_1) + (5 * (K^4) * C_1 * C_2) \quad (3-320)$$

$$X_2 = (5 * (K^4) * C_1 * J_2) + (10 * (K^4) * J * C_2) + (5 * (K^4) * J_1 * C_2) \quad (3-321)$$

$$+ (10 * (K^4) * C_1 * J)$$

$$X_3 = (5 * (K^4) * J_1 * J_2) + (20 * (K^3) * C_1 * J * C_2) + (10 * (K^4) * J_1 \quad (3-322)$$

$$* J) + (10 * (J^2) * (K^4)) + (10 * (K^4) * J * J_2)$$

$$X_4 = (15 * (K^3) * C_1 * (J^2)) + (15 * (K^3) * (J^2) * C_2) + (20 * (K^3) \quad (3-323)$$

$$* C_1 * J * J_2) + (20 * (K^3) * J_1 * J * C_2)$$

$$X_5 = (15 * (K^3) * (J^2) * J_2) + (20 * (K^3) * J_1 * J * J_2) + (6 * (J^3) \quad (3-324)$$

$$* (K^3)) + (15 * (K^3) * J_1 * (J^2)) + (21 * (K^2) * C_1$$

$$* (J^2) * C_2)$$

$$X_6 = (21 * (K^2) * J_1 * (J^2) * C_2) + (7 * C_1 * (J^3) * (K^2)) + (21 * (K^2) \quad (3-325)$$

$$* C_1 * (J^2) * J_2) + (7 * (K^2) * (J^3) * C_2);$$

$$X_7 = (7 * J_1 * (J^3) * (K^2)) + (21 * (K^2) * J_1 * (J^2) * J_2) + ((K^2) \quad (3-326)$$

$$* (J^4)) + (8 * K * C_1 * (J^3) * C_2) + (7 * (K^2) * (J^3) * J_2)$$

$$X_8 = (K * C_1 * (J^4)) + (8 * K * C_1 * (J^3) * J_2) + (8 * K * J_1 * (J^3) \quad (3-327)$$

$$* C_2) + (K * (J^4) * C_2)$$

$$X_9 = (K * (J^4) * J_2) + (8 * K * J_1 * (J^3) * J_2) + (K * J_1 * (J^4)) + (C_1 * (J^4) * C_2) \quad (3-328)$$

$$X_{10} = (C_1 * (J^4) * J_2) + (J_1 * (J^4) * C_2) \quad (3-329)$$

$$X_{11} = (J_1 * (J^4) * J_2) \quad (3-330)$$

Matrix Y:

$$Y_0 = (K^5) \quad (3-331)$$

$$Y_1 = (5 * (K^4) * C_2) \quad (3-332)$$

$$Y_2 = (5 * (K^4) * J_2) + (10 * (K^4) * J) \quad (3-333)$$

$$Y_3 = (20 * (K^3) * J * C_2) \quad (3-334)$$

$$Y_4 = (15 * (K^3) * (J^2)) + (20 * (K^3) * J * J_2) \quad (3-335)$$

$$Y_5 = (21 * (K^2) * (J^2) * C_2) \quad (3-336)$$

$$Y_6 = (7 * (J^3) * (K^2)) + (21 * (K^2) * (J^2) * J_2) \quad (3-337)$$

$$Y_7 = (8 * K * (J^3) * C_2) \quad (3-338)$$

$$Y_8 = (8 * K * (J^3) * J_2) + (K * (J^4)) \quad (3-339)$$

$$Y_9 = ((J^4) * C_2) \quad (3-10)$$

$$Y_{10} = ((J^4) * J_2) \quad (3-341)$$

Main Shaft:

Setting the variables of the system:

$$\text{syms } S \ T_{22} \ T_2 \ C_4 \ C_{B1} \ J_4 \ J_{B1} \ J_{22} \ K_{MRS} \quad (3-342)$$

Properties of finite elements:

$$K_{MRS} = 5 * K_{MRS} \quad (3-342)$$

$$J_{22} = \frac{J_{1MRS}}{5} \quad (3-343)$$

The A Matrix is composed of:

$$\begin{aligned} KF_2 = [& K_{MRS} - K_{MRS} \ 0 \ 0 \ 0 \ 0; \ -K_{MRS} \ K_{MRS} + K_{MRS} - K_{MRS} \ 0 \ 0 \ 0; \ 0 \\ & - K_{MRS} \ K_{MRS} + K_{MRS} - K_{MRS} \ 0 \ 0; \ 0 \ 0 - K_{MRS} \ K_{MRS} \\ & + K_{MRS} - K_{MRS} \ 0; \ 0 \ 0 \ 0 - K_{MRS} \ K_{MRS} + K_{MRS} \\ & - K_{MRS}; \ 0 \ 0 \ 0 \ 0 - K_{MRS} \ K_{MRS}]; \end{aligned} \quad (3-344)$$

$$C_{22} = [C_4 \ 0 \ 0 \ 0 \ 0 \ 0; \ 0 \ 0 \ 0 \ 0 \ 0 \ 0; \ 0 \ 0 \ 0 \ 0 \ 0 \ 0; \ 0 \ 0 \ 0 \ 0 \ 0 \ 0; \ 0 \ 0 \ 0 \ 0 \ 0 \ C_{B1}]; \quad (3-345)$$

$$\begin{aligned} JF_2 = [& J_4 \ 0 \ 0 \ 0 \ 0 \ 0; \ 0 \ J_{22} \ 0 \ 0 \ 0 \ 0; \ 0 \ 0 \ J_{22} \ 0 \ 0 \ 0; \ 0 \ 0 \ 0 \ J_{22} \ 0 \ 0; \\ & 0 \ 0 \ 0 \ 0 \ J_{22} \ 0; \ 0 \ 0 \ 0 \ 0 \ 0 \ J_{B1}]; \end{aligned} \quad (3-346)$$

$$A_4 = JF_2 * S^2 \quad (3-347)$$

$$A_5 = C_{22} * S \quad (3-348)$$

$$A_6 = KF_2 \quad (1)$$

$$A_{22} = A_4 + A_5 + A_6 \quad (2)$$

The Inverse of A Matrix:

$$Y_{22} = inv(A_{22}) \quad (3-349)$$

The Torque Vector:

$$T_{22} = [T_2; \ 0; \ 0; \ 0; \ 0; \ 0]; \quad (3-350)$$

The Angular Speed Vector:

$$WF_2 = Y_{22} * T_{22} \quad (3-351)$$

After obtaining the equations in variable form, the variables are re arranged in terms of S, in a matrix form:

Matrix V:

$$V_0 = ((K^5) * C_4) + ((K^5) * C_{B1}) \quad (3-352)$$

$$V_1 = ((K^5) * J_{B1}) + (4 * (K^5) * J) + ((K^5) * J_4) + (5 * (K^4) * C_4 * C_{B1}) \quad (3-353)$$

$$V_2 = (5 * (K^4) * C_4 * J_{B1}) + (10 * (K^4) * J * C_{B1}) + (5 * (K^4) * J_4 * C_{B1}) + (10 * (K^4) * C_4 * J) \quad (3-354)$$

$$V_3 = (5 * (K^4) * J_4 * J_{B1}) + (20 * (K^3) * C_4 * J * C_{B1}) + (10 * (K^4) * J_4 * J) + (10 * (J^2) * (K^4)) + (10 * (K^4) * J * J_{B1}) \quad (3-355)$$

$$V_4 = (15 * (K^3) * C_4 * (J^2)) + (15 * (K^3) * (J^2) * C_{B1}) + (20 * (K^3) * C_4 * J * J_{B1}) + (20 * (K^3) * J_4 * J * C_{B1}) \quad (3-356)$$

$$V_5 = (15 * (K^3) * (J^2) * J_{B1}) + (20 * (K^3) * J_4 * J * J_{B1}) + (6 * (J^3) * (K^3)) + (15 * (K^3) * J_4 * (J^2)) + (21 * (K^2) * C_4 * (J^2) * C_{B1}) \quad (3-357)$$

$$V_6 = (21 * (K^2) * J_4 * (J^2) * C_{B1}) + (7 * C_4 * (J^3) * (K^2)) + (21 * (K^2) * C_4 * (J^2) * J_{B1}) + (7 * (K^2) * (J^3) * C_{B1}) \quad (3-358)$$

$$V_7 = (7 * J_4 * (J^3) * (K^2)) + (21 * (K^2) * J_4 * (J^2) * J_{B1}) + ((K^2) * (J^4)) + (8 * K * C_4 * (J^3) * C_{B1}) + (7 * (K^2) * (J^3) * J_{B1}) \quad (3-359)$$

$$V_8 = (K * C_4 * (J^4)) + (8 * K * C_4 * (J^3) * J_{B1}) + (8 * K * J_4 * (J^3) * C_{B1}) + (K * (J^4) * C_{B1}) \quad (3-5360)$$

$$V_9 = (K * (J^4) * J_{B1}) + (8 * K * J_4 * (J^3) * J_{B1}) + (K * J_4 * (J^4)) + (C_4 * (J^4) * C_{B1}) \quad (3-361)$$

$$V_{10} = (C_4 * (J^4) * J_{B1}) + (J_4 * (J^4) * C_{B1}) \quad (3-362)$$

$$V_{11} = (J_4 * (J^4) * J_{B1}) \quad (3-363)$$

Matrix W:

$$W_0 = (K^5) \quad (3-364)$$

$$W_1 = (5 * (K^4) * C_{B1}) \quad (3-365)$$

$$W_2 = (5 * (K^4) * J_{B1}) + (10 * (K^4) * J) \quad (3-366)$$

$$W_3 = (20 * (K^3) * J * C_{B1}) \quad (3-367)$$

$$W_4 = (15 * (K^3) * (J^2)) + (20 * (K^3) * J * J_{B1}) \quad (3-368)$$

$$W_5 = (21 * (K^2) * (J^2) * C_{B1}) \quad (3-369)$$

$$W_6 = (7 * (J^3) * (K^2)) + (21 * (K^2) * (J^2) * J_{B1}) \quad (3-370)$$

$$W_7 = (8 * K * (J^3) * C_{B1}) \quad (3-371)$$

$$W_8 = (8 * K * (J^3) * J_{B1}) + (K * (J^4)) \quad (3-372)$$

$$W_9 = ((J^4) * C_{B1}) \quad (3-373)$$

$$W_{10} = ((J^4) * J_{B1}) \quad (3-374)$$

Resonance Equations:

$$w_3 = [-X_{10} \ 0 \ X_8 \ 0 \ -X_6 \ 0 \ X_4 \ 0 \ -X_2 \ 0 \ X_0] \quad (3-375)$$

$$w_4 = [-V_{10} \ 0 \ V_8 \ 0 \ -V_6 \ 0 \ V_4 \ 0 \ -V_2 \ 0 \ V_0] \quad (3-376)$$

roots(w₃);

roots(w₄);

Only real positive values are taken into consideration.

3.5.3 Hybrid (Distributed-Lumped) Model Equations

Main Rotor Shaft:

System Characteristics:

Compliance/Inverse of Stiffness (Equivalent to Capacitance):

$$COM_1 = \frac{\rho * L_{1MS}}{G * J_{1MS}} \quad (3-377)$$

Inductance (Equivalent to Polar moment of inertia, mass):

$$LIN_1 = \frac{J_{1MS}}{L_{1MS}} \quad (3-378)$$

The Impedance:

$$\zeta_1 = \sqrt{\left(\frac{LIN_1}{COM_1}\right)} \quad (3-379)$$

Time Constants and Delays:

$$\tau_{s1} = \sqrt{LIN_1 * COM_1} \quad (3-380)$$

$$\tau_1 = 2 * L_{1MS} * TAW_{S1} \quad (3-381)$$

Transfer Function Equivalence Equations (For Convenience):

$$\gamma_{11} = [J_1 C_1] \quad (3-382)$$

$$\gamma_{12} = [J_2 C_2] \quad (3-383)$$

$$DS_{11} = J_1 * J_2 \quad (3-384)$$

$$DS_{12} = (J_1 * C_2) + (J_2 * C_1) \quad (3-385)$$

$$DS_{13} = (C_1 * C_2) + (\zeta_1^2) \quad (3-386)$$

Main Shaft:

System Characteristics:

Compliance/Inverse of Stiffness (Equivalent to Capacitance):

$$COM_2 = \frac{\rho * L_{1MRS}}{G * J_{1MRS}} \quad (3-387)$$

Inductance (Equivalent to Polar moment of inertia, mass):

$$LIN_2 = \frac{J_{1MRS}}{L_{1MRS}} \quad (3-388)$$

The Impedance:

$$\zeta_2 = \sqrt{\left(\frac{LIN_2}{COM_2}\right)} \quad (3-389)$$

Time Constants and Delays:

$$\tau_{s2} = \sqrt{LIN_2 * COM_2} \quad (3-390)$$

$$\tau_2 = 2 * L_{1MRS} * TAWS2 \quad (3-391)$$

Transfer Function Equivalence Equations (For Convenience):

$$\gamma_{21} = [J_4 C_4] \quad (3-392)$$

$$\gamma_{22} = [J_{B1} C_{B1}] \quad (3-393)$$

$$DS_{21} = J_4 * J_{B1} \quad (3-394)$$

$$DS_{22} = (J_4 * C_{B1}) + (J_{B1} * C_4) \quad (3-395)$$

$$DS_{23} = (C_4 * C_{B1}) + (\zeta_2^2) \quad (3-396)$$

Chapter IV: Simulation, Results & Discussion of Results

4.1 Lumped Parameter Model Simulation

By inserting these equations into MATLAB it is possible to simulate the response of $W_1(s)$ and $W_2(s)$ using SIMULINK block models.

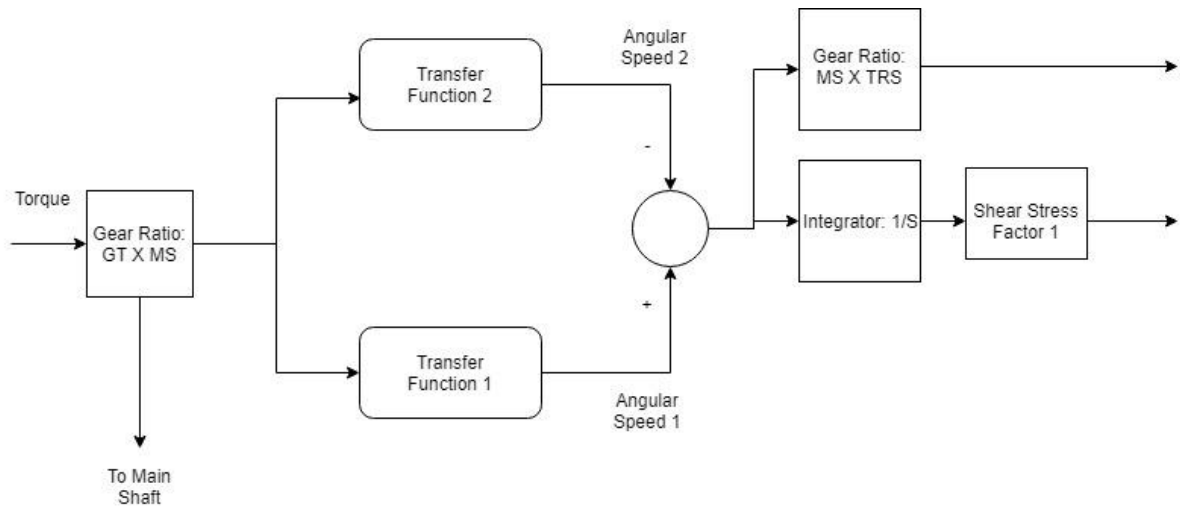


Figure 19: Representation of SIMULINK Model of Main Rotor Shaft

From the left, first comes the signal generator. This generator produces a sine wave with the determined torque and frequency. Next, the signal goes to an amplifier, representing the gear ratio between gear 3 and gear 1, to transmit the torque. The signal moves to a parallel representation of the vector $[W(s)]$. Each speed at the ends of the shaft is represented by a transfer function, found from the equations solved previously. Each output from each transfer function is the aim of this study, so both resulted are graphed.

From $[W_2(s)]$, the torque is transferred from the Main Rotor Shaft to the Tail Rotor Shaft through a gear ratio between gear 2 and 5: $GR_2 = \frac{N_2}{N_5}$

The Tail Rotor Shaft is small and its mechanics are ignored (for simplicity purposes). The same goes for the tail blades and the speed of the blades are estimated to be the same of the shaft. This speed is graphed.

In SIMULINK the block model of vector $[W(s)]$ is represented as $W_1(s) - W_2(s)$. This is because due to the torque is transmitted through gear 1 along the Main Rotor Shaft. For the moment the shaft moves from rest, $W_1(s)$ will be leading while $W_2(s)$ will be lagging. The difference of both angular speeds is used to calculate the Shear Stress of the Shaft.

The Shear Stress is defined as: $SS = G * \rho * \frac{\theta}{L}$

θ here is the difference of $\theta_1 - \theta_2$ that is produced from the signal multiplied by an integrator. The Shear Stress behavior of the Main Rotor Shaft is recorded and graphed.

The Shear Stress is calculated to know the mechanical limits of the shaft when studying its response. Another property that limits the shaft rotation would be resonance. Resonance, as defined in *Understanding of resonance essential for solving vibration problems*, is the maximum frequency attained when the natural frequency of the shaft is equal to the forced frequency (2018). By replacing S by iW , taking the modulus, and differentiating the real part of the equation, and equating it to zero, the equation becomes:

$$w = \sqrt{\left(\frac{K * (C_1 + C_2)}{(J_1 * C_2) + (J_2 * C_1)}\right)} \quad (5-1)$$

Covering the second path, the Intermediate Shaft mechanics is ignored due to the size of the shaft and for simplicity purposes. However, the gear ratio between gear 6 and 4 is still considered and is equal to: $GR_3 = \frac{N_6}{N_4}$

Building the model blocks in SIMULINK:

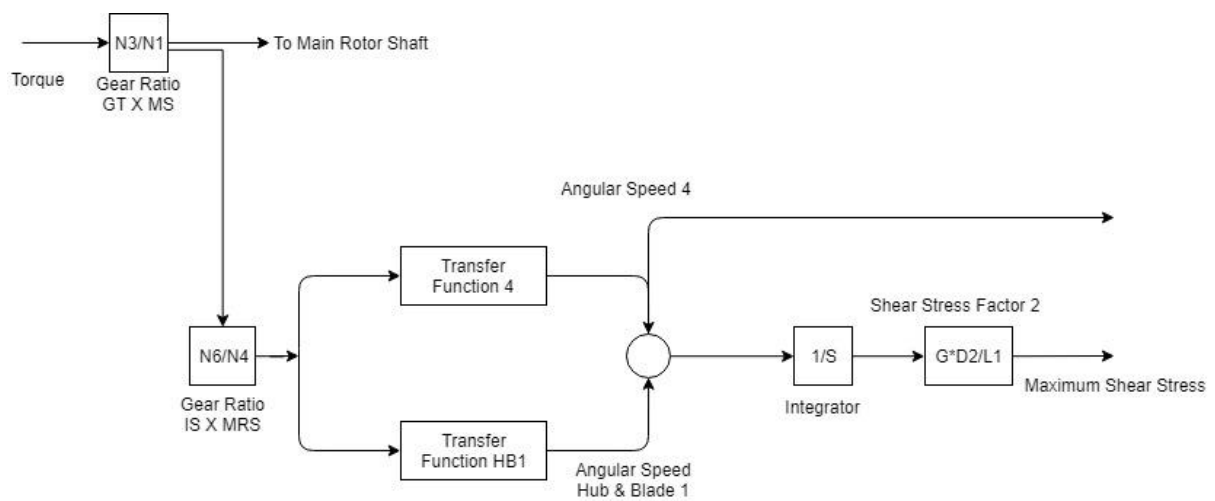


Figure 20: Representation of SIMULINK Model Main Shaft

As shown in the figure above, the layout is similar to the previous block model. A signal generator into gear ratios into parallel transfer function blocks. Each block represents angular speed at the end of the Main Shaft, the difference is used to calculate the Shear Stress of the shaft. Both angular speed 4 and of the blades 1 as well as the Shear Stress are recorded and graphed.

The resonance speeds of the Main Shaft are also calculated:

$$w_2 = \sqrt{\left(\frac{K_2 * (C_4 + C_{B1})}{(J_4 * C_{B1}) + (J_{B1} * C_4)} \right)} \quad (5-2)$$

4.2 Lumped Parameter Model Results

The source of the signal generator was adjusted by a BIAS of 2812. This would give the angular speed in the main rotor shaft, to settle to 100 radians per second. This is done only for convenience of display. Other shafts however will have varying speeds according to the gear ratio calculated respectively. The simulation is run for 0.05 seconds; enough time to study the behavior and for the speed to settle.

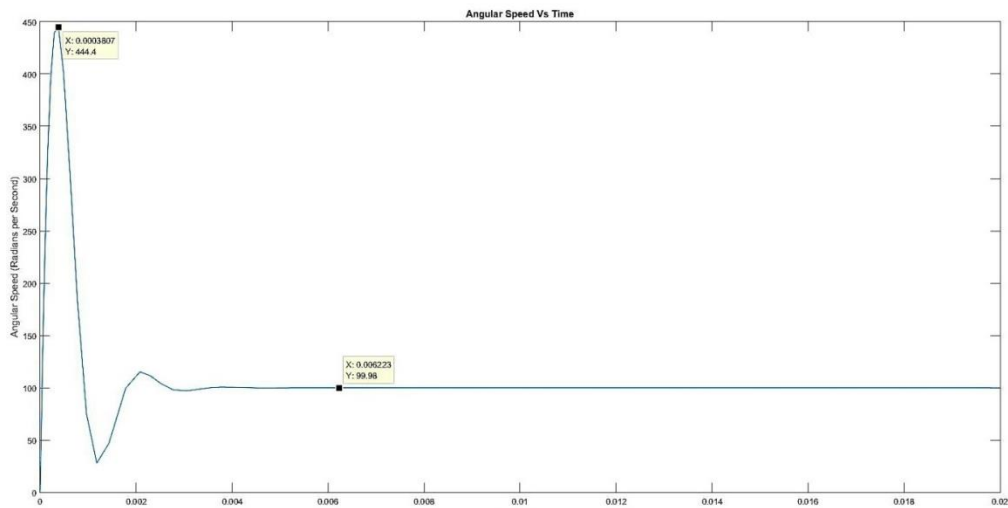


Figure 21: Load End (Angular Speed 1) of Lumped Model

The settling time for the angular speed 1 is around 0.006223 seconds. The maximum over shoot is 444.4 radians per second at the first 0.0003807 seconds. The wave has one and half propagation which makes this an under damped response of a transfer function. The Settling speed is 99.98 radians per second.

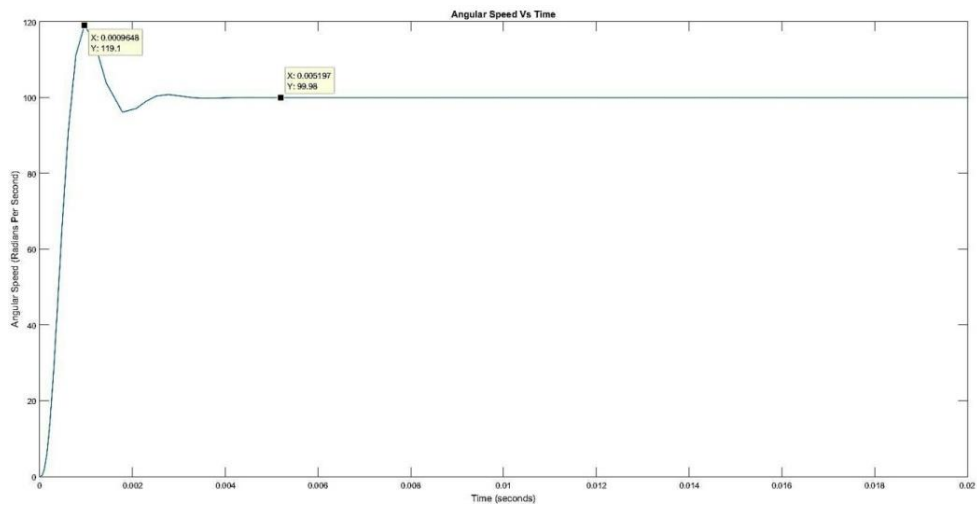


Figure 22: Drive End (Angular Speed 2) of Lumped Model

The settling time for the angular speed 2 is around 0.005197 seconds. The maximum over shoot is 119.1 radians per second at the first 0.0009648 seconds. The wave has one and half propagation which makes this an under damped response of a transfer function. The Settling speed is 99.98 radians per second.

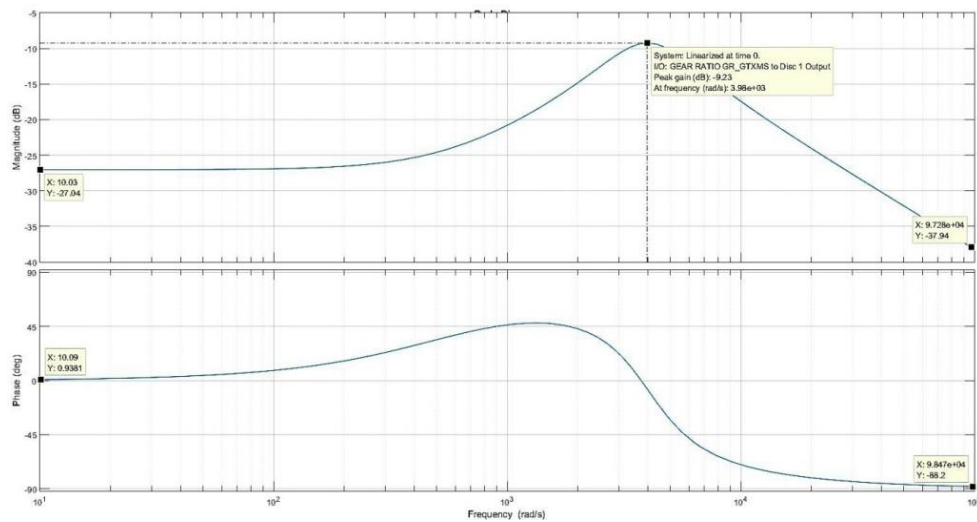


Figure 23: Load End (Angular Speed 1) Bode Plot for Lumped Model

At Low Frequencies, the magnitude is -27 DB. The input is almost in phase with the output of the transfer function at angle of 0.938 degrees. At high frequencies, the magnitude decreases constantly to -37.9 DB. The input and output have a phase difference of 90 degrees or $\pi/2$. Resonance peak is predicted at $4.03 \cdot 10^3$ radians per second.

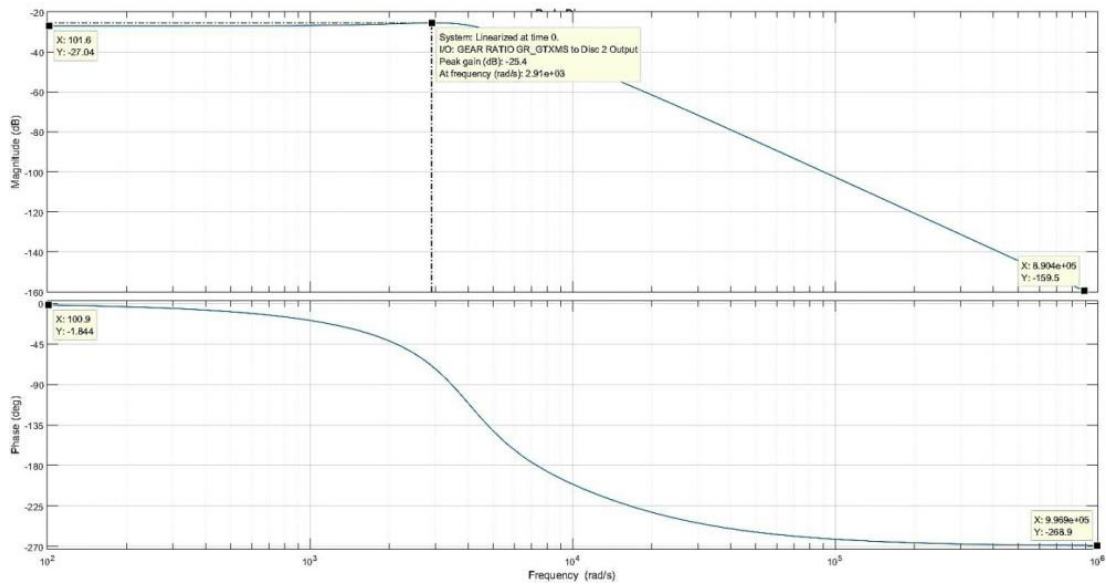


Figure 24: Load End (Angular Speed 2) Bode Plot for Lumped Model

At Low Frequencies, the magnitude is -27 DB. The input is almost in phase with the output of the transfer function at angle of -1.84. At high frequencies, the magnitude decreases constantly to -160 DB. The input and output have a phase difference of 270 degrees or $3 \cdot \pi/2$. Resonance peak is predicted at $4.07 \cdot 10^3$ radians per second.

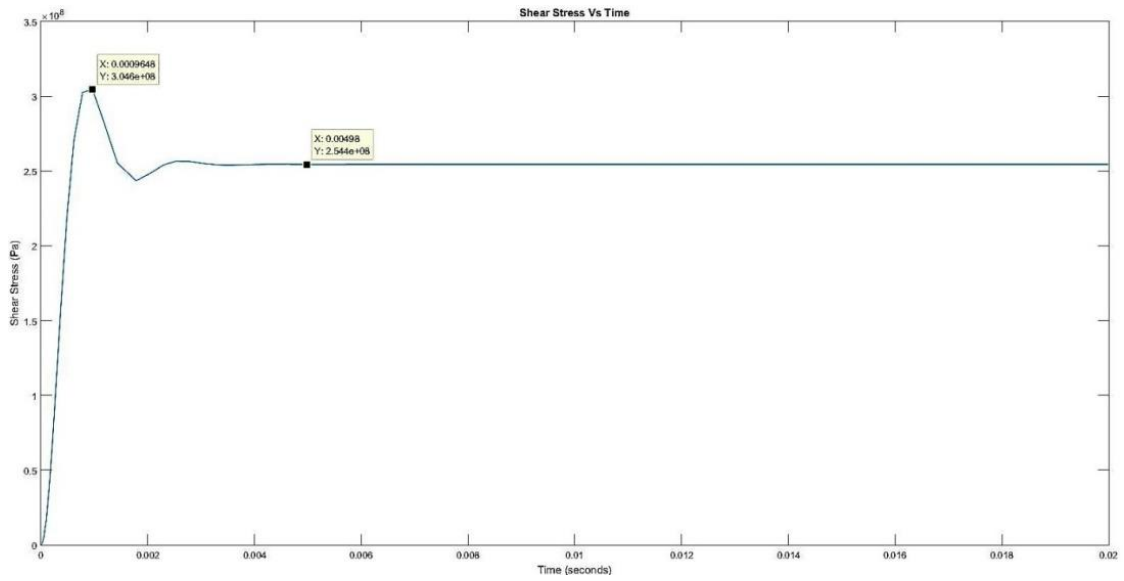


Figure 25: Shear Stress of Main Rotor Shaft for Lumped Model

The settling time for the Shear Stress is around 0.00498 seconds. The maximum overshoot is 3.046×10^8 Pa at the first 0.0009648 seconds. The wave has one and half propagation which makes this an under damped response of a transfer function. The Settling Stress is 2.544×10^8 Pa.

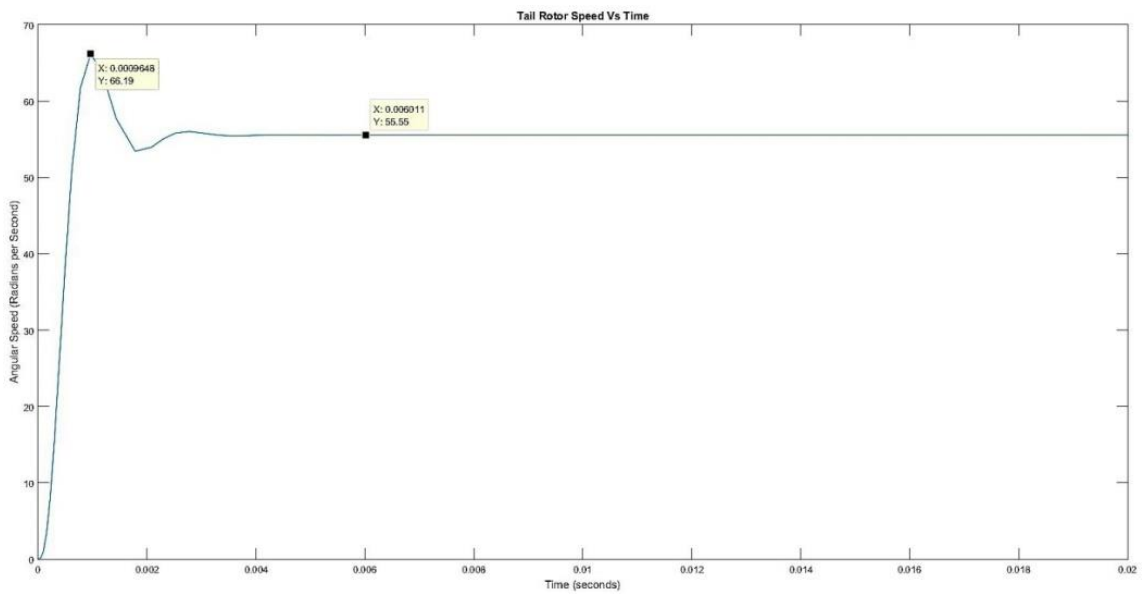


Figure 26: Tail Rotor Speed for Lumped Model

The settling time for the Tail Rotor Speed is around 0.00601 seconds. The maximum over shoot is 66.19 radians per second at the first 0.0009648 seconds. The wave has one and half propagation which makes this an under damped response of a transfer function. The Settling speed is 55.55 radians per second.

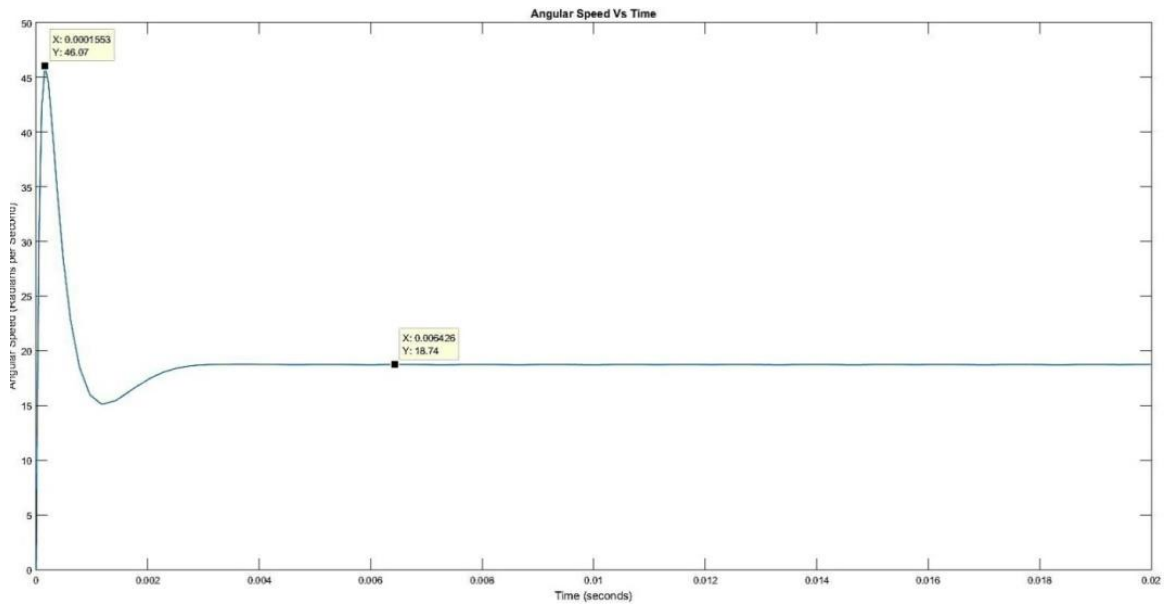


Figure 27: Drive End (Angular Speed 4) of Main Shaft for Lumped Model

The settling time for the Angular speed 4 is around 0.006426 seconds. The maximum over shoot is 46.07 radians per second at the first 0.0009648 seconds. The wave has one and half propagation which makes this an under damped response of a transfer function. The Settling speed is 18.74 radians per second.

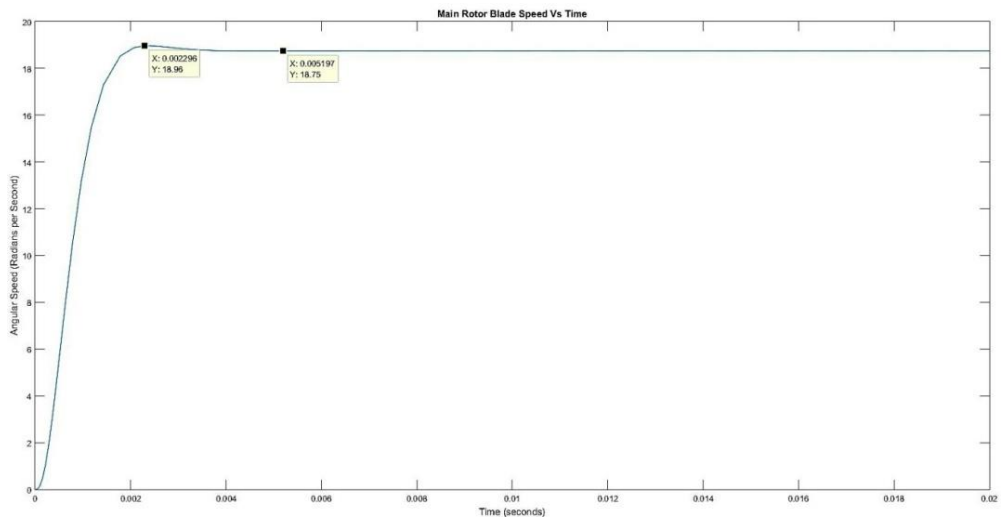


Figure 28: Blade Angular Speed of Main Shaft for Lumped Model

The settling time for the Angular speed of the Blade is around 0.005197 seconds. The maximum over shoot is 18.96 radians per second at the first 0.002296 seconds. The wave barely has one propagation, which makes this an under damped response that is very close to the critical damping value of a transfer function. The Settling speed is 18.75 radians per second.

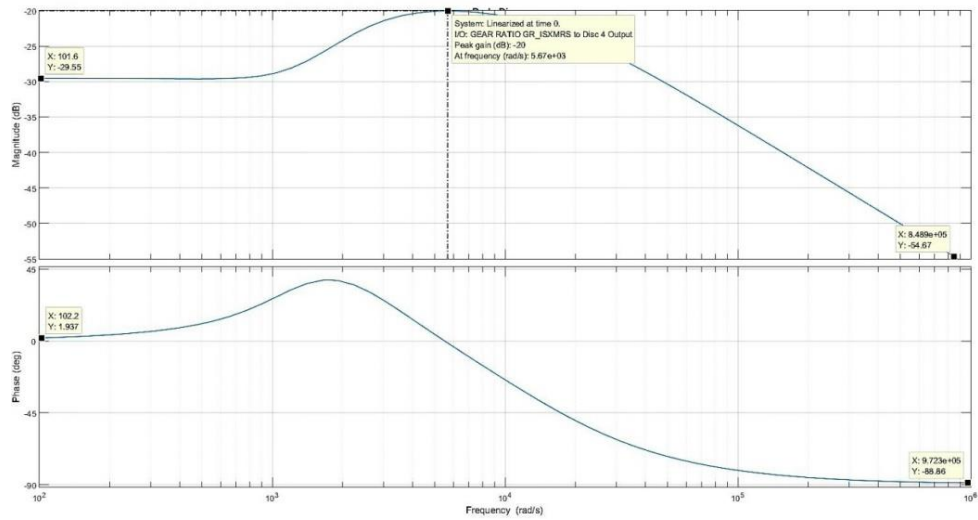


Figure 29: Drive End (Angular Speed 4) of Main Shaft Bode plot for Lumped Model

At Low Frequencies, the magnitude is -29.5 DB. The input is approximately in phase with the output of the transfer function at a phase difference of 1.94 degrees. At high frequencies, the magnitude decreases constantly to -54.7 DB. The input and output have a phase difference of 90 degrees or $\pi/2$. Resonance peak is predicted at $5.64 \cdot 10^3$ radians per second.

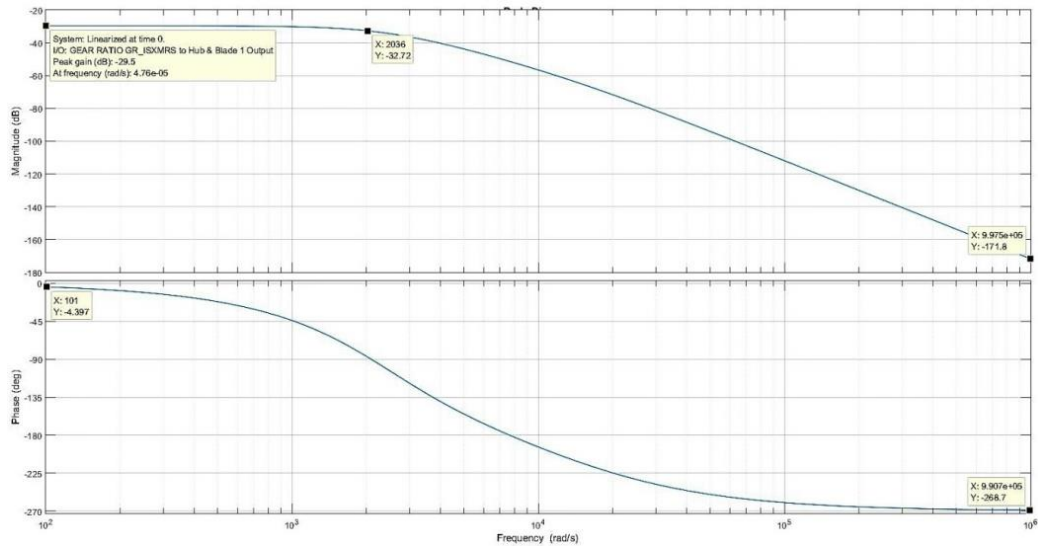


Figure 30: Blade Angular Speed of Main Shaft Bode Plot for Lumped Model

At Low Frequencies, the magnitude is -29.5 DB. The input is approximately in phase with the output of the transfer function at a phase difference of -4.4 degrees. At high frequencies, the magnitude decreases constantly to -172 DB. The input and output have a phase difference of 270 degrees or $3\pi/2$. Resonance peak is predicted at 2.04×10^3 radians per second.

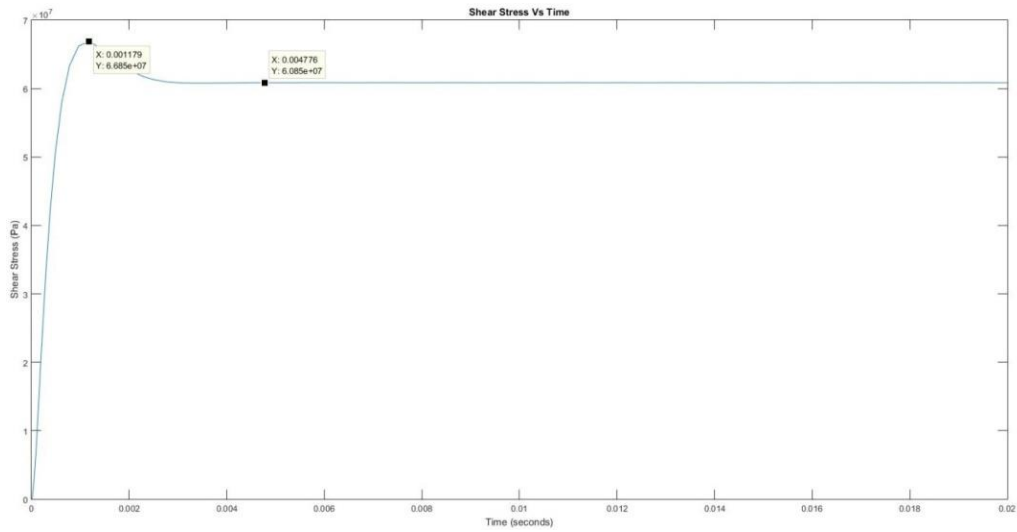


Figure 31: Shear Stress of Main Shaft for Lumped Model

The settling time for the Shear Stress is around 0.004776 seconds. The maximum overshoot is 6.685×10^7 Pa at the first 0.001179 seconds. The wave has one and half propagation which makes this an under damped response of a transfer function. The Settling Stress is 6.085×10^7 Pa.

4.3 Lumped Parameter Model Analysis

Main Rotor Shaft:

Figure 14 shows the response of the angular speed 1. The settling speed is set to 99.98 radians (100) by setting a bias in the sine wave generator signal to 2812. This is so the speed can be easily compared with just the gear ratios (to other shafts and elements). The percentage overshoot of the response is very high:

$$\%overshoot = \frac{444.4 - 99.98}{99.98} * 100\% = 344.49\%$$

This corresponding to R.Whalley's and M.Ibrahimi's work where they reach an overshoot of 80% (April, 2005). Both results being outliers to a typical stable system where the % overshoot would be a lot lower. The discrepancy between the results is a matter of shaft and gear design as well the system application. A high % overshoot is usually followed by tendency to either instability of the system, or a very high maximum shear stress where the shaft breaks due to forces of rotation. Neither of this is happening as shown in Figure 18, the response of the shaft to the shear stress. The settling stress is reached in 0.00498 seconds (very small value) and the Main Rotor Shaft has a percentage overshoot of:

$$\%overshoot = \frac{3.046 - 2.544}{2.544} * 100\% = 19.73\%$$

The value is in an acceptable range and is less than what the hollow shaft can handle [from design point of view]. This gives the conclusion that the high overshoot is acceptable. Another supporting detail would be that the overshoot is for a very small amount of time, typically after the first 0.0003807 seconds starting the system the shaft starts to stabilize and at the settling time of 0.006223 seconds the shaft is completely stable.

The system behavior is that of an under damped system is completely expected, as the value of the damping at gear 1 is $C_1 = 0.5$

This value is very small, and even though both values of the damping (at both ends) affect the behavior response of this end of the shaft, the damping C_1 holds more weight, and thus giving this expectation.

A controller can be designed to reduce the overshoot of this system, however it is not needed (nor it is the scope of this study) and the behavior of this section is stable.

Figure 15, shows a similar behavior of the angular speed at the other end of the shaft. The response is almost identical except for the over shoot:

$$\%overshoot = \frac{119.1 - 99.98}{99.98} * 100\% = 19.12\%$$

There seems to be a lot less risk involved in this section of the shaft, although the behavior is similar to the angular speed 1, with a lot less overshoot. The under damped system behavior is stable.

Figure 16 shows the bode plot of the angular speed 1 which in fact shows the magnitude and the phase. The values are all self-explanatory with the phase angle between the output signal and the input signal being almost 0 [0.938] in the beginning and settles down to 90 degrees at the end [very high frequencies]. The resonance value can be compared with that of the calculated value:

Calculated resonance: $3.4647 * 10^3$ *radians per second*

Captured resonance (Bode Plot): $4.03 * 10^3$ *radians per second*

The results are similar but not identical, the bode plot does not completely agree with the results from the equation, neither does it disagree. The discrepancy between the two could be a result of effective damping of the shaft and not taking the inertia of the shaft into consideration.

Figure 17 Shows the bode plot of the angular speed 2. The magnitude and phase angle of the section of the shaft is displayed. The value of the phase angle of -1.84 is expected to be small at the beginning. The phase angle output at high frequencies is 3 times (270) the phase of the output at the first end of the shaft. This could be due to the inertia difference between the two (inertia of gear 2 is almost 2x inertia of gear 1 by design). This is consistent with the results of R.Whalley's and M.Ibrahimi's work in their paper of "Torsional Response of Rotor Systems" (April, 2005). The resonance value is compared to the calculated value:

Calculated resonance: $3.4647 * 10^3 \text{ radians per second}$

Captured resonance (Bode Plot): $4.07 * 10^3 \text{ radians per second}$

This is consistent with the previous resonance results, as it is almost the same prediction from both ends of the shaft. This resonance was a lot harder to predict due to the fact that the magnitude graph had no "hump". The unseen resonance peak can still be determined from phase angle change and is shown to be almost the same prediction as the other bode plot.

Figure 19 shows the assumed tail rotor speed (since the mechanics of tail rotor shaft is ignored, tail rotor shaft = tail rotor blade speed). The tail rotor speed is a fraction of the main rotor shaft speed due to the gear ratio. The speed is equal to 55.55 radians. The behavior is neat similar to that of under damped system. The overshoot is:

$$\%Over\ shoot = \frac{66.19 - 55.55}{55.55} * 100\% = 19.15\%$$

The behavior is similar to other parts of the transmission, the percentage overshoot is acceptable and the behavior is deemed stable.

Main Shaft:

Figure 20 shows the angular speed 4. The setting speed is 18.74 radians per second; this is low due to the gear ratio between the intermediate shaft and the main shaft.

The percentage overshoot can be calculated:

$$\% \text{ overshoot} = \frac{46.07 - 18.74}{18.74} * 100\% = 145.8\%$$

The percentage overshoot here is similar to the behavior of angular speed 1 of the main rotor shaft. An outlier value of a high overshoot, although lower than the angular speed 1, could be a sign of dangerous instability of the system. However, the value overshoots only for 0.0009648 second, which is approximately 1 mili second. The amount of time the system is in a dangerous amount of speed is very low which lowers the risk of undergoing major issues within the shaft. The shear stress behavior of the shaft can also confirm this conclusion from Figure 24. In fact, the shear stress behavior seems to be closer to the critical damping behavior with only a half wave propagation through the first 0.002 seconds. The overshoot of the shear stress is:

$$\% \text{ Overshoot} = \frac{6.685 - 6.085}{6.085} * 10^7 * 100\% = 9.86\%$$

The overshoot as shown above is very low, and with this it is possible to deduce that angular speed 4 behavior is not dangerous. An explanation for the behavior could come from the low damping at gear 4: $C_4 = 10$

While this value is not low, it is not particularly high either, and its effectiveness depends on the gear design and inertia as well as the shaft. The under damped behavior of this section of the shaft is deemed to be stable.

Figure 21 shows the behavior response of the angular speed of the blades. The behavior seems to be a lot more stable than the first end of the shaft, with the overshoot being:

$$\% \text{Overshoot} = \frac{18.96 - 18.75}{18.75} * 100 = 1.12\%$$

With such a low overshoot the system can be assumed to be almost critically damped.

Figure 22 shows the bode plot of the angular speed 4 transfer function. The phase starts from 1.94 degrees difference up to 90 degrees, which seems similar to the main rotor shaft first end behavior. Comparing the resonance values:

Calculated resonance: $2.0983 * 10^3 \text{ radians per second}$

Captured resonance (Bode Plot): $5.64 * 10^3 \text{ radians per second}$

There seems to be a large discrepancy between the calculated value and the value from the graph. The bode plot predicts the resonance at much later frequency. This could be due to the imaginary poles of the under damped system.

Figure 23 shows the bode plot of the angular speed of the blades. The phase angle varies from -4.4 to 270 degrees, a behavior seen before in the main rotor shaft of this end. The resonance frequency is predicted to be:

Calculated resonance: $2.0983 * 10^3$ *radians per second*

Captured resonance (Bode Plot): $2.04 * 10^3$ *radians per second*

The captured resonance seems to be in line with the calculated resonance. Although the graph has no “humps” the resonance can be predicted at certain phase change. This end seems to be a lot more in phase with the calculated prediction possibly due to increased damping on this end of the shaft.

4.4 Finite Element Model Simulation

The equations are put into MATLAB and a SIMULINK model is drawn:

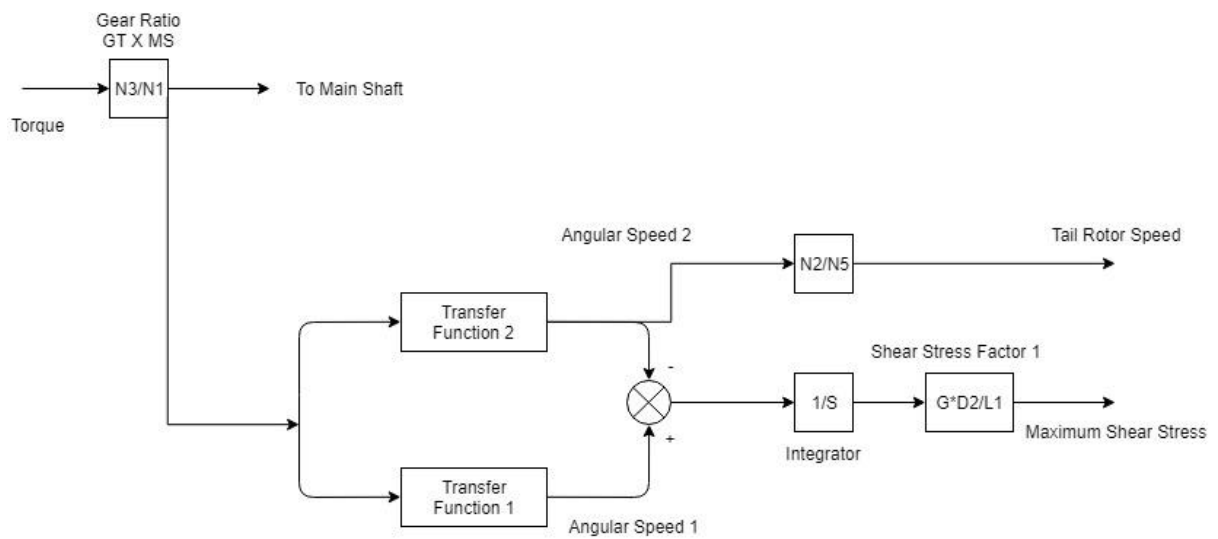


Figure 32: Representation of SIMULINK Model of Finite Elements on Main Rotor Shaft

As it is shown in the figure above, there is not much difference in representation from the lumped model, only the parallel transfer function blocks are exchanged for much more sophisticated transfer functions of higher power polynomials in terms of created matrixes of X and Y. The angular speeds $W1(s)$ and $W2(s)$ response is recorded and graphed. The difference of the angular speeds is turned into angular position with the use of the integrator, and multiplied by the gain (the shear stress factor) in order to obtain the Shear Stress response of the Main Rotor Shaft. The response is recorded and graphed.

The other mechanical limit set by the shaft (other than the shear stress) is the resonance speed. This can be found by replacing s by $(i\omega)$ and differentiating the real part, and equating it to 0. This can be easily represented by MATLAB as a function of matrix X.

The resonance speed of the Main Rotor Shaft is calculated by:

$$w_3 = [-X_{10} \ 0 \ X_8 \ 0 \ -X_6 \ 0 \ X_4 \ 0 \ -X_2 \ 0 \ X_0] \quad (5-3)$$

The roots of this equation is the resonance speed of the shaft, the values will be represented in the RESULTS section.

The equations are put into MATLAB and a SIMULINK block model is drawn for the finite element model:

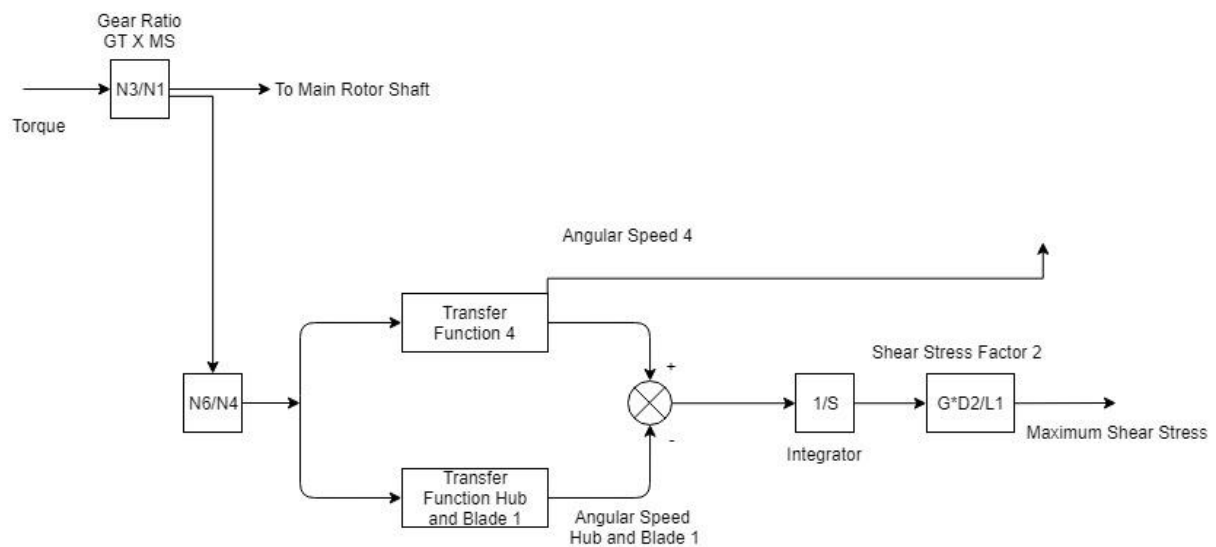


Figure 33: Representation of SIMULINK Model of Main Shaft for the Finite Elements

The signal generator produces the torque which goes through a gain simulating the gear ratio, into another gain of the second gear ratio, into the main shaft analysis of two parallel blocks containing the transfer functions calculated above. The speeds of the blades and the gear 4 is studied and graphed.

The difference in speeds goes through an integrator to become angle difference, and is then multiplied by a gain. This gain simulates the shear stress factor to find the

shear stress behavior of the main shaft. The shear stress response is studied and graphed.

The next limit to be found is the resonance, and is done the same as above. The real values of the substituted (iW) is differentiated and modeled in a MATLAB as a polynomial, the equation is:

$$w_4 = [-V_{10} \ 0 \ V_8 \ 0 \ -V_6 \ 0 \ V_4 \ 0 \ -V_2 \ 0 \ V_0]; \quad (5-4)$$

4.5 Finite Element Model Results

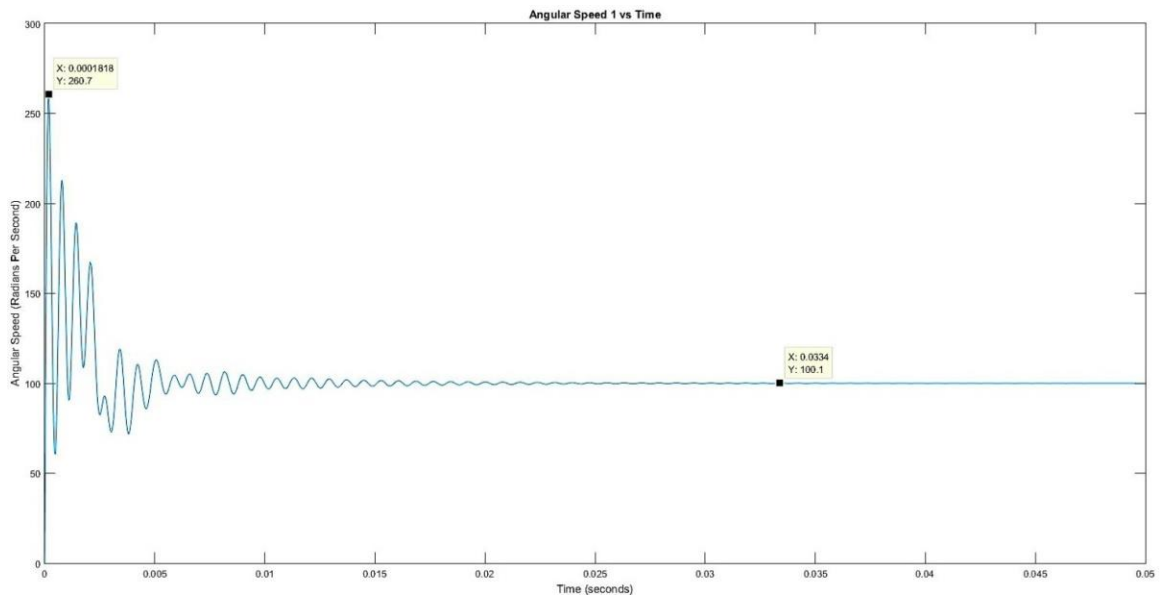


Figure 34: Load End (Angular Speed 1) of Finite Model

The settling time for the angular speed 1 is around 0.0334 seconds. The maximum over shoot is 260.7 radians per second at the first 0.0001818 seconds. The wave has a lot of propagations because of all the finite elements, but the behavior is similar to

that of the under damped response of a transfer function. The Settling speed is propagation between 100 and 99.96 radians per second.

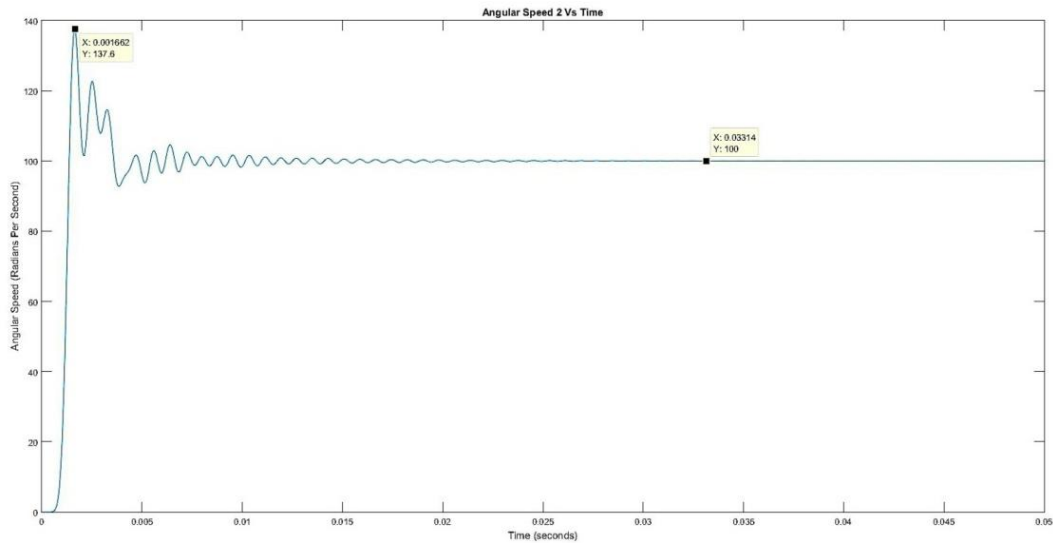


Figure 35: Drive End (Angular Speed 2) of Finite Element Model

The settling time for the angular speed 2 is around 0.03314 seconds. The maximum overshoot is 137.6 radians per second at the first 0.001662 seconds. The wave has a lot of propagations because of all the finite elements, but the behavior is similar to that of the under damped response of a transfer function. The Settling speed is propagation between 100 and 99.96 radians per second.

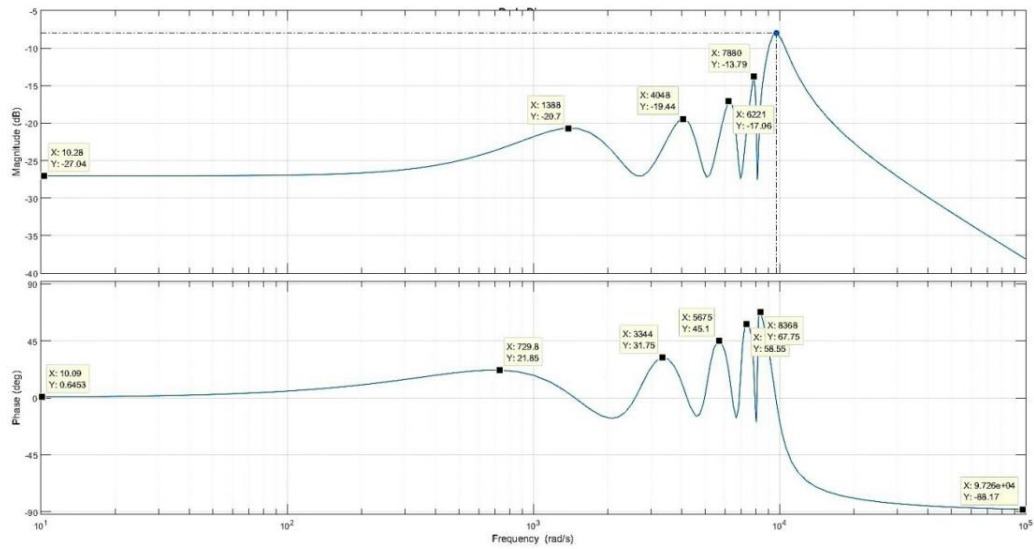


Figure 36: Load End (Angular Speed 1) Bode Plot for Finite Element Model

At Low Frequencies, the magnitude is -27 DB. The input is approximately in phase with the output of the transfer function at a phase difference of 0.644 degrees. At high frequencies, the magnitude decreases constantly to -37.9 DB. The input and output have a phase difference of 90 degrees or $\pi/2$. Different resonance peaks are predicted at $1.39 \cdot 10^3$, $4.05 \cdot 10^3$, $6.22 \cdot 10^3$, $7.88 \cdot 10^3$, $9.71 \cdot 10^3$, radians per second, each corresponding to one finite element.

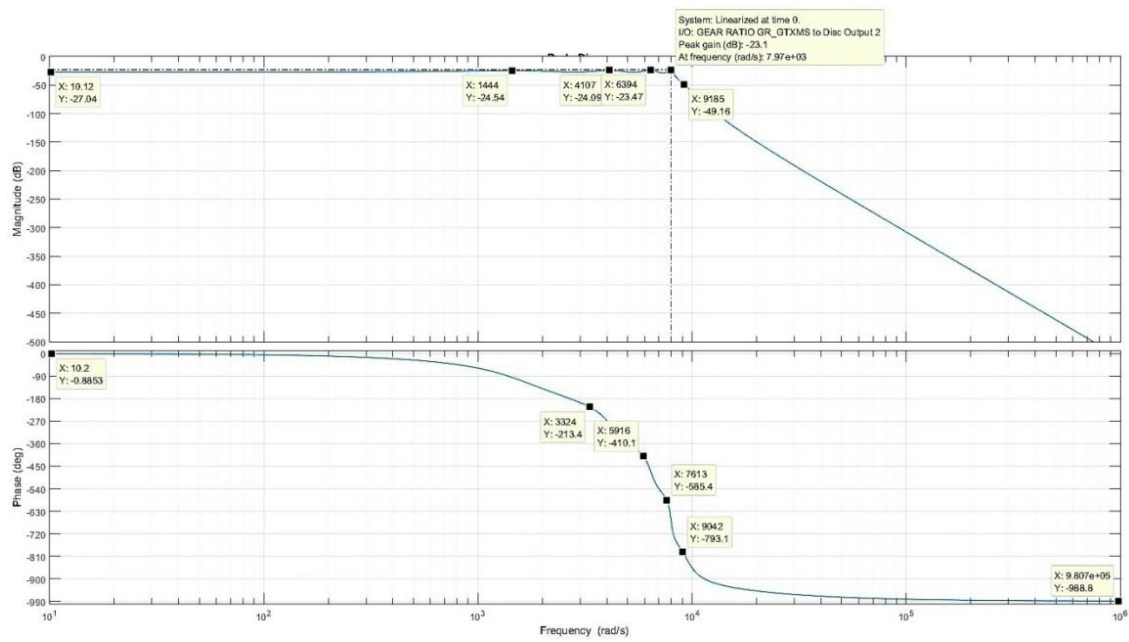


Figure 37: Load End (Angular Speed 2) Bode Plot for Finite Element Model

At Low Frequencies, the magnitude is -27 DB. The input is approximately in phase with the output of the transfer function at a phase difference of -0.89 degrees. At high frequencies, the magnitude decreases constantly to -498. The input and output have a phase difference of 990 degrees or $11 \cdot \pi/2$. Different resonance peaks are predicted at $1.44 \cdot 10^3$, $4.11 \cdot 10^3$, $6.39 \cdot 10^3$, $7.97 \cdot 10^3$, $9.18 \cdot 10^3$ radians per second, each corresponding to one finite element.

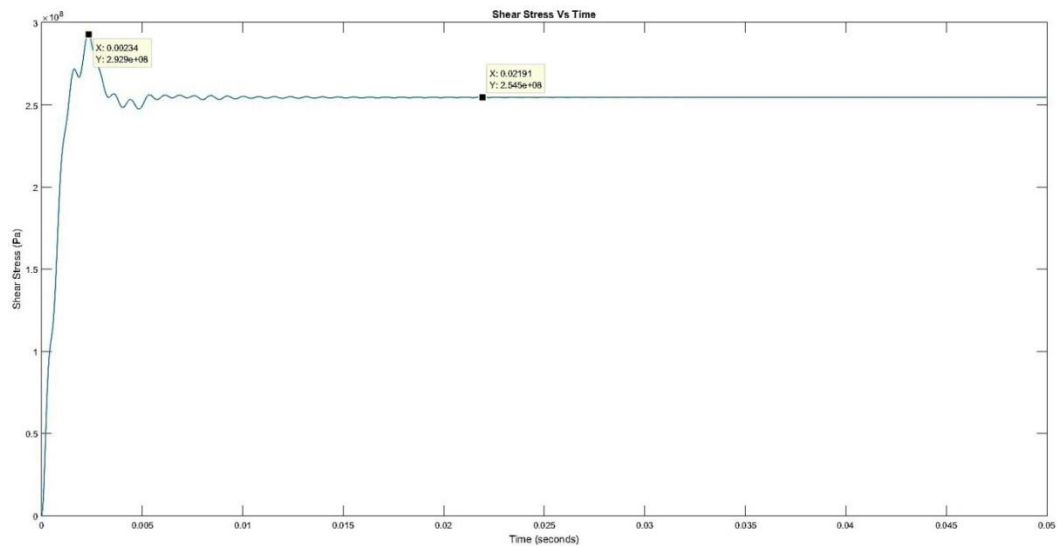


Figure 38: Shear Stress of Main Rotor Shaft for Finite Element Model

The settling time for the Shear Stress is around 0.02191 seconds. The maximum over shoot is 2.929×10^8 Pa at the first 0.00234 seconds. The wave has a lot of propagations because of all the finite elements, but the behavior is similar to that of the under damped response of a transfer function. The Settling Stress is propagation between 2.544×10^8 and 2.545×10^8 Pa.

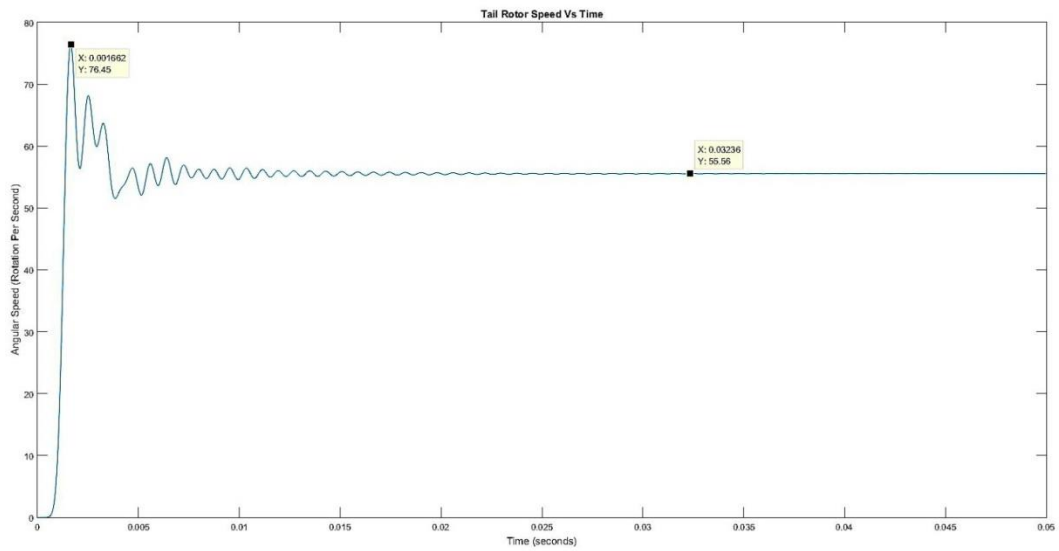


Figure 39: Tail Rotor Speed for Finite Element Model

The settling time for the Tail Rotor Speed is around 0.03236 seconds. The maximum over shoot is 76.45 radians per second at the first 0.001662 seconds. The wave has a lot of propagations because of all the finite elements, but the behavior is similar to that of the under damped response of a transfer function. The Settling speed is propagation between 55.56 and 55.53 radians per second.

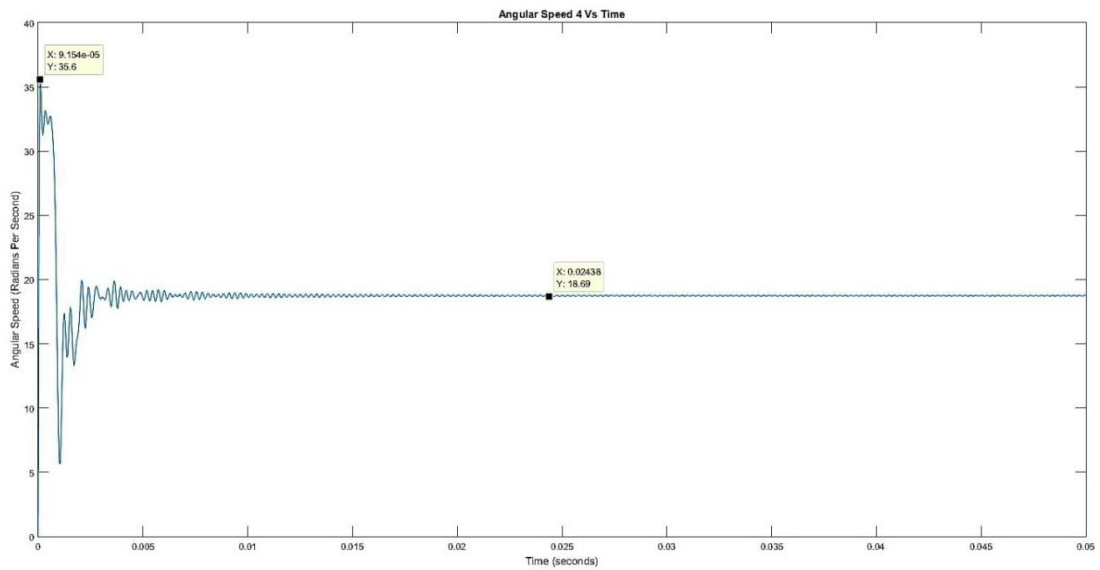


Figure 40: Drive End (Angular Speed 4) of Main Shaft for Finite Element Model

The settling time for the angular speed 4 is around 0.02438 seconds. The maximum over shoot is 35.6 radians per second at the first 9.154×10^{-5} seconds. The wave has a lot of propagations because of all the finite elements, but the behavior is similar to that of the under damped response of a transfer function. The Settling speed is propagation between 18.74 and 18.69 radians per second.

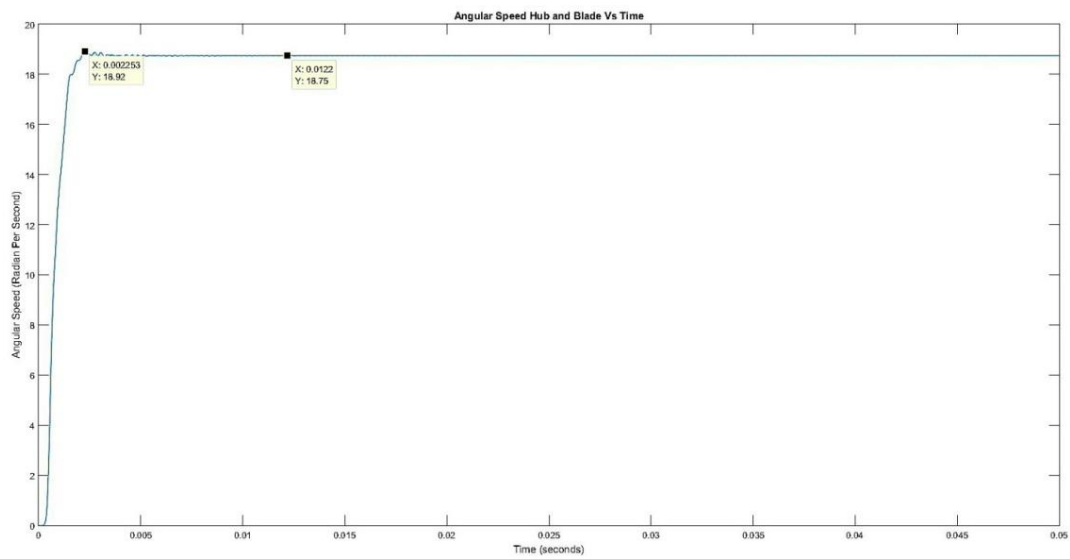


Figure 41: Blade Angular Speed of Main Shaft for Finite Element Model

The settling time for the angular speed of the blade is around 0.0122 seconds. The maximum overshoot is 18.92 radians per second at the first 0.002253 seconds. The wave has a lot of propagations because of all the finite elements, but the behavior is similar to that of the under damped response of a transfer function; it is also closer to critical damping than other functions. The settling speed is propagation between 18.75 and 18.74 radians per second.

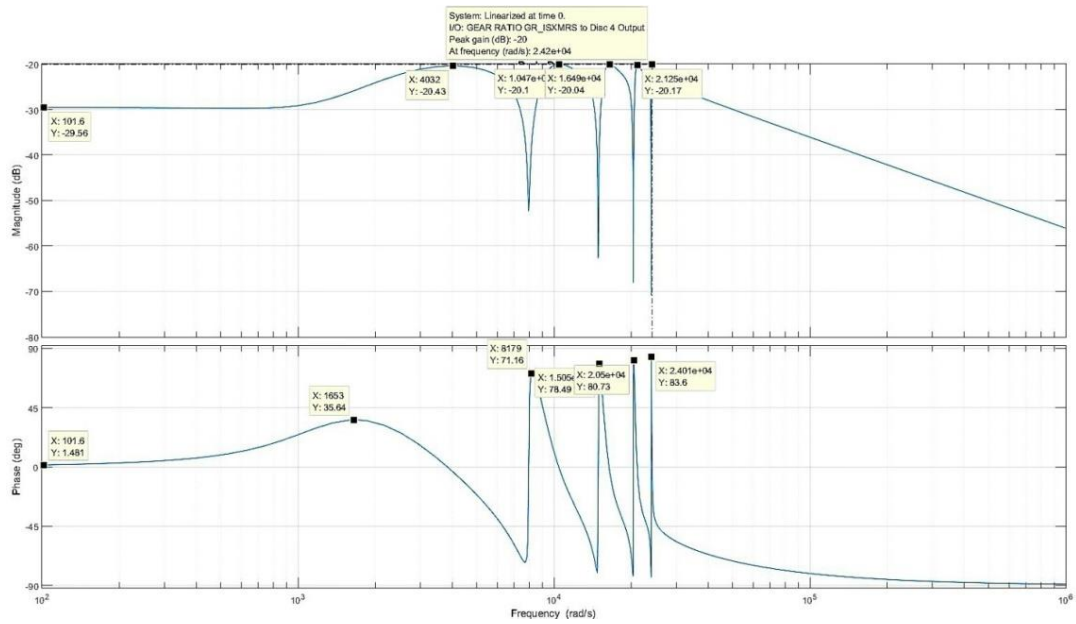


Figure 42: Drive End (Angular Speed 4) of Main Shaft Bode plot for Finite Element Model

At Low Frequencies, the magnitude is -29.6 DB. The input is approximately in phase with the output of the transfer function at a phase difference of 1.49 degrees. At high frequencies, the magnitude decreases constantly to -55.7. The input and output have a phase difference of 90 degrees or $\pi/2$. Different resonance peaks are predicted at $4.03 \cdot 10^3$, $1.05 \cdot 10^4$, $1.65 \cdot 10^4$, $2.12 \cdot 10^4$, $2.42 \cdot 10^4$ radians per second, each corresponding to one finite element.

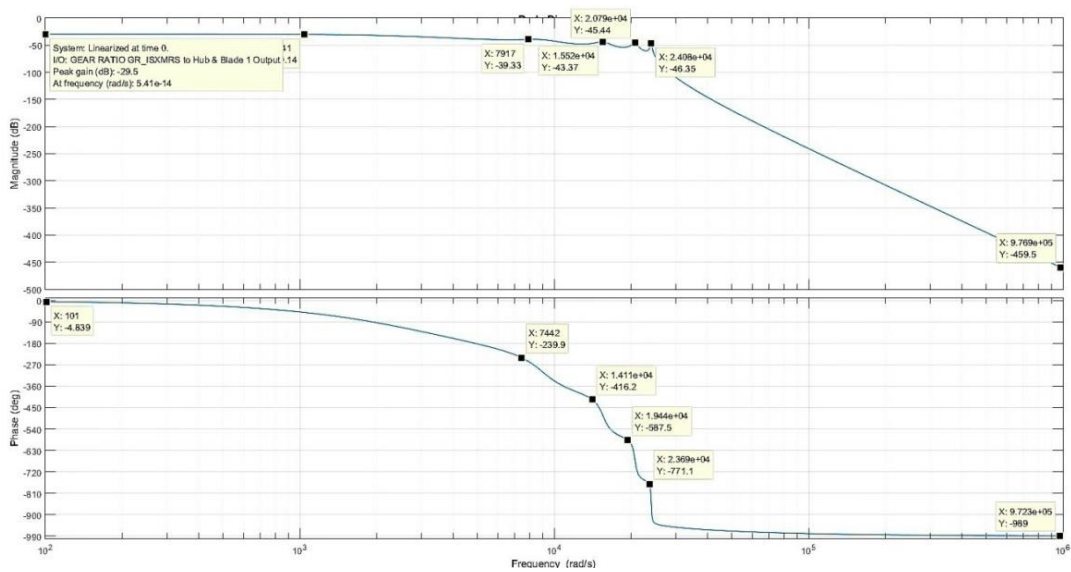


Figure 43: Blade Angular Speed of Main Shaft Bode Plot for Finite Element Model

At Low Frequencies, the magnitude is -29.5 DB. The input is approximately in phase with the output of the transfer function at a phase difference of -4.84 degrees. At high frequencies, the magnitude decreases constantly to -459. The input and output have a phase difference of 990 degrees or $11 \cdot \pi/2$. Different resonance peaks are predicted at $1.04 \cdot 10^3$, $7.93 \cdot 10^3$, $1.55 \cdot 10^4$, $2.08 \cdot 10^4$, $2.41 \cdot 10^4$, radians per second, each corresponding to one finite element.

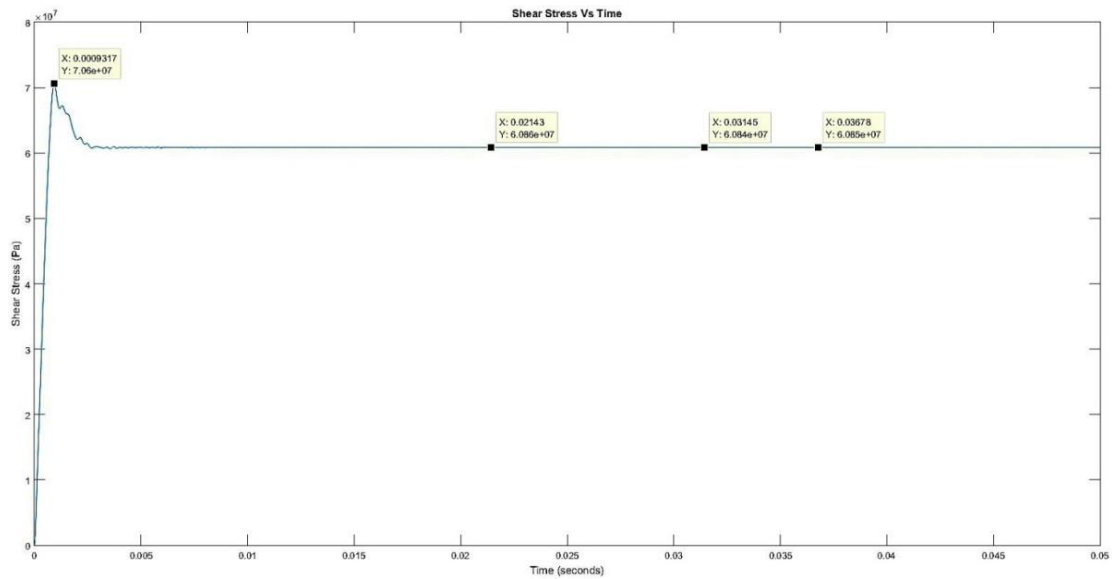


Figure 44: Shear Stress of Main Shaft for Finite Element Model

The settling time for the Shear Stress is around 0.02143 seconds. The maximum overshoot is 7.06×10^7 Pa at the first 0.0009317 seconds. The wave has a lot of propagations because of all the finite elements, but the behavior is similar to that of the underdamped response of a transfer function. The Settling Stress is propagation between 6.084×10^7 and 6.085×10^7 Pa.

4.6 Finite Element Model Analysis

The signals on all ends of the shafts have propagation after settling of very low frequency. This is due to the model design. Unlike lumped analysis, this is considered to be stable. This is because the model is more accurate to a practical situation (at the cost of being more complicated and prone to computational errors).

Main Rotor Shaft:

Figure 25 shows the response of the angular speed 1. Mind the propagations of the wave, the overall shape of the signal is similar to the under damped behavior. These propagations are due to the shaft being distributed into 5 elements. Similarly, to the lumped model, the overshoot is calculated:

$$\% \text{ over shoot} = \frac{260.7 - 100}{100} * 100\% = 160.7\%$$

This is similar to the lumped model, except the overshoot now is almost half of what is predicted before. This is not considered unhealthy as it only stays for the first 0.18 milliseconds of the response. The transfer function of the first end is still considered to be under damped.

Figure 26 shows the response behavior of angular speed 2. Comparing the finite model to the lumped model, the speed seems to settle a lot later than the lumped model (from 0.005 seconds to 0.03 seconds), however, since the time itself is very short, this is not an issue at all. The overshoot is calculated to be:

$$\% \text{ over shoot} = \frac{137.6 - 100}{100} * 100\% = 37.6\%$$

The overshoot seems to be a little bit higher than the lumped model; this means that a lot more vibrations should be expected in this section of the shaft. To get a better conclusion the shear stress behavior is observed.

Figure 29 shows the shear stress behavior of the main rotor shaft. This response is approximately identical to that of the lumped model, mind the propagations caused by the finite elements model. The over shoot of this is calculated:

$$\% \text{Overshoot} = \frac{2.929 - 2.544}{2.544} * 100\% = 45.29\%$$

Although the behavior is the same, the overshoot is twice as high; this explains the higher overshoot at the gear 2 end of the shaft. However, it is concluded that the system is not in danger of approaching instability, due to the short time to reach the overshoot, and the overall behavior of the speed and stress signals.

Figure 30 shows the tail rotor speed. This speed is predicted to be similar to the angular speed 2, but only a fraction of it in value as of the gear ratio between them.

The over shoot is:

$$\% \text{Overshoot} = \frac{76.45 - 55.56}{55.56} * 100\% = 37.59\%$$

The over shoot behavior is also similar and occurs only during the first 0.001662 seconds and is not considered to be an issue to the stability of the system.

Figure 27 shows the bode plot of angular speed 1 transfer function. There seems to be a lot of propagations compared the lumped model analysis. In fact it's assumed to be one real resonance peak for each finite element. The resonance values are:

Calculated resonance: $1.0 * 10^3 * (9.2826, 7.8770, 6.2746, 4.0327, 1.3900)$

Captured resonance (Bode Plot): $1.39 * 10^3, 4.05 * 10^3, 6.22 * 10^3, 7.88 * 10^3, 9.71 * 10^3$

The values from the graph seem to be in line with the calculated values, which seems to conclude that this method is a lot more accurate than the lumped model analysis, with increased consistency.

Figure 28 shows the bode plot of angular speed 2. The graph seems a lot harder to read than angular speed 1 perhaps due to damping. This is consistent with the lumped model on the other hand. The resonance values are found to be:

Calculated resonance: $1.0 * 10^3 * (9.2826, 7.8770, 6.2746, 4.0327, 1.3900)$

Captured resonance (Bode Plot): $1.44 * 10^3, 4.11 * 10^3, 6.39 * 10^3, 7.97 * 10^3, 9.18 * 10^3$

Although the values appear to have a little higher discrepancy, they are still very consistent with both calculated results, and the bode results from the other end of the shaft.

Main Shaft:

Figure 31 shows the angular speed 4 behavior response. The shape of the signal indicates this is an under damped response with the over shoot to be:

$$\% \text{Overshoot} = \frac{35.6 - 18.74}{18.74} * 100 = 89.97\%$$

As expected the overshoot is higher on the first end of the shaft. This was also seen in the lumped model analysis. For a conclusion to be made, the time and stress must be looked at.

Figure 35 shows the shear stress in the main shaft. The response seems to be close to that of a critical damped system. The overshoot is:

$$\% \text{ Over shoot} = \frac{7.06 - 6.084}{6.084} * 100\% = 16.04\%$$

The over shoot seems to be very low. Even though this is the finite element model analysis there are a lot less propagations than expected, this is a hint towards the system's stability. The time it takes for the angular speed 4 to reach the overshoot is 0.02438 seconds. These two low values excel at concluding that the high overshoot is not of large concern towards system stability.

Figure 32 shows the speed of the blade end. The behavior of the response is a sign that shows that the transfer function of this speed is almost critically damped. The over shoot is calculated to be:

$$\% \text{ Overshoot} = \frac{18.92 - 18.75}{18.75} * 100\% = 0.91\%$$

This value is agreeable of the analysis of the lumped model and this section is considered to be stable.

Figure 33 shows the bode plot of angular speed 4. Similarly to the main rotor shaft, there are 5 peaks considered to hold the frequency for resonance speed, because of the 5 finite element modeling. The resonance frequency is compared:

Calculated resonance: $1.0 * 10^4 * (2.4012, 2.0489, 1.5032, 0.8299, 0.1936)$

Captured resonance (Bode Plot): $4.03 * 10^3, 1.05 * 10^4, 1.65 * 10^4, 2.12 * 10^4, 2.42 * 10^4$

As seen from the comparison of the values, the first two resonance frequencies have a large discrepancy while the last three values are similar. This seems to be consistent with what was found from the lumped analysis and might be a damping issue. However this is but a prediction and is not enough to dismiss it as instability, although it is not entirely out of concern.

Figure 34 shows the bode plot of the blade transfer function. The peaks are hard to read as seen in the lumped model but still can be deduced from the phase change and be used for comparison between:

Calculated resonance: $1.0 * 10^4 * (2.4012, 2.0489, 1.5032, 0.8299, 0.1936)$

Captured resonance (Bode Plot): $1.04 * 10^3, 7.93 * 10^3, 1.55 * 10^4, 2.08 * 10^4, 2.41 * 10^4$

These values are much more in line with the calculated values and approved for consistency and precision.

4.7 Hybrid (Distributed-Lumped) Model Simulation

Putting the necessary equations in MATLAB in order to produce the following simulation in SIMULINK:

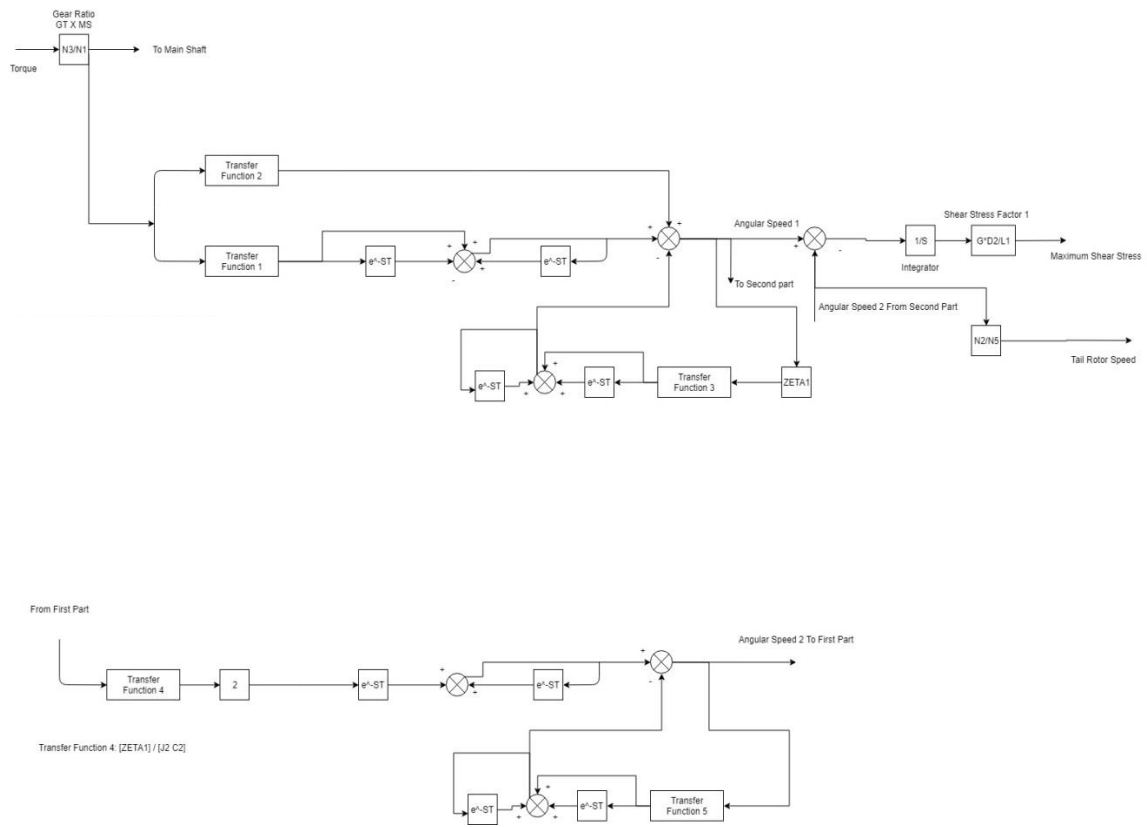


Figure 45: Representation of SIMULINK Model on Main Rotor Shaft for Hybrid Model

From the left, the signal generator into the gain of gear ratio GR_1 up until the signal reaches the transfer function. This model is of series blocks which results in the speed $W_1(s)$ is multiplied into the function of $W_2(s)$. The Angular speed 1 itself is split up into two parallel blocks as they both are two functions of S (the frequency domain). $G(s)$ which is an exponential function can be modeled as a finite time delay. Since there are two delays in the function (numerator and denominator), the numerator delay is forward, and the denominator delay is feed backed. The separate parallel lines represent the addition and subtraction of 1 (equation term). Both function blocks of $G(s)$ and $\gamma_2(s)$ are added. The denominator of $W_1(s)$ can be

represented as a transfer function on its own through a feed back to the numerator. That function is also multiplied by a finite delay as it is a function of $G(s)$. The denominator signal is subtracted from the numerator and that would be the first Angular speed represented by simout block. The response is recorded and graphed. The same split is done on the second Angular speed. The signals of W_2 and W_1 are subtracted and go through an integrator in order to obtain the angle. This angle difference signal is multiplied by a gain to obtain the Shear Stress. The Angular speed 2 and shear stress responses are graphed and recorded. From the Angular speed 2 signal, the speed is multiplied by the gear ratio to simulate the speed of the tail rotor. This speed response is also graphed and recorded.

In “Torsional response of Rotor Systems” a similar model is derived for a rotor shaft. After replacing s by $i\omega$, the resonance for that model is found to be at the cross section between hyperbolic cotan (from $P(s)$ and $G(s)$) and a linear line (from $\Delta(s)$). “There will be an infinite number of interceptions” quoting R. Whalley (2005), and therefore, it is decided that the resonance frequencies of this model will not be further analyzed.

Building the SIMULINK block models on top of the model for the main shaft becomes:

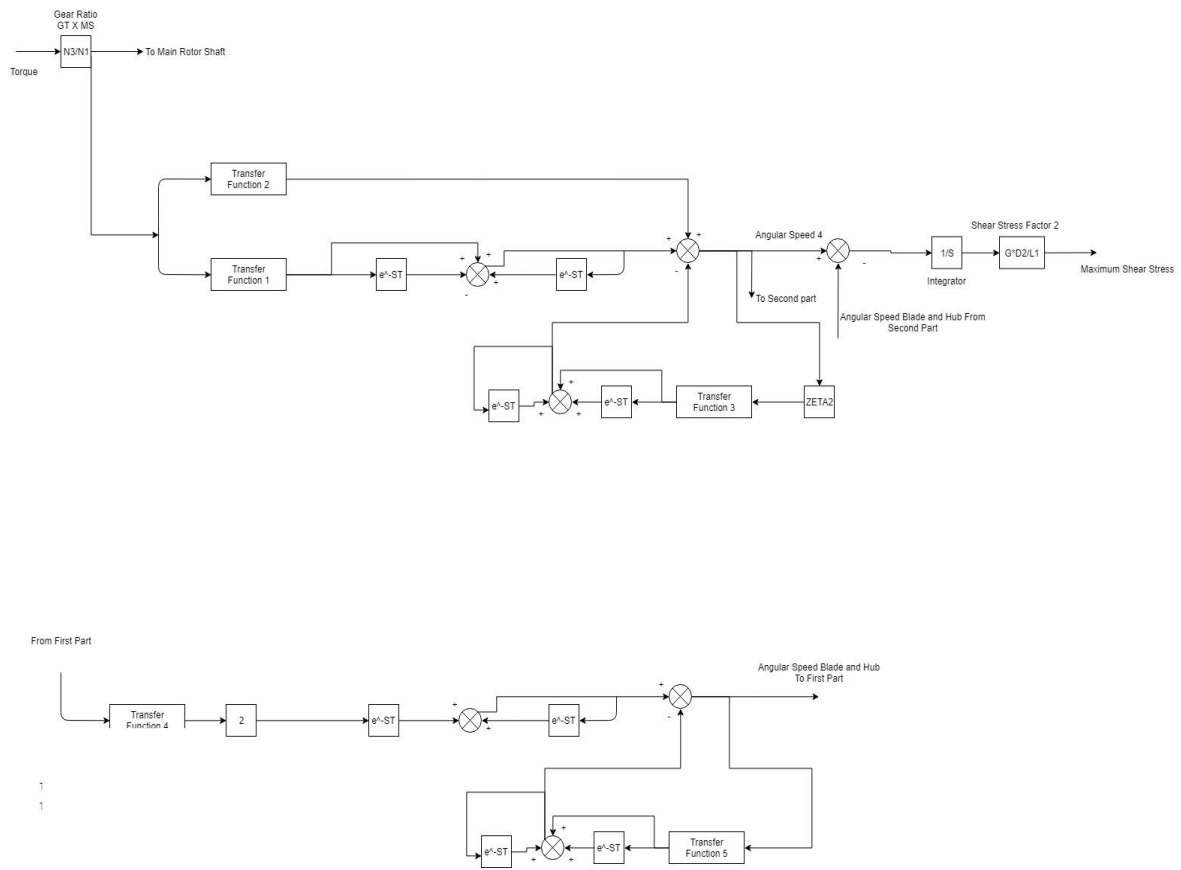


Figure 46: Representation of SIMULINK Model on Main Shaft for Hybrid Model

The signal coming from the generator is multiplied by gain of gear ratio 1 (shown in Figure 12) is split into two routes. The second route is shown in the figure above. This signal is further multiplied into another gear ratio based on the model of the transmission. This signal goes into the transfer functions. The model is also based on a Series block diagram that represents the angular speed W_1 then W_2 . The first angular speed transfer function is split into two terms of blocks each represents the numerator and denominator respectively. The numerator is split into two parallel transfer function blocks of $\gamma_4(s)$ and $G_2(s)$. The function of $G_2(s)$ itself can be represented as a time delay function block of numerator and denominator. The

parallel the lines represent the 1 term in the equation of $G_2(s)$. These parallel transfer functions are added. The denominator is further represented by its own transfer function and fed back to the numerator. This function is a function of the time delay and thus represented as above. The subtraction of these signals (numerator and denominator) is the angular speed 1. The same representation method is used for the angular speed 2 in series with angular speed 1. Both these speed responses are recorded and graphed. The difference of the angular speeds is represented by a signal going through the integrator making it represent the angle difference. The signal is further multiplied by the shear stress factor of the main shaft. The Shear stress response is recorded and graphed.

4.8 Hybrid (Distributed-Lumped) Model Results

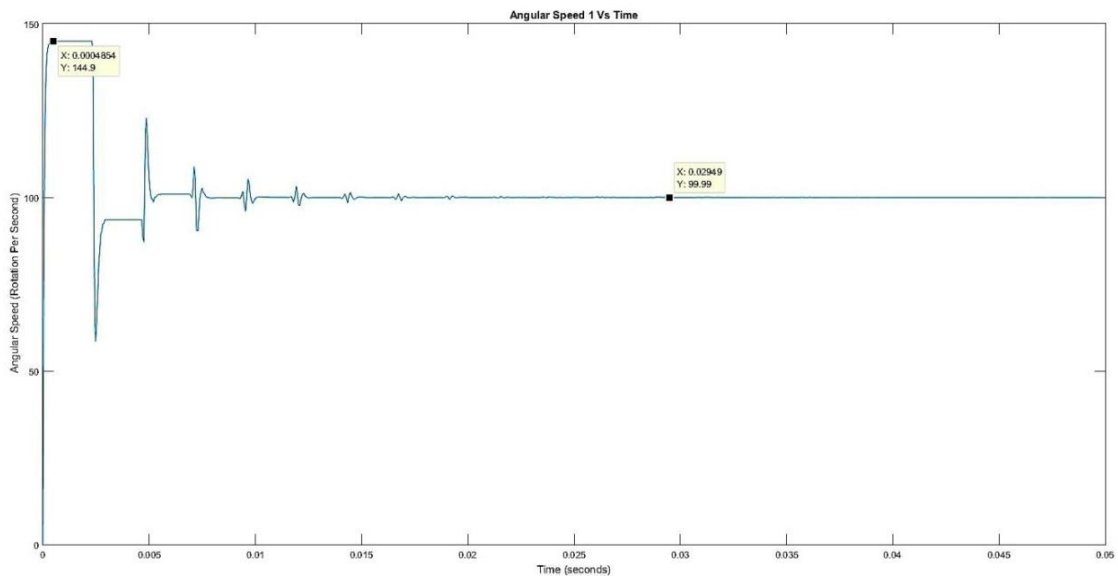


Figure 47: Load End (Angular Speed 1) of Hybrid Model

The settling time for the angular speed 1 is around 0.02949 seconds. The maximum over shoot is 144.9 radians per second at the first 0.0004854 seconds. The wave has

a lot of propagations because the shaft is modeled as many distributed elements, but the behavior is similar to that of the under damped response of a transfer function. The propagation is not as continuous as the finite element model due the finite time delay of 0.0023 seconds. The Settling speed is propagation between 99.97 and 99.98 radians per second.

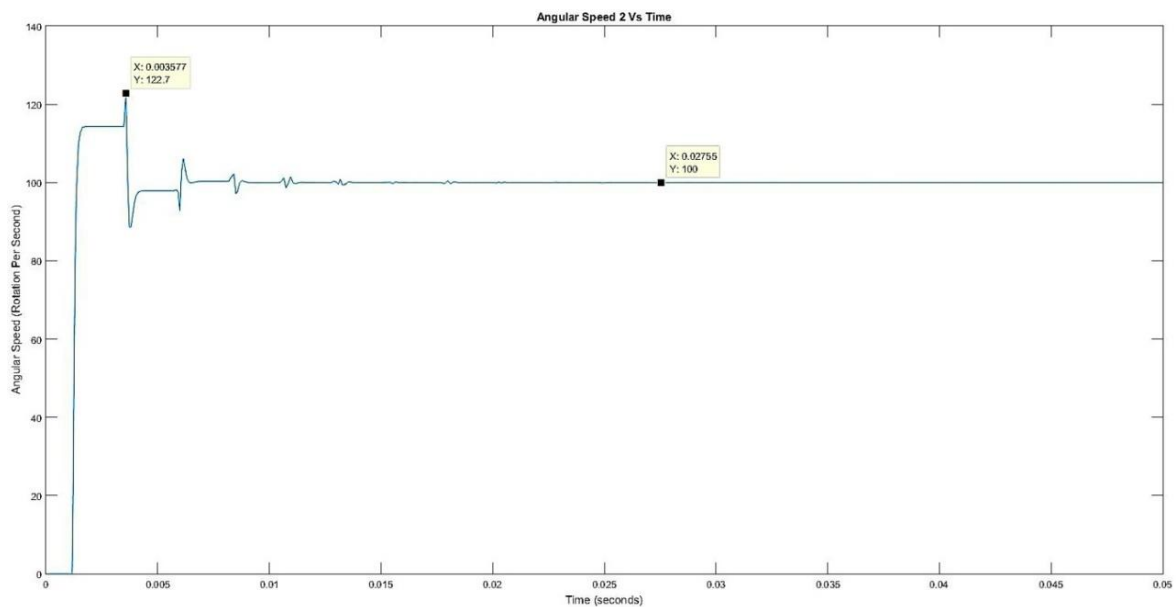


Figure 48: Drive End (Angular Speed 2) of Hybrid Model

The settling time for the angular speed 2 is around 0.02755 seconds. The maximum over shoot is 122.7 radians per second at the first 0.003577 seconds. The wave has a lot of propagations because the shaft is modeled as many distributed elements, but the behavior is similar to that of the under damped response of a transfer function. The propagation is not as continuous as the finite element model due the finite time delay of 0.0023 seconds. The Settling speed is propagation between 99.97 and 99.98 radians per second.

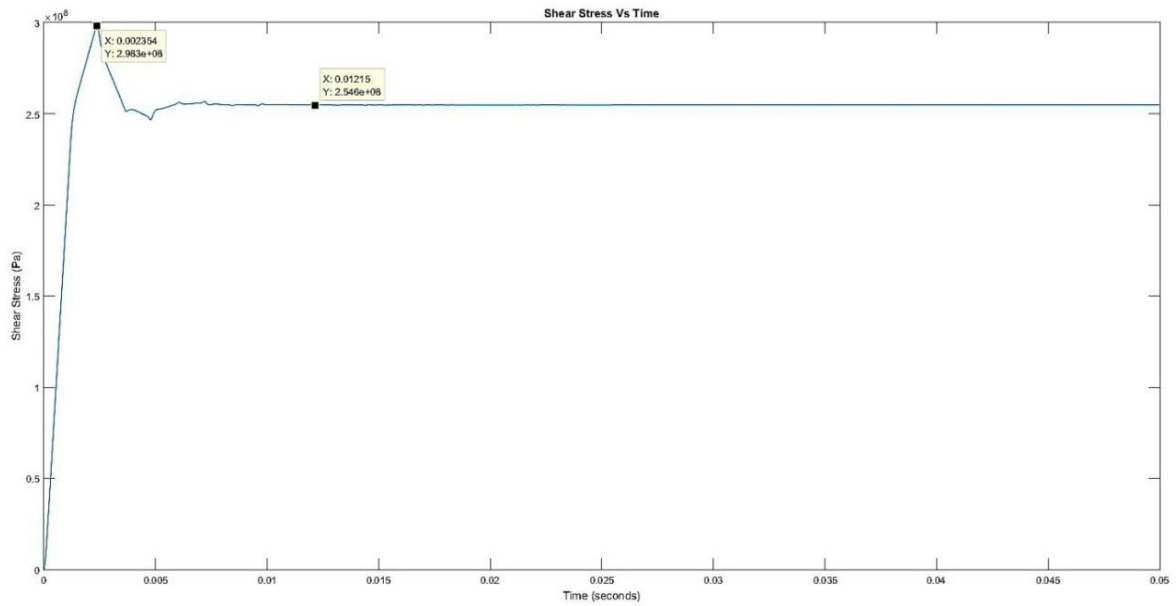


Figure 49: Shear Stress Main Rotor Shaft Hybrid Model

The settling time for the shear stress in the main rotor shaft is around 0.001215 seconds. The maximum overshoot is 2.983×10^8 Pa at the first 0.002354 seconds. The wave has a lot of propagations because the shaft is modeled as many distributed elements, but the behavior is similar to that of the under damped response of a transfer function. The propagation is not as continuous as the finite element model due to the finite time delay of $[0.0023-7.9275 \times 10^{-4}]$ seconds. The Settling Shear Stress is 2.548×10^8 Pa.

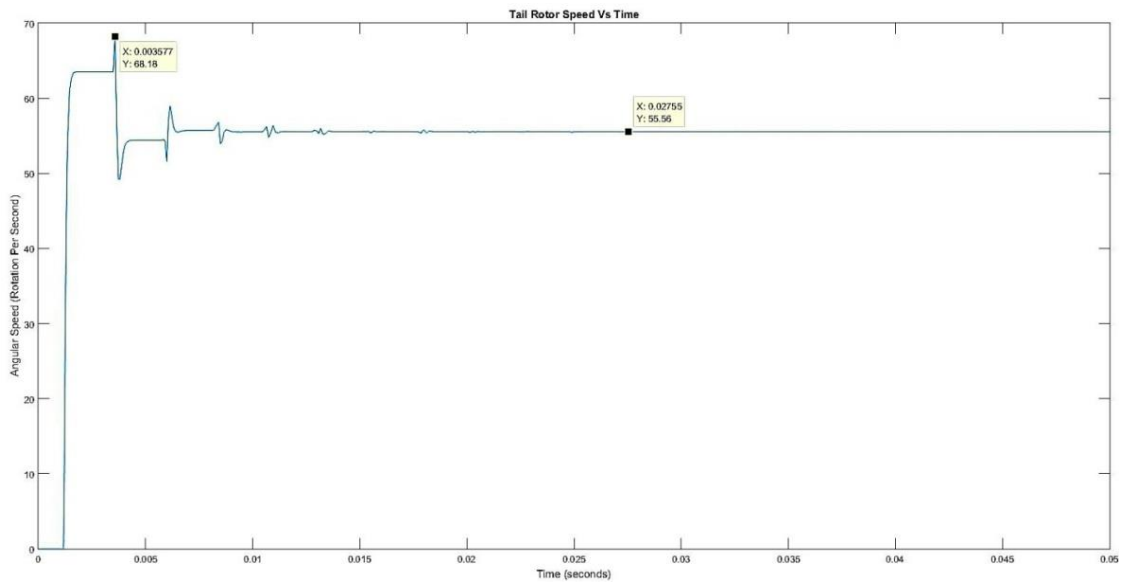


Figure 50: Tail Rotor Speed Hybrid Model

The settling time for the Tail Rotor angular speed is around 0.02755 seconds. The maximum over shoot is 68.18 radians per second at the first 0.003577 seconds. The wave has a lot of propagations because the shaft is modeled as many distributed elements, but the behavior is similar to that of the under damped response of a transfer function. The propagation is not as continuous as the finite element model due the finite time delay of 0.0023 seconds. The Settling speed is propagation between 55.54 and 55.55 radians per second.

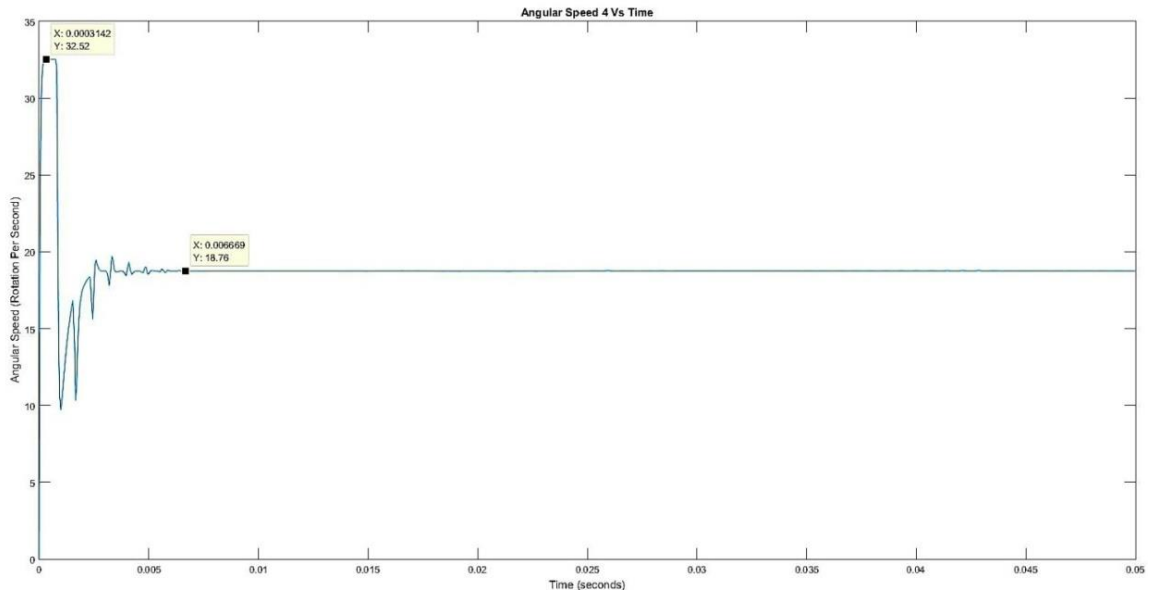


Figure 51: Drive End (Angular Speed 4) of Main Shaft for Hybrid Model

The settling time for the angular speed 4 is around 0.006669 seconds. The maximum over shoot is 32.52 radians per second at the first 0.0003142 seconds. The wave has a lot of propagations because the shaft is modeled as many distributed elements, but the behavior is similar to that of the under damped response of a transfer function. The propagation is not as continuous as the finite element model due the finite time delay of 7.9275×10^{-04} seconds. The Settling speed is propagation between 18.75 and 18.76 radians per second.

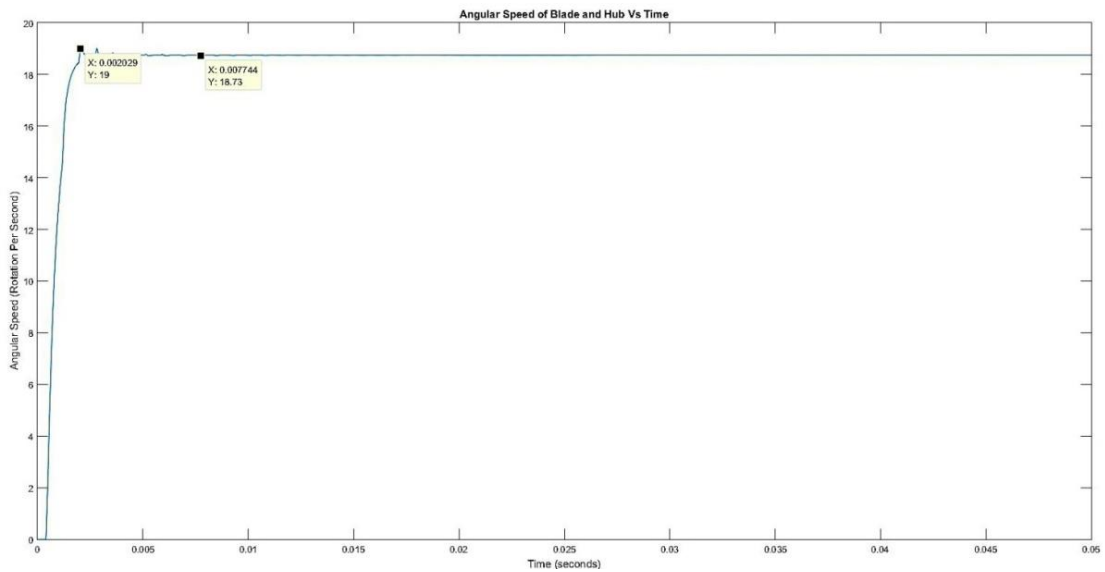


Figure 52: Blade Angular Speed of Main Shaft for Hybrid Model

The settling time for the angular speed of the blade is around 0.007744seconds. The maximum overshoot is 32.52 radians per second at the first 0.002029 seconds. The wave has a lot of propagations because the shaft is modeled as many distributed elements, but the behavior is similar to that of the under damped response of a transfer function (closer to critical damping response behavior). The propagation is not as continuous as the finite element model due the finite time delay of 7.9275×10^{-4} seconds. The Settling speed is propagation between 18.74 and 18.75 radians per second.

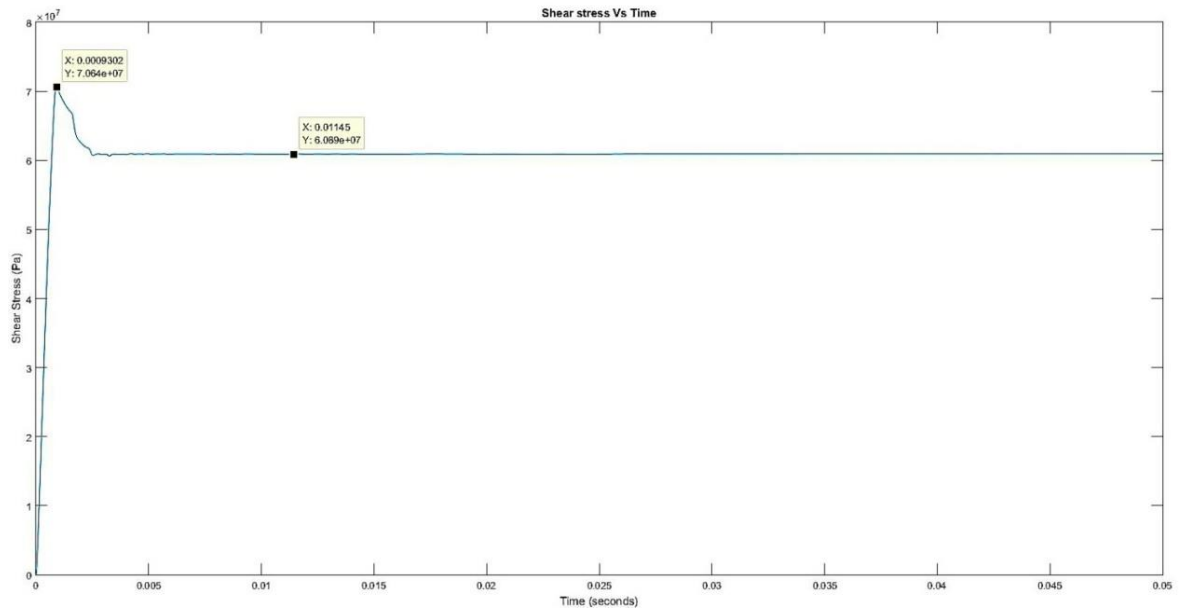


Figure 53: Shear Stress Main Shaft Hybrid Model

The settling time for the shear stress in the main shaft is around 0.01145seconds. The maximum over shoot is 7.604×10^7 Pa at the first 0.0009302 seconds. The wave has a lot of propagations because the shaft is modeled as many distributed elements, but the behavior is similar to that of the under damped response of a transfer function. The propagation is not as continuous as the finite element model due the finite time delay of $[0.0023-7.9275 \times 10^{-04}]$ seconds. The Settling Shear Stress is 6.094×10^7 Pa.

4.9 Hybrid (Distributed-Lumped) Model Analysis

The signals on all ends of the shafts have finite time delays due to the design and modeling of the hybrid distributed and lumped system. Therefore, the responses are expected to be straight lines between propagations similar to the finite element

analysis but less severe and continuous. This model is most accurate for long shaft lengths.

Main Rotor Shaft:

Figure 36 shows the response of the angular speed 1. As expected the behavior is propagations with straight lines showing the effect of finite time delays. The behavior is still that of an under damped system, and the over shoot is found to be:

$$\% \text{Overshoot} = \frac{144.9 - 99.98}{99.98} * 100\% = 44.92\%$$

Out of all models, this model gives off the least amount of overshoot for this particular speed and is because of the effect of the finite time delay (cuts the signal behavior until after the time delay where it starts to decrease).

Figure 37 shows the behavior of angular speed 2. Unlike angular speed 1 this response starts with a delay due the function block of the SIMULINK modeling, in other words, the nature of the transfer function. The over shoot of the system is effected by this:

$$\% \text{Over shoot} = \frac{122.7 - 99.98}{99.98} * 100\% = 22.72\%$$

Although the overshoot of angular speed 1 is greatly affected by the time delay compared to other models, the overshoot for angular speed 2 does not seem to be that much affected. This is because it starts with the time delay 0.0023 which is smaller than the rise time (to reach the overshoot) which is 0.02755 seconds.

Figure 38 shows the shear stress behavior along the main rotor shaft. The shear stress does not seem very different in all models of study. However, it is still possible to see the small effects of the time delays in the difference of angular speeds (1 and 2). The overshoot is:

$$\% \text{Overshoot} = \frac{2.983 - 2.548}{2.548} * 100\% = 17.07\%$$

The overshoot behavior is also similar to other models.

Figure 30 shows the tail rotor speed response. Like other models this model is exactly similar to the angular speed 2 model but with a difference in settling speed due to the gear ratio. The overshoot can still be calculated to be:

$$\% \text{Over shoot} = \frac{68.18 - 55.55}{55.55} * 100\% = 22.73\%$$

Figure 40 shows the behavior of the angular speed 4. The response is similar to the finite element model due to the small time constant of the finite time delay ($7.9275 * 10^{-04}$ seconds). The overshoot of the signal is:

$$\% \text{Overshoot} = \frac{32.52 - 18.76}{18.76} * 100\% = 73.33\%$$

The overshoot is still high as the other models have also shown but due to the shear stress behavior shown next and a small rise time of 0.3 milliseconds, this behavior is accepted.

Figure 42 shows the shear stress along the main shaft. The response shows similar characteristics of previous models to due to very small finite time delay difference.

The overshoot becomes:

$$\% \text{ Over shoot} = \frac{7.604 - 6.094}{6.094} * 100\% = 24.78\%$$

Just as the other models have predicted the over shoot is small and in an acceptable range, making the over shoot in angular speed 4 also acceptable.

Figure 41 shows the angular speed of the blades. The finite time delay effect can be seen in forms of stagnation between small propagations. The system response here is still close to critical damping as other models have shown. The over shoot is:

$$\% \text{ Overshoot} = \frac{32.52 - 18.75}{18.75} * 100\% = 1.33\%$$

The small overshoot corresponds to an almost critically damped system, and the speed is deemed to be stable.

Chapter V: Conclusions & Recommendations

This section explains the behavior of the corresponding response, based on analysis, model, and actual behavior of the shafts, gears and blades. The respective results are referenced from their figure number.

To summarize, the three modeling techniques for rotor drive line system were derived. The mathematical equations were extracted as ordinary differential equations from the lumped and finite element model, and as partial differential equations in the hybrid (transmission line) model. The transmission of the helicopter was designed element by element, including shafts, gears, dampers, hubs and blades. Using both, the mathematical model and element design a simulation has been run on the system to find the output response. This response is in terms of angular velocity and torsional shear stress. The lumped model was a more direct approach to the theoretical derivation of the drive line system. The response was smooth for the most part; with a small exception regarding the overshoots. However, this was observed in all of the models, making it more of a design flaw than a modeling flaw. The lumped model is simple and easy to derive and simulate but less accurate as it is affected by assumptions and non linearities. The finite element model holds more complexity in terms of mathematical derivation. This gives the value of the behavior (of the responses) a lot more weight. However, with more complexity comes more difficulty in solving the equations, and with more difficulty comes less accuracy. The more the finite elements the higher the order of the polynomial, the more prone to making mistakes the designer is. The hybrid model shows closer behavior to that

of the finite element, adding more weight to the value of the response found. The hybrid model weakness is shown from the difficulty of obtaining the resonance or critical speeds of the shaft. This becomes a nuisance as this information is needed to prevent mechanical failure.

References

- 2018, *Understanding of resonance essential for solving vibration problems | Control Engineering*. [online] Available at: <https://www.controleng.com/single-article/understanding-of-resonance-essential-for-solving-vibration-problems/d488603700c4d41d9797cece595e8e74.html> [Accessed 15 Nov. 2018].
- 2019, [online] Available at: http://navybmr.com/study%20material/14008a/14008A_ch7.pdf [Accessed 6 Jan. 2019].
- Ameer, A. (2010). *Distributed Parameter System Modeling, Lecture 1*.
- Ameer, A. (2010). *Distributed Parameter System Modeling, Lecture 2*.
- Ameer, A. (2010). *Distributed Parameter System Modeling, Lecture 3*.
- Asmar, N. (2017). *Partial Differential Equations with Fourier Series and Boundary Value Problems*. Dover Publications.
- Bartlett, H. and Whalley, R. (1998). Analogue solution to the modelling and simulation of distributed-lumped parameter systems. *Proceedings of the Institution of Mechanical Engineers, Part I: Journal of Systems and Control Engineering*, 212(2), pp.99-114.
- Bathe K. J. (1976) *Numerical methods in finite element analysis*, Prentice-Hall
- Budynas. (n.d.). *Shigleys mechanical engineering design, 9th ed.* Mc Graw Hill: 2010.
- C. Hibbeler, R. (2015). *Engineering Mechanics + Mastering Engineering With Pearson Etext*. 14th ed. Pearson College Div.
- Çengel, Y., Kanoglu, M. and Boles, M. (2007). *Thermodynamics*. 6th ed. New York: McGraw-Hill.
- Doebelin, E. (1998). *System dynamics*. New York: Marcel Dekker.
- Dorf, R. and Bishop, R. (2010) *Modern Control Systems, 12th Edition*, Pearson.
- Ebrahimi, M. and Whalley, R. (2000). *Analysis, Modeling and Simulation of stiffness in machine tool drives*. *Computers & Industrial Engineering*, 38(1), pp.93-105.
- Fundamentals of Gas Turbine Engines*. (n.d.).
- Gregersen, E. (2017). *Torque | Equation, Definition, & Units*. [online] Encyclopedia Britannica. Available at: <https://www.britannica.com/science/torque> [Accessed 28 Jun. 2017].
- Gunston, B. (2006). *The development of jet and turbine aero engines*. Sparkford, Somerset: Patrick Stephens.

Helicopter instructor's handbook. (2012). New Castle, Wash.: Aviation Supplies & Academics, Inc.

Industries, P. (2015). *A History of the Helicopter | Prime Industries*. [online] Prime Industries. Available at: <https://primeindustriesusa.com/history-of-the-helicopter/> [Accessed 27 Jan. 2019].

Jiang, Y., Yang, Z. and Gao, J. (2011). The Application and Development of the High Speed Overrunning Clutch in the Transmission System of the Helicopter. *Applied Mechanics and Materials*, 86, pp.283-286.

John, S., Mishra, R. and Shetty, B. (2017). Development of Reclamation Technology for a Turbo-Shaft Engine. *Journal of Failure Analysis and Prevention*, 17(2), pp.255-261.

Kalkat, M., Yıldırım, Ş. and Uzmay, I. (2003). Rotor Dynamics Analysis of Rotating Machine Systems Using Artificial Neural Networks. *International Journal of Rotating Machinery*, 9(4), pp.255-262.

Karakash, J. (1951). *Transmission lines and filter networks*. Macmillan.

Modeling of Mechanical Vibrations, n.d.

Mohaideen, M. (2012). Optimization and Analysis on Turbine Rotor of a Turbo Shaft Engine. *Procedia Engineering*, 38, pp.867-871.

MVR, R. (2015). Aerodynamic Load Estimation of Helicopter Rotor in Hovering Flight. *Journal of Aeronautics & Aerospace Engineering*, 05(01).

Padfield, R. (n.d.). *Learning to fly helicopters*.

Poluiyanin, A. and Zaëutysev, V. (2003). *Handbook of exact solutions for ordinary differential equations*. Boca Raton: Chapman & Hall/CRC.

Seddon, J. and Newman, S. (2011). *Basic Helicopter Aerodynamics*. Hoboken: Wiley.

Siemens Gas Turbine. (2015). [ebook] Mahmood El Naggar. Available at: <https://www.slideshare.net/manojg1990/236407565-gasturbinenotes> [Accessed 6 Jan. 2019].

Slager, A. (2015). Examination of a Helicopter Main Transmission Spiral Bevel Gear Fractures Due to Intergranular Attack and Fatigue. *Journal of Failure Analysis and Prevention*, 15(3), pp.441-444.

Sontag, E. (1998). *Mathematical control theory : deterministic finite dimensional systems*. New York: Springer.

Turboshaft Engine. (2019). [ebook] Thirumalvalavan. Available at: <https://www.slideshare.net/manothirumal/turbo-shaft-engine> [Accessed 6 Jan. 2019].

Whalley, R. (1990). Interconnected spatially distributed systems. *Transactions of the Institute of Measurement and Control*, 12(5), pp.262-270.

Whalley, R. (1998). Three-term control of lightly damped mechanical systems. *Proceedings of the Institution of Mechanical Engineers, Part C: Journal of Mechanical Engineering Science*, 212(2), pp.153-164.

Whalley, R. and A-Ameer, A. (2009). The computation of torsional, dynamic stresses. *Proceedings of the Institution of Mechanical Engineers, Part C: Journal of Mechanical Engineering Science*, 223(8), pp.1799-1814.

Whalley, R. and Abdul-Ameer, A. (2009). Contoured shaft and rotor dynamics. *Mechanism and Machine Theory*, 44(4), pp.772-783.

Whalley, R. and Ebrahimi, M. (2000). The regulation of mechanical drive systems. *Applied Mathematical Modelling*, 24(4), pp.247-262.

Whalley, R., Abdul-Ameer, A. and Ebrahimi, M. (2008). Machine tool modelling and profile following performance. *Applied Mathematical Modelling*, 32(11), pp.2290-2311.

Whalley, R., Ebrahimi, M. and Abdul-Ameer, A. (2005). Hybrid modelling of machine tool axis drives. *International Journal of Machine Tools and Manufacture*, 45(14), pp.1560-1576.

Whalley, R., Ebrahimi, M. and Abdul-Ameer, A. (2007). High-speed rotor-shaft systems and whirling identification. *Proceedings of the Institution of Mechanical Engineers, Part C: Journal of Mechanical Engineering Science*, 221(6), pp.661-676.

Whalley, R., Ebrahimi, M. and Jamil, Z. (2005). The torsional response of rotor systems. *Proceedings of the Institution of Mechanical Engineers, Part C: Journal of Mechanical Engineering Science*, 219(4), pp.357-380.

White, G. (1998). Design study of a split-torque helicopter transmission. *Proceedings of the Institution of Mechanical Engineers, Part G: Journal of Aerospace Engineering*, 212(2), pp.117-123.

Images:

https://upload.wikimedia.org/wikipedia/commons/thumb/6/69/Turboshaft_operation_%28multilanguage%29.svg/440px-Turboshaft_operation_%28multilanguage%29.svg.png

https://www.faasafety.gov/gslac/ALC/course_content.aspx?cID=105&sID=461&preview=true [Accessed 6 Jan. 2019]

Appendix I

MATLAB EQUATIONS:

% All Gears

H = 0.02; %m

D = 7000; %kg/m³

% All Blades

DB = 3000; %kg/m³

% Main Shaft (Tail Rotor,Hollow)

% Inertia of the Shaft:

D1MS = 0.0655; %m

D2MS = 0.07; %m

L1MS = 3.96; %m

I1MS = $\pi * D * L1MS * (1/32) * ((D2MS^4) - (D1MS^4))$; %kgm²

% Inertia of the disc 1:

% Number of Teeth = 50

NTD1 = 50;

% Rotation = 2040 rpm

D1D1 = 0.08; %m

D2D1 = 0.10; %m

I1 = $\pi * D * H * (1/32) * ((D2D1^4) - (D1D1^4))$; %kgm²

% Inertia of the disc 2:

% Number of Teeth = 27

NTD2 = 25;

% Rotation = 2040 rpm

D1D2 = 0.08; %m

D2D2 = 0.115; %m

I2 = $\pi * D * H * (1/32) * ((D2D2^4) - (D1D2^4))$; %kgm2

% Gas Turbine Shaft (Not Hollow)

% Power = 350 HP

% Number of Teeth = 17

NTD3 = 40;

% Rotation = 6000 rpm

% Inertia of the Shaft

D1GTS = 0.1; %m

L1GTS = 0.2; %m

I1GTS = $\pi * D * L1GTS * (1/32) * (D1GTS^4)$; %kgm2

% Inertia of the disc 3

D1D3 = 0.03; %m

D2D3 = 0.05; %m

I3 = $\pi * D * H * (1/32) * ((D2D3^4) - (D1D3^4))$; %kgm2

% Main Rotor Shaft

% Inertia of the Shaft

D1MRS = 0.042; %m

D2MRS = 0.05; %m

L1MRS = 1.34; %m

I1MRS = pi*D*L1MRS*(1/32)*((D2MRS^4)-(D1MRS^4)); %kgm2

% Inertia of the disc 4:

% Number of Teeth = 61

NTD4 = 60;

% Rotation = 468 rpm

D1D4 = 0.1; %m

D2D4 = 0.11; %m

I4 = pi*D*H*(1/32)*((D2D4^4)-(D1D4^4)); %kgm2

% Inertia of the Blades 1

NB1 = 5;

LB1 = 4.03; %m

D1B1 = 0.02; %m

IB1 = NB1*pi*DB*LB1*(1/32)*(D1B1^4); %kgm2

% Inertia of the Hub 1

DH1 = 0.1; %m

LH1 = 0.35; %m

IH1 = pi*DB*LH1*(1/32)*(DH1^4); %kgm2

% Tail Rotor Shaft

% Inertia of the Shaft = IGNORED because the shaft is too small

% Inertia of the Hub = IGNORED because the mass is too small

% Inertia of the blades 2 (Fixed on a small shaft)

NB2 = 4;

LB2 = 0.7; %m

D1B2 = 0.01; %m

I1B2 = NB2*pi*DB*LB2*(1/32)*(D1B2^4); %kgm2

% Inertia of the disc 5:

% Number of Teeth = 29

NTD5 = 45;

% Rotation = 1899 rpm

D1D5 = 0.01; %m

D2D5 = 0.1; %m

I5 = pi*D*H*(1/32)*((D2D5^4)-(D1D5^4)); %kgm2

% Intermediate Shaft

% Inertia of the Shaft = IGNORED because the shaft is too small

% Inertia of the disc 6:

% Number of Teeth = 14

NTD6 = 15;

% Rotation = 2040 rpm

D1D6 = 0.01; %m

D2D6 = 0.1; %m

I6 = pi*D*H*(1/32)*((D2D6^4)-(D1D6^4)); %kgm2

% Gear Ratios

% Gas Turbine X Main Shaft

GR_GTXMS = NTD3/NTD1;

% Main Shaft x Tail Rotor Shaft

GR_MSXTRS = NTD2/NTD5;

% Intermediate Shaft x Main Rotor Shaft

GR_ISXMRS = NTD6/NTD4;

% Maximum Shear Stress:

% TAW = Angle*G*R/L

% R = Outer Radius

% L = Length of Shaft

% Substitution:

% K = G*J/L EQUATION

% SSF = G*R/L EQUATION

J1 = I1;

J2 = I2;

J1MS = I1MS;

G = 80*10⁹; % N/m²

C1 = 2.5; % 20;

C2 = 20; % 5;

K = (G*J1MS)/(D*(L1MS²));

$$J4 = I4;$$

$$J1B1 = IB1;$$

$$JH1 = IH1;$$

$$J1MRS = I1MRS;$$

% back

$$JB1 = J1B1 + JH1;$$

$$C4 = 10;$$

$$CB1 = 20;$$

$$KMRS = (G*J1MRS)/(D*(L1MRS^2));$$

$$SSF1 = G*D2MS/L1MS;$$

$$SSF2 = G*D2MRS/L1MRS;$$

% Torque

$$WT = 6000*2*pi/60;$$

$$PT = 350*745.7;$$

$$TT = PT/WT;$$

% Resonance

$$w = \sqrt{(K*(C1+C2))/((J1*C2)+(J2*C1))};$$

$$w2 = \sqrt{(KMRS*(C4+CB1))/((J4*CB1)+(JB1*C4))};$$

syms S T1 T2

% Values

$K = 5 * K;$

$J = J1MS/5;$

% Matrices

$KF = [K \ -K \ 0 \ 0 \ 0 \ 0;$

$\ -K \ K+K \ -K \ 0 \ 0 \ 0;$

$\ 0 \ -K \ K+K \ -K \ 0 \ 0;$

$\ 0 \ 0 \ -K \ K+K \ -K \ 0;$

$\ 0 \ 0 \ 0 \ -K \ K+K \ -K;$

$\ 0 \ 0 \ 0 \ 0 \ -K \ K];$

$C = [C1 \ 0 \ 0 \ 0 \ 0 \ 0;$

$\ 0 \ 0 \ 0 \ 0 \ 0 \ 0;$

$\ 0 \ 0 \ 0 \ 0 \ 0 \ 0;$

$\ 0 \ 0 \ 0 \ 0 \ 0 \ 0;$

$\ 0 \ 0 \ 0 \ 0 \ 0 \ 0;$

$\ 0 \ 0 \ 0 \ 0 \ 0 \ C2];$

$JF = [J1 \ 0 \ 0 \ 0 \ 0 \ 0;$

$\ 0 \ J \ 0 \ 0 \ 0 \ 0;$

$\ 0 \ 0 \ J \ 0 \ 0 \ 0;$

$\ 0 \ 0 \ 0 \ J \ 0 \ 0;$

$\ 0 \ 0 \ 0 \ 0 \ J \ 0];$

```
0 0 0 0 0 J2];
```

```
A1 = JF*S^2;
```

```
A2 = C*S;
```

```
A3 = KF;
```

```
A = A1+A2+A3;
```

```
Y = inv (A);
```

```
%R = S*Y;
```

```
T = [T1;
```

```
0;
```

```
0;
```

```
0;
```

```
0;
```

```
0];
```

```
WF = Y*T;
```

```
% SIMULINK EQUATIONS:
```

```
X0 = ((K^5)*C1) + ((K^5)*C2);
```

```
X1 = ((K^5)*J2) + (4*(K^5)*J) + ((K^5)*J1) + (5*(K^4)*C1*C2);
```

```
X2 = (5*(K^4)*C1*J2) + (10*(K^4)*J*C2) + (5*(K^4)*J1*C2) + (10*(K^4)*C1*J);
```

```
X3 = (5*(K^4)*J1*J2) + (20*(K^3)*C1*J*C2) + (10*(K^4)*J1*J) + (10*(J^2)*(K^4)) +  
(10*(K^4)*J*J2);
```

$$X4 = (15*(K^3)*C1*(J^2)) + (15*(K^3)*(J^2)*C2) + (20*(K^3)*C1*J*J2) + (20*(K^3)*J1*J*C2);$$

$$X5 = (15*(K^3)*(J^2)*J2) + (20*(K^3)*J1*J*J2) + (6*(J^3)*(K^3)) + (15*(K^3)*J1*(J^2)) + (21*(K^2)*C1*(J^2)*C2);$$

$$X6 = (21*(K^2)*J1*(J^2)*C2) + (7*C1*(J^3)*(K^2)) + (21*(K^2)*C1*(J^2)*J2) + (7*(K^2)*(J^3)*C2);$$

$$X7 = (7*J1*(J^3)*(K^2)) + (21*(K^2)*J1*(J^2)*J2) + ((K^2)*(J^4)) + (8*K*C1*(J^3)*C2) + (7*(K^2)*(J^3)*J2);$$

$$X8 = (K*C1*(J^4)) + (8*K*C1*(J^3)*J2) + (8*K*J1*(J^3)*C2) + (K*(J^4)*C2);$$

$$X9 = (K*(J^4)*J2) + (8*K*J1*(J^3)*J2) + (K*J1*(J^4)) + (C1*(J^4)*C2);$$

$$X10 = (C1*(J^4)*J2) + (J1*(J^4)*C2);$$

$$X11 = (J1*(J^4)*J2);$$

$$Y0 = (K^5);$$

$$Y1 = (5*(K^4)*C2);$$

$$Y2 = (5*(K^4)*J2) + (10*(K^4)*J);$$

$$Y3 = (20*(K^3)*J*C2);$$

$$Y4 = (15*(K^3)*(J^2)) + (20*(K^3)*J*J2);$$

$$Y5 = (21*(K^2)*(J^2)*C2);$$

$$Y6 = (7*(J^3)*(K^2)) + (21*(K^2)*(J^2)*J2);$$

$$Y7 = (8*K*(J^3)*C2);$$

$$Y8 = (8*K*(J^3)*J2) + (K*(J^4));$$

$$Y9 = ((J^4)*C2);$$

Y10 = ((J^4)*J2);

% Values

KMRS = 5*KMRS;

J22 = J1MRS/5;

% Matrices

KF2 = [KMRS -KMRS 0 0 0 0;

-KMRS KMRS+KMRS -KMRS 0 0 0;

0 -KMRS KMRS+KMRS -KMRS 0 0;

0 0 -KMRS KMRS+KMRS -KMRS 0;

0 0 0 -KMRS KMRS+KMRS -KMRS;

0 0 0 0 -KMRS KMRS];

C22 = [C4 0 0 0 0 0;

0 0 0 0 0 0;

0 0 0 0 0 0;

0 0 0 0 0 0;

0 0 0 0 0 0;

0 0 0 0 0 CB1];

JF2 = [J4 0 0 0 0 0;

0 J22 0 0 0 0;

0 0 J22 0 0 0;

0 0 0 J22 0 0;

```
0 0 0 0 J22 0;
```

```
0 0 0 0 0 JB1];
```

```
A4 = JF2*S^2;
```

```
A5 = C22*S;
```

```
A6 = KF2;
```

```
A22 = A4+A5+A6;
```

```
Y22 = inv (A22);
```

```
%R = S*Y;
```

```
T22 = [T2;
```

```
0;
```

```
0;
```

```
0;
```

```
0;
```

```
0];
```

```
WF2 = Y22*T22;
```

```
% SIMULINK EQUATIONS:
```

```
V0 = ((KMRS^5)*C4) + ((KMRS^5)*CB1);
```

```
V1 = ((KMRS^5)*JB1) + (4*(KMRS^5)*J22) + ((KMRS^5)*J4) + (5*(KMRS^4)*C4*CB1);
```

```
V2 = (5*(KMRS^4)*C4*JB1) + (10*(KMRS^4)*J22*CB1) + (5*(KMRS^4)*J4*CB1) +
```

```
(10*(KMRS^4)*C4*J22);
```

$$V3 = (5*(KMRS^4)*J4*JB1) + (20*(KMRS^3)*C4*J22*CB1) + (10*(KMRS^4)*J4*J22) + (10*(J22^2)*(KMRS^4)) + (10*(KMRS^4)*J22*JB1);$$

$$V4 = (15*(KMRS^3)*C4*(J22^2)) + (15*(KMRS^3)*(J22^2)*CB1) + (20*(KMRS^3)*C4*J22*JB1) + (20*(KMRS^3)*J4*J22*CB1);$$

$$V5 = (15*(KMRS^3)*(J22^2)*JB1) + (20*(KMRS^3)*J4*J22*JB1) + (6*(J22^3)*(KMRS^3)) + (15*(KMRS^3)*J4*(J22^2)) + (21*(KMRS^2)*C4*(J22^2)*CB1);$$

$$V6 = (21*(KMRS^2)*J4*(J22^2)*CB1) + (7*C4*(J22^3)*(KMRS^2)) + (21*(KMRS^2)*C4*(J22^2)*JB1) + (7*(KMRS^2)*(J22^3)*CB1);$$

$$V7 = (7*J4*(J22^3)*(KMRS^2)) + (21*(KMRS^2)*J4*(J22^2)*JB1) + ((KMRS^2)*(J22^4)) + (8*KMRS*C4*(J22^3)*CB1) + (7*(KMRS^2)*(J22^3)*JB1);$$

$$V8 = (KMRS*C4*(J22^4)) + (8*KMRS*C4*(J22^3)*JB1) + (8*KMRS*J4*(J22^3)*CB1) + (KMRS*(J22^4)*CB1);$$

$$V9 = (KMRS*(J22^4)*JB1) + (8*KMRS*J4*(J22^3)*JB1) + (KMRS*J4*(J22^4)) + (C4*(J22^4)*CB1);$$

$$V10 = (C4*(J22^4)*JB1) + (J4*(J22^4)*CB1);$$

$$V11 = (J4*(J22^4)*JB1);$$

$$W0 = (KMRS^5);$$

$$W1 = (5*(KMRS^4)*CB1);$$

$$W2 = (5*(KMRS^4)*JB1) + (10*(KMRS^4)*J22);$$

$$W3 = (20*(KMRS^3)*J22*CB1);$$

$$W4 = (15*(KMRS^3)*(J22^2)) + (20*(KMRS^3)*J22*JB1);$$

$$W5 = (21*(KMRS^2)*(J22^2)*CB1);$$

$$W6 = (7*(J22^3)*(KMRS^2)) + (21*(KMRS^2)*(J22^2)*JB1);$$

$$W7 = (8*KMRS*(J22^3)*CB1);$$

$$W8 = (8*KMRS*(J22^3)*JB1) + (KMRS*(J22^4));$$

$$W9 = ((J22^4)*CB1);$$

$$W10 = ((J22^4)*JB1);$$

% Resonance

$$w3 = [-X10 \ 0 \ X8 \ 0 \ -X6 \ 0 \ X4 \ 0 \ -X2 \ 0 \ X0];$$

roots(w3);

$$w4 = [-V10 \ 0 \ V8 \ 0 \ -V6 \ 0 \ V4 \ 0 \ -V2 \ 0 \ V0];$$

roots(w4);

%Givens

%shaft MRS

$$COM1 = (D*L1MS)/(G*J1MS); \text{ \% Compliance/m (inverse of stiffness)}$$

$$LIN1 = J1MS/L1MS; \text{ \% Polar moment of inertia/m (Inductance)}$$

$$ZETA1 = \text{sqrt}(LIN1/COM1);$$

$$NEW11 = [J1 \ C1];$$

$$NEW12 = [J2 \ C2];$$

$$TAWS1 = \text{sqrt}(LIN1*COM1); \text{ \%R(s)}$$

$$TAW1 = 2*L1MS*TAWS1; \text{ \% Time Constant (Delay)}$$

$$DS11 = J1 * J2;$$

$$DS12 = (J1 * C2) + (J2 * C1);$$

$$DS13 = (C1 * C2) + (ZETA1^2);$$

% shaft MS

$$COM2 = (D * L1MRS) / (G * J1MRS); \text{ \% Compliance/m (inverse of stiffness)}$$

$$LIN2 = J1MRS / L1MRS; \text{ \% Polar moment of inertia/m (Inductance)}$$

$$ZETA2 = \text{sqrt}(LIN2 / COM2);$$

$$NEW21 = [J4 \ C4];$$

$$NEW22 = [JB1 \ CB1];$$

$$TAWS2 = \text{sqrt}(LIN2 * COM2); \text{ \% R(s)}$$

$$TAW2 = 2 * L1MRS * TAWS2; \text{ \% Time Constant (Delay)}$$

$$DS21 = J4 * JB1;$$

$$DS22 = (J4 * CB1) + (JB1 * C4);$$

$$DS23 = (C4 * CB1) + (ZETA2^2);$$

Appendix II

8.1 Definition of Concepts

Some mechanical engineering concepts must be understood to grasp the modelling of the system.

8.1.1 Torque& Torsion

Torque is the moment of force, the tendency of a force to cause a rotation of the body along a certain axis (Gregerson, 2017). The torque itself as a quantity is calculated by the multiplication of the force vector that is acting on the concerned body by the shortest distance between the axis and the force's direction. Torque is measured in Newton meter (SI units). In vector form, the torque is the cross product between the force and the radius (distance from force to centre of axis).

$$T = r \times F \text{ [cross product]}$$

Torsion is the effect of such torque on the rigid body subjected to it; in other words, the twisting effect on the rigid body (Nibsett, 2011). Torsion is usually indicated by the angle of twist:

$$\theta = \frac{T * L}{G * J}$$

Where:

θ = angle of twist in radians

G = modulus of rigidity in Pa (shear stress/shear strain)

J = polar moment of inertia in $\text{Kg}\cdot\text{m}^2$ (resistance to torsion)

8.1.2 Shear Stress

Stress on a rigid body is also called pressure. The stress is caused by a force on a certain area of contact. Shear stress is specifically caused by the force that is parallel to the plane of action or perpendicular to the axis of rotation (Nibsett, 2011). These types of forces are also known as torque. When a rigid body is affected by a torque, it deforms due to torsion. This deformation causes shear stress to develop across the cross section.

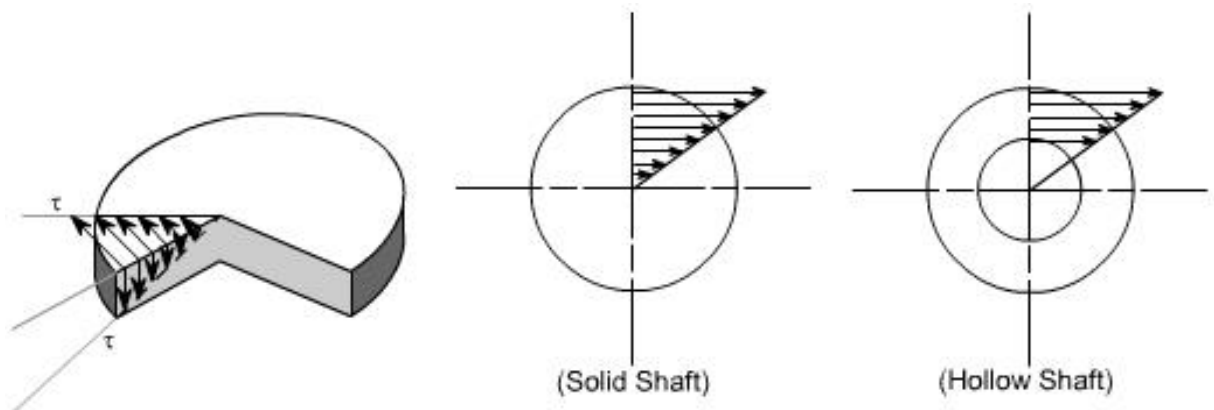


Figure 54: Shear stress distribution across Solid and Hollow Shafts

8.1.3 Angular Displacement, Velocity, Acceleration

The angular displacement is the angle made by the body when moving from one place to another along a circular path. When an object rotates around its axis, rotational motion is analysed by taking the angular displacement into consideration (instead of linear). The difference in angles from the new position

of the rotated object to the original position is called the angular displacement. The derivative of the angular displacement with respect to time is the angular velocity; similarly, the double derivative is the angular acceleration (Hibbeler, 2015).

Angular Displacement: $\theta_f - \theta_i$ in radians.

Angular Velocity: $\omega = \frac{d\theta}{dt}$ in radians per second.

Angular Acceleration: $\alpha = \frac{d^2\theta}{dt^2}$ in radians per second squared.

8.1.4 Inertia & Moment of inertia

Inertia is, as stated in Newton's first law of motion, the tendency to resist change in the object's state of motion. This tendency is measured with the aspect called the moment of inertia.

The moment of inertia is used in rotational motion, and usually refers to the measure of the tendency to resist angular acceleration caused by the torque. The moment of inertia is used to determine the torque needed in angular acceleration. For a point mass, the moment of inertia is given by the mass of the object multiplied by the square of the perpendicular distance (Hibbeler, 2015). For a rigid body, it is dependent on the shape and dimensions.

The polar moment of inertia is the measure of the tendency to resist change in torsion when torque is applied. Torsion means the angle of deflection; therefore, the polar moment of inertia deals with angular displacement of a rigid body.

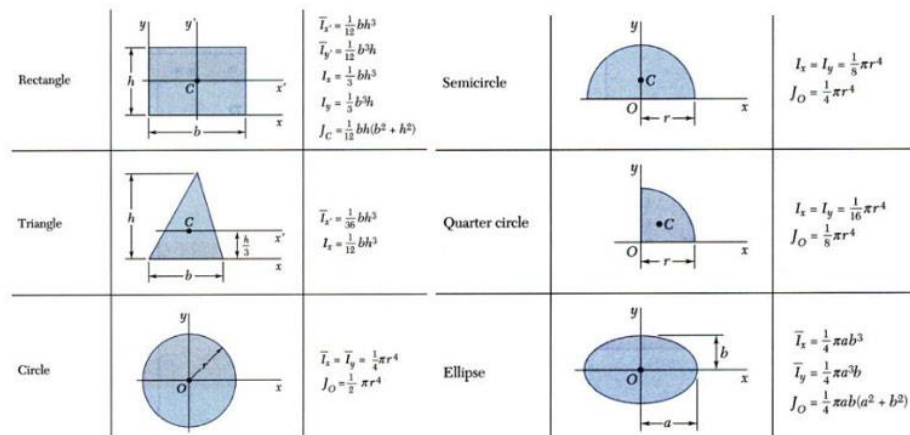


Figure 55: Equations of moment and polar moment of inertia for different shapes of rigid bodies

8.1.5 Power

Power is the rate of doing work, or the rate of energy/heat transfer. In terms of rigid bodies, it is the product of the torque multiplied by the angular velocity. It is measured in Watts or Joules per second.

8.1.6 Density

Density is simply put as the mass of a substance per its unit volume. It is measured in Kilograms per meters cubed.

8.2 Differential Equations

Solving each type of model require a set number of mathematical skills dealing with differential equations. In general, there are many ways to solve a differential equation, but the most used and reliable way in control system engineering is the frequency response method. The frequency response method utilizes the Laplace transform to change the differential equation from the time domain to the

frequency domain. This change causes the model equations to change from derivatives to polynomials; and polynomials are much easier to solve from classic algebra. Now the solved equations can be brought back to the time domain, but in today's simulation software, it is possible to study and understand the behaviour of the model just from the frequency response. Normally there are two types of differential equations; ordinary and partial. Ordinary equations would be in terms of one independent and one dependent variable. Partial differential equations on the other hand, are equations in terms of more than one independent variable. The Lumped and Finite element drive line mathematical models utilize ordinary differential equations, while the transmission model utilises the partial differential equations.